December 30, 2015

USFS Idaho and Montana Forests LiDAR 2015

Blocks 2 - 4

Technical Data Report

Ken Marshall
USDA Forest Service
Nez Perce-Clearwater National Forests
12730 Hwy 12
Orofino, ID 83544-9333

QSI Environmental
517 SW 2nd St., Suite 400
Corvallis, OR 97333
PH: 541-752-1204

Cover Photo: A view of Little Salmon River Canyon, Idaho.

Table of Contents

Introduction 1
Planning 4
Acquisition 4
Ground Control 5
Airborne Survey 11
LiDAR 11
LiDAR Data 12
Processing 12
LiDAR Density 14
Results and Discussion 14
LiDAR Accuracy Assessments 22
LiDAR Absolute Accuracy 22
LiDAR Relative Accuracy 24
Selected Images 25
Glossary 27
Appendix A - Accuracy Controls 29
Appendix B - 2015 Data Report 31
Appendix C - 2014 Data Report 59

Introduction

Little Salmon River near Riggins, Idaho.

WSI, a Quantum Spatial company (QSI), was contracted by the USDA Forest Service (USFS) to collect Light Detection and Ranging (LiDAR) data in the fall of 2014 for the Idaho and Montana Forests project. Data were collected to aid the USFS in assessing the topographic properties of the study area to support resource management.

This report accompanies the delivered LiDAR data and products for Blocks 2, 3, and 4 of the 2015 USFS Idaho and Montana Forests project. Contract specifications, data acquisition procedures, processing methods, and analysis of the final dataset including LiDAR accuracy and density are included in delivery. A complete list of contracted deliverables provided to the USFS is shown in Table 1, acquisition dates and acreage are shown in Table 2 and the project extent is shown in Figure

Table 1: Products delivered to the USFS Idaho and Montana Forests 2015 project area for Blocks 2, 3, and 4.

Idaho and Montana Forests Products Projection: UTM Zones 11 North Horizontal Datum: NAD83 (CORS96) Vertical Datum: NAVD88 (GEOID03) Units: Meters	
Points	LAS v 1.2 • All Returns • Ground Returns
Rasters	1.0 Meter ESRI Grids • Bare Earth DEM • Canopy Height DEM 0.5 Meter GeoTiffs • Intensity Images
Vectors	Shapefiles (*.shp) • Site Boundary • LiDAR Tile Index • DEM Tile Index • Ground Survey Shapes • Survey Monuments • Ground Check Points • Land Class Points • Quality Assurance Points

Table 2: Acquisition dates, acreage, and delivery dates for Idaho and Montana Forests project areas

Delivery Block	UTM	AOI	Contracted Acres	Buffered Acres	Acquisition Date(s)	Delivery Date
2	11	Grangeville South	36,820	38,463	6/17/2015	12/30/2015
		Cove Restoration	7,870	8,539	6/16/2015	
3		Palouse Additions 1	16,574	19,877	5/30/2015 - 6/5/2015	
		Palouse Additions 2	9,337	10,991	6/6/2015 -6/7/2015	
		Palouse Additions 3	2,208	2,691	6/6/2015	
		Meadow Creek	25,618	27,141	6/1/20105 - 6/6/2015	
		Headwaters Palouse River	20,528	21,599	5/31/2015 - 6/6/2015	
		Big Sand Creek	23,871	25,415	5/31/2015 - 6/6/2015	
4		Cougar Leggett	41,513	43,275	6/8/2015 - 6/13/2015	
		SF Clearwaters (HUC-10) Additions	58,087	62,349	6/8/2015 - 6/15/2015	
		Ten Twenty Mile	30,224	31,659	6/13/2015 - 6/15/2015	
		Meadow Creek Addition	8,650	9,377	6/8/2015 - 6/13/2015	

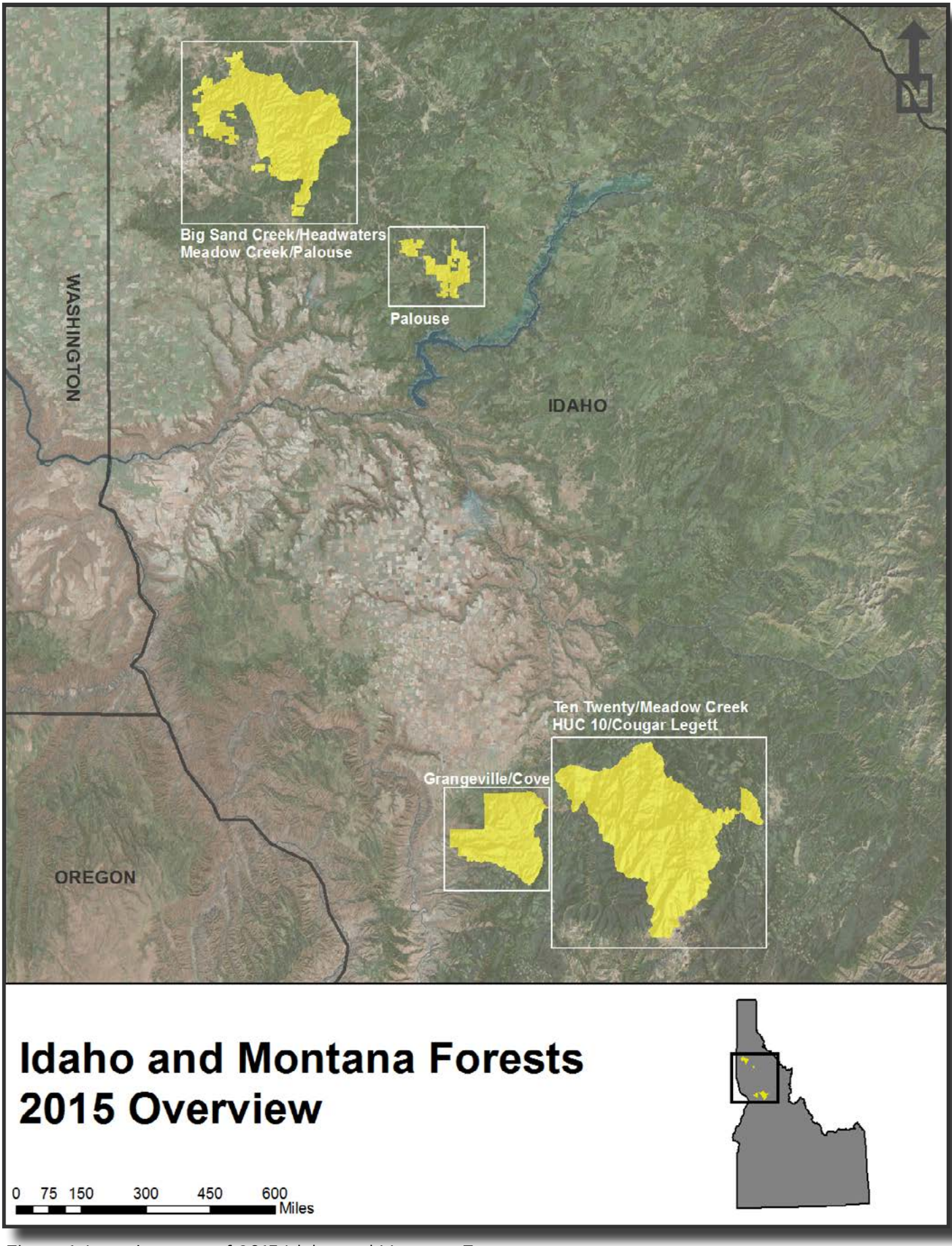

Figure 1: Location map of 2015 Idaho and Montana Forests

Acquisition

QSI Cessna 208-B Grand Caravan

Planning

In preparation for data collection, QSI reviewed the project area and developed a specialized flight plan to ensure complete coverage of the Idaho and Montana LiDAR study area at the target point density of ≥8.0 points/m^2 (0.74 points/ft^2). Acquisition parameters including orientation relative to terrain, flight altitude, pulse rate, scan angle, and ground speed were adapted to optimize flight paths and flight times while meeting all contract specifications.

Factors such as satellite constellation availability and weather windows must be considered during the planning stage. Any weather hazards or conditions affecting the flight were continuously monitored due to their potential impact on the daily success of airborne and ground operations. In addition, logistical considerations including private property access and potential air space restrictions were reviewed.

Ground Control

Ground control surveys, including monumentation, aerial targets and ground survey points (GSPs), were conducted to support the airborne acquisition. Ground control data were used to geospatially correct the aircraft positional coordinate data and to perform quality assurance checks on final LiDAR data and orthoimagery products.

QSI-Established Monument

Monumentation

The spatial configuration of ground survey monuments provided redundant control within 13 nautical miles of the mission areas for LiDAR flights. Monuments were also used for collection of ground survey points using the real time kinematic (RTK) survey technique.

Monument locations were selected with consideration for satellite visibility, field crew safety, and optimal location for GSP coverage. QSI utilized 17 existing monuments and established 43 monuments for the Idaho and Montana Forests LiDAR project (Table 3, Figures 2a, 2b, 2c). New monumentation was set using 5/8" x 30" rebar topped with stamped 2" aluminum caps.

To correct the continuously recorded onboard measurements of the aircraft position, QSI concurrently conducted multiple static Global Navigation Satellite System (GNSS) ground surveys (1 Hz recording frequency) over each monument. During post-processing, the static GPS data were triangulated with nearby Continuously Operating Reference Stations (CORS) using the Online Positioning User Service (OPUS*) for precise positioning. Multiple independent sessions over the same monument were processed to confirm antenna height measurements and to refine position accuracy.

Table 3: Monuments established for the Idaho and Montana Forests acquisition. Coordinates are on the NAD83 (CORS96) datum, epoch 2002.00. Geoid03 was used to establish orthometric heights.

UTM Zone	Monument ID	Latitude	Longitude	Ellipse	NAVD88 Height (meters)
11	DUTCH_01	N45°49'45.26290"	W115°36'10.35256"	1204.157	1219.586
11	DUTCH_02	N45°49'04.40532"	W115°27'25.95805"	1184.307	1199.613
11	ELK_01A	N46°47'28.03198"	W116°10'26.76338"	844.749	861.749
11	ELK_01B	N46°47'26.96376"	W116°10'26.31241"	845.398	862.398
11	ID_MT_FOR_01	N46°17'22.58039"	W115°28'10.51282"	1593.435	1609.501
11	ID_MT_FOR_02	N46°18'52.77536"	W115°25'27.32450"	1591.161	1607.184
11	ID_MT_FOR_03	N46°50'29.54312"	W115°25'41.56738"	1422.701	1438.543
11	ID_MT_FOR_04	N46°51'25.68990"	W115°22'08.56449"	1407.036	1422.739
11	ID_MT_FOR_05	N46°44'49.01540"	W115°19'06.78184"	1391.325	1406.924
11	ID_MT_FOR_06	N46°47'19.19859"	W115°26'14.13932"	1203.404	1219.311
11	ID_MT_FOR_07	N45°50'25.67201"	W116°04'43.89199"	1510.339	1526.230
11	ID_MT_FOR_08	N45°45'54.82620"	W116°05'37.63340"	1625.654	1641.378
11	ID_MT_FOR_09	N45°22'56.30848"	W116°27'09.23563"	1920.629	1935.886
11	ID_MT_FOR_10	N45°20'49.47449"	W116°29'31.58828"	2245.68	2260.817
11	IDMT_1A	N47°50'18.42046"	W116°15'17.98418"	899.617	916.284
11	IDMT_1B (SV0057)	N47°50'18.24062"	W116°15'16.93899"	899.767	916.433

* OPUS is a free service provided by the National Geodetic Survey to process corrected monument positions. http://www.ngs.noaa.gov/OPUS.

Table 3 cont'd: Monuments established for the Idaho and Montana Forests acquisition. Coordinates are on the NAD83 (CORS96) datum, epoch 2002.00. Geoid03 was used to establish orthometric heights.

UTM Zone	Monument ID	Latitude	Longitude	Ellipse	NAVD88 Height (meters)
11	IDMT_2A	N46°57'27.12561"	W116°40'06.18645"	787.818	805.595
11	IDMT_2B	N46°57'28.08788"	W116°40'06.25244"	787.466	805.242
11	IDMT_5A	N45°32'00.80369"	W116°20'41.82002"	939.974	955.616
11	IDMT_5B	N45°32'01.16174"	W116°20'42.70169"	939.980	955.621
11	IDMT_5C	N45°32'54.30483"	W116°24'36.58737"	1582.283	1597.879
11	IDMT_7A	N45°50'21.72930"	W115°41'14.47764"	1634.779	1650.308
11	IDMT_7B	N45°49'53.60076"	W115°41'54.41542"	1687.737	1703.268
11	IDMT_9A	N45°44'57.02027"	W115°42'14.93166"	1773.361	1788.658
11	IDMT_9B	N45°44'56.75974"	W115°42'14.53746"	1773.187	1788.483
11	IDNP	N45°56'22.93594"	W116°07'16.53072"	997.096	1013.322
11	LOLO	N46°45'46.24714"	W114°05'48.67315"	1109.860	1124.614
11	LWST	N46°22'23.42428"	W117°00'08.24812"	427.607	445.852
11	P023	N44°53'54.34204"	W116°06'10.76576"	1522.130	1537.060
11	P025	N48°43'51.63137"	W116°17'14.98404"	695.902	712.342
11	P372	N45°25'41.27722"	W117°15'05.91188"	1208.817	1224.945
11	P422	N46°47'52.29765"	W116°58'46.80446"	844.199	862.601
11	RIG_01	N45°20'26.05061"	W116°23'05.08261"	1192.416	1207.805
11	RIG_02	N45°18'37.38776"	W116°22'58.98879"	1242.471	1257.785
11	RIG_03	N45°32'55.16792"	W116°24'36.66711"	1583.564	1599.162
11	SPN6	N47°31'06.10734"	W117°25'24.00164"	720.997	739.314
12	AI7923	N47°21'50.97066"	W113°35'58.61712"	1243.997	1257.895
12	AI7923-B	N47°21'51.31615"	W113°35'53.28186"	1242.297	1256.192
12	IDMT_11A	N47°52'42.03773"	W113°47'51.73762"	1000.579	1015.440
12	IDMT_11B	N47°52'45.60200"	W113°47'56.03164"	999.058	1013.924
12	IDMT_13A	N47°35'29.44346"	W113°45'20.86851"	1066.545	1081.086
12	IDMT_13B	N47°35'26.21433"	W113°45'19.28065"	1067.183	1081.722
12	IDMT_16A	N47°20'41.09926"	W113°31'20.21364"	1882.270	1895.933
12	IDMT_16B	N47°20'41.88195"	W113°31'22.51814"	1879.058	1892.724
12	IDMT_17A	N47°09'20.06465"	W113°19'00.36234"	1484.274	1497.813
12	IDMT_17B	N47°09'18.66519"	W113°19'02.82768"	1499.362	1512.904
12	IDMT_17C	N47°09'20.13816"	W113°19'00.26068"	1484.236	1497.775
12	IDMT_19A	N47°07'17.61634"	W112°59'10.39571"	1742.360	1755.295
12	IDMT_19B	N47°07'18.91084"	W112°59'10.79992"	1741.331	1754.265
12	IDMT_23A	N46°51'00.57362"	W112°43'21.63439"	1928.477	1941.441
12	IDMT_23B	N46°51'01.16231"	W112°43'21.76271"	1927.876	1940.841
12	IDMT_25A	N46°57'18.62103"	W112°30'30.38888"	1791.196	1803.960
12	IDMT_25B	N46°57'18.77823"	W112°30'28.94686"	1784.119	1796.880
12	MSOL	N46°55'45.83748"	W114°06'31.84582"	960.622	975.562
12	MTDT	N46°35'18.59106"	W111°59'36.96383"	1217.751	1230.826
12	MTFV	N48°13'38.89075"	W114°19'36.54418"	905.677	921.802
12	P046	N47°01'46.52350"	W113°19'54.18626"	1290.837	1304.661
12	PLS5	N47°39'49.55360"	W114°06'50.07818"	974.604	990.000
12	RX0477	N46°56'23.78108"	W112°40'06.70709"	1374.622	1387.584
12	RX0477B	N46°56'24.95725"	W112°40'06.69684"	1374.287	1387.249

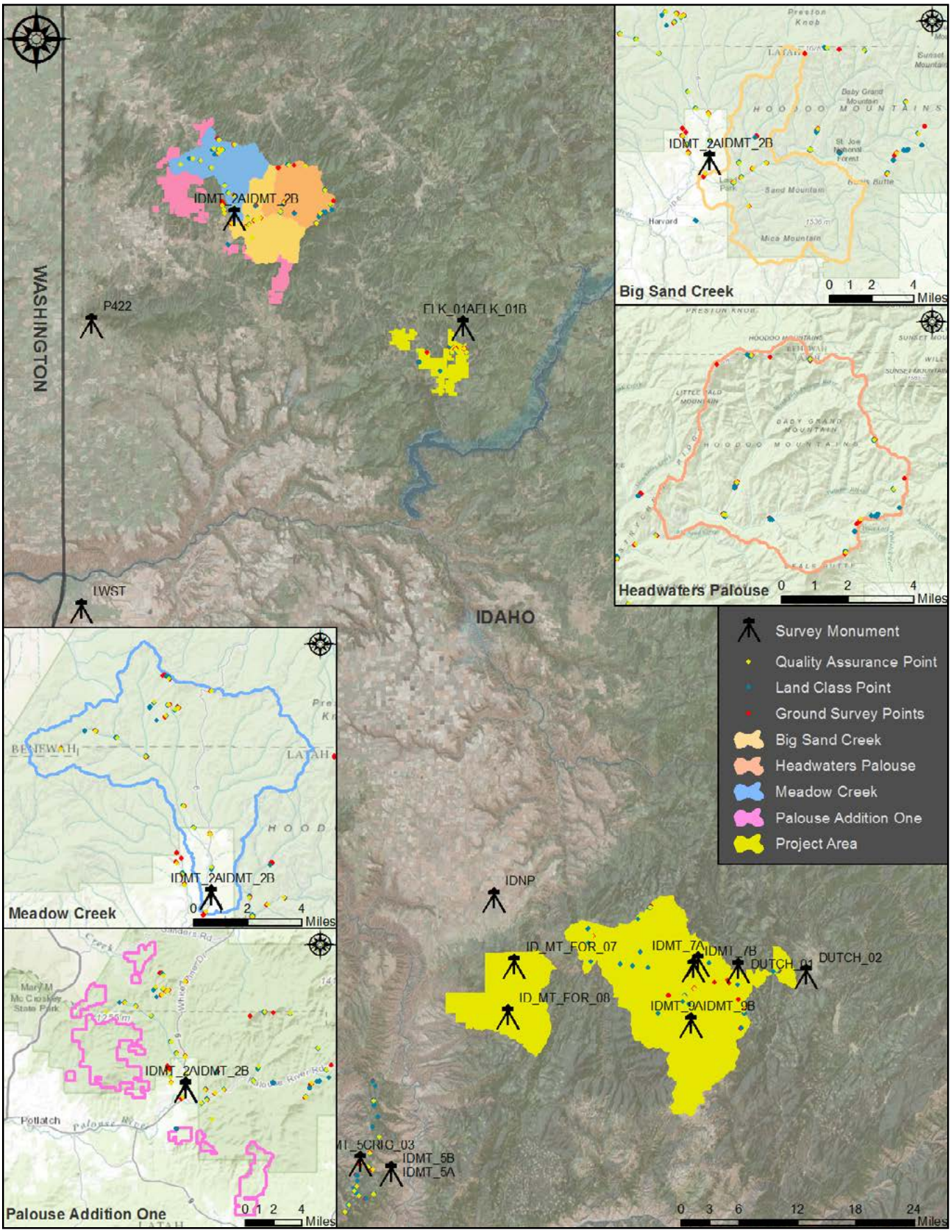

Figure 2a: Ground control location map for UTM 11.

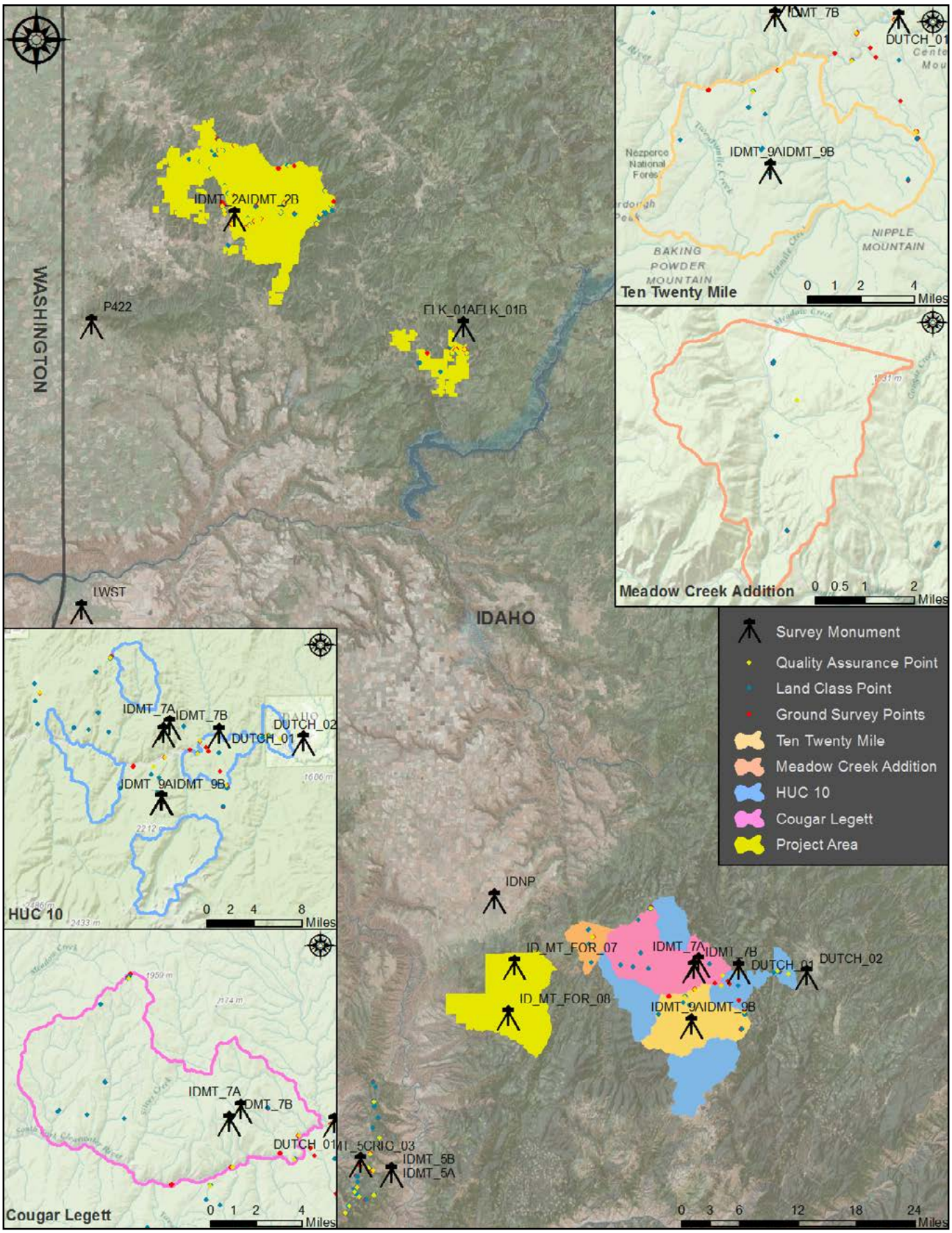

Figure 2b: Ground control location map for UTM 11 continued.

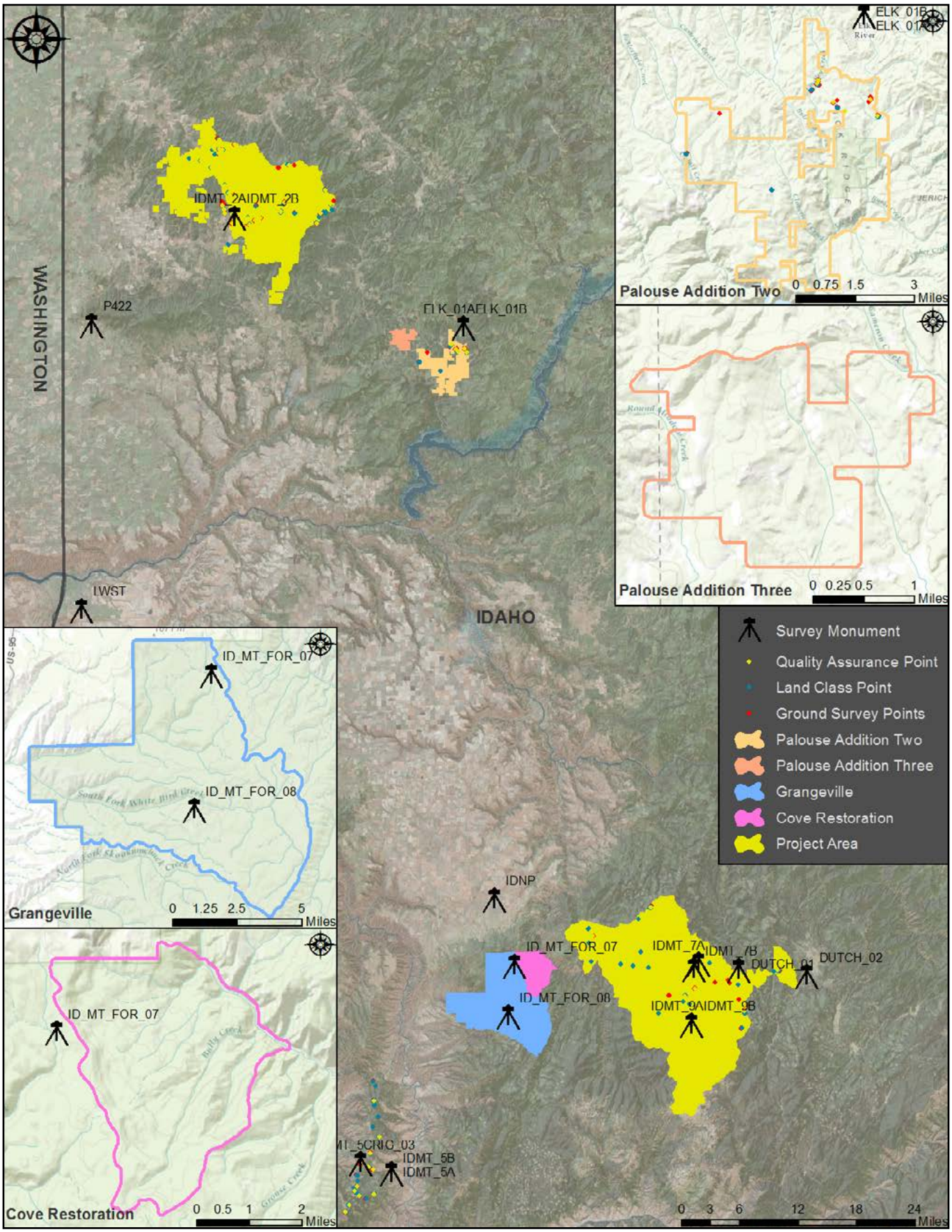

Figure 2c: Ground control location map for UTM 11 continued.

Ground Survey Points (GSPs)

Ground survey points were collected using real time kinematic, roving Trimble R6 or R8 survey techniques. A Trimble R7 base unit was positioned at a nearby monument to broadcast a kinematic correction to a roving Trimble R8 GNSS receiver. All GSP measurements were made during periods with a Position Dilution of Precision (PDOP) of ≤ 3.0 with at least six satellites in view of the stationary and roving receivers. When collecting RTK data, the rover records data while stationary for five seconds, then calculates the pseudorange position using at least three one-second epochs. Relative errors for any GSP position must be less than 1.5 cm horizontal and 2.0 cm vertical in order to be accepted. Relative errors for the position must be less than 1.5 cm horizontal and 2.0 cm vertical in order to be accepted. See Table 5 for Trimble unit specifications.

GSPs were collected in areas where good satellite visibility was achieved on paved roads and other hard surfaces such as gravel or packed dirt roads. GSP measurements were not taken on highly reflective surfaces such as center line stripes or lane markings on roads due to the increased noise seen in the laser returns over these surfaces. GSPs were collected within as many flightlines as possible, however the distribution of GSPs depended on ground access constraints and monument locations and may not be equitably distributed throughout the study area (Figures 2a and 2b).

Table 5: Trimble equipment identification

Receiver Model	Antenna	OPUS Antenna ID	Use
Trimble R6	Integrated GNSS Antenna R6	TRM_R6	Rover
Trimble R7 GNSS	Zephyr GNSS Geodetic Model 2 RoHS	TRM57971.00	Static
Trimble R8	Integrated Antenna R8 Model 2	TRM_R8_GNSS	Static, Rover

Airborne Survey

LiDAR

The LiDAR survey was accomplished using Leica ALS70 sensor systems mounted in a Cessna 208-B Grand Caravan and Partenavia P68 aircraft. Table 6 summarizes the settings used to yield an average pulse density of 8 pulses/m^2 over the Idaho and Montana Forests project area. The Leica laser system records up to four range measurements (returns) per pulse. It is not uncommon for some types of surfaces (e.g., dense vegetation or water) to return fewer pulses to the LiDAR sensor than the laser originally emitted. The discrepancy between first return and overall delivered density will vary depending on terrain, land cover, and the prevalence of water bodies. All discernible laser returns were processed for the output dataset.

Table 6: LiDAR specifications and survey set-

LiDAR Survey Settings & Specifications	
Acquisition Dates	5/30/2015 - 6/17/2015
Aircraft Used	Cessna 208 Grand Caravan Partenavia P68
Sensor	Leica ALS70
Survey Altitude (AGL)	1,450 m
Target Pulse Rate	180-192.6 kHz
Pulse Mode	Single Pulse in Air (SPiA)
Laser Pulse Diameter	32 cm
Mirror Scan Rate	39 Hz
Field of View	30°
GPS Baselines	≤13 nm
GPS PDOP	≤3.0
GPS Satellite Constellation	≥6
Maximum Returns	Up to four per pulse
Intensity	8-bit
Resolution/Density	Average 8 pulses/m2

Leica ALS70 LiDAR sensor

All areas were surveyed with an opposing flight line side-lap of ≥56% (≥100% overlap) in order to reduce laser shadowing and increase surface laser painting. To accurately solve for laser point position (geographic coordinates x, y and z), the positional coordinates of the airborne sensor and the attitude of the aircraft were recorded continuously throughout the LiDAR data collection mission. Position of the aircraft was measured twice per second (2 Hz) by an onboard differential GPS unit, and aircraft attitude was measured 200 times per second (200 Hz) as pitch, roll and yaw (heading) from an onboard inertial measurement unit (IMU). To allow for post-processing correction and calibration, aircraft and sensor position and attitude data are indexed by GPS time.

View looking west at a regenerated clearcut on the north edge of the Woodward area of interest. The image was created from the gridded LiDAR surface colored by elevation and overlaid with the 3-D LiDAR point cloud.

LiDAR Data

Upon completion of data acquisition, QSI processing staff initiated a suite of automated and manual techniques to process the data into the requested deliverables. Processing tasks included GPS control computations, smoothed best estimate trajectory (SBET) calculations, kinematic corrections, calculation of laser point position, sensor and data calibration for optimal relative and absolute accuracy, and LiDAR point classification (Table 7). Processing methodologies were tailored for the landscape. Brief descriptions of these tasks are shown in Table 8.

Table 7: ASPRS LAS classification standards applied to the Idaho and Montana Forests dataset

Classification Number	Classification Name	Classification Description
1	Default/ Unclassified	Laser returns that are not included in the ground class, composed of vegetation and man-made structures
2	Ground	Laser returns that are determined to be ground using automated and manual cleaning algorithms
6	Buildings	Permanent structures
7	Noise	Identified by height from ground
11	Noise	Identified by intensity values of 0 or 255

Table 8: LiDAR processing workflow

Resolve kinematic corrections for aircraft position data using kinematic aircraft GPS and static ground GPS data. Develop a smoothed best estimate of trajectory (SBET) file that blends post-processed aircraft position with sensor head position and attitude recorded throughout the survey.	IPAS TC v.3.1 Waypoint Inertial Explorer v.8.5
Calculate laser point position by associating SBET position to each laser point return time, scan angle, intensity, etc. Create raw laser point cloud data for the entire survey in *.las (ASPRS v. 1.2) format. Convert data to orthometric elevations by applying a geoid correction.	ALS Post Processing Software v.2.75
Import raw laser points into manageable blocks (less than 500 MB) to perform manual relative accuracy calibration and filter erroneous points. Classify ground points for individual flight lines.	TerraScan v.15
Using ground classified points per each flight line, test the relative accuracy. Perform automated line-to-line calibrations for system attitude parameters (pitch, roll, heading), mirror flex (scale) and GPS/IMU drift. Calculate calibrations on ground classified points from paired flight lines and apply results to all points in a flight line. Use every flight line for relative accuracy calibration.	TerraMatch v.15
Classify resulting data to ground and other client designated ASPRS classifications (Table 7). Assess statistical absolute accuracy via direct comparisons of ground classified points to ground control survey data.	TerraScan v.15 TerraModeler v.15
Generate bare earth models as triangulated surfaces. Generate highest hit models as a surface expression of all classified points. Export all surface models as ESRI GRIDs in ERDAS Imagine (.img) format at a 3.0 foot 1 meter pixel resolution.	TerraScan v.15 TerraModeler v.15 ArcMap v. 10.1
Correct intensity values for variability and export intensity images as GeoTIFFs at a 1.5 foot 0.5 meter pixel resolution.	TerraScan v.15 TerraModeler v.15 ArcMap v. 10.2

Project area under snow

LiDAR Density

The acquisition parameters were designed to acquire an average first-return density of 8 points/m^2. First return density describes the density of pulses emitted from the laser that return at least one echo to the system. Multiple returns from a single pulse were not considered in first return density analysis. Some types of surfaces (e.g., breaks in terrain, water and steep slopes) may have returned fewer pulses than originally emitted by the laser. First returns typically reflect off the highest feature on the landscape within the footprint of the pulse. In forested or urban areas the highest feature could be a tree, building or power line, while in areas of unobstructed ground, the first return will be the only echo and represents the bare earth surface.

The density of ground-classified LiDAR returns was also analyzed for this project. Terrain character, land cover, and ground surface reflectivity all influenced the density of ground surface returns. In vegetated areas, fewer pulses may penetrate the canopy, resulting in lower ground density.

The average first-return density of LiDAR data for the final delivery of the 2015 Idaho and Montana Forests project was 17.01 points/m^2 and the average ground classified density was 1.46 points/m^2 (Table 9).

Table 9: Average LiDAR point densities

Classification	Point Density
First Return	1.46 points/ft^2
	17.01 points/m^2
Ground Classified	0.14 points/ft^2
	1.46 points/m^2

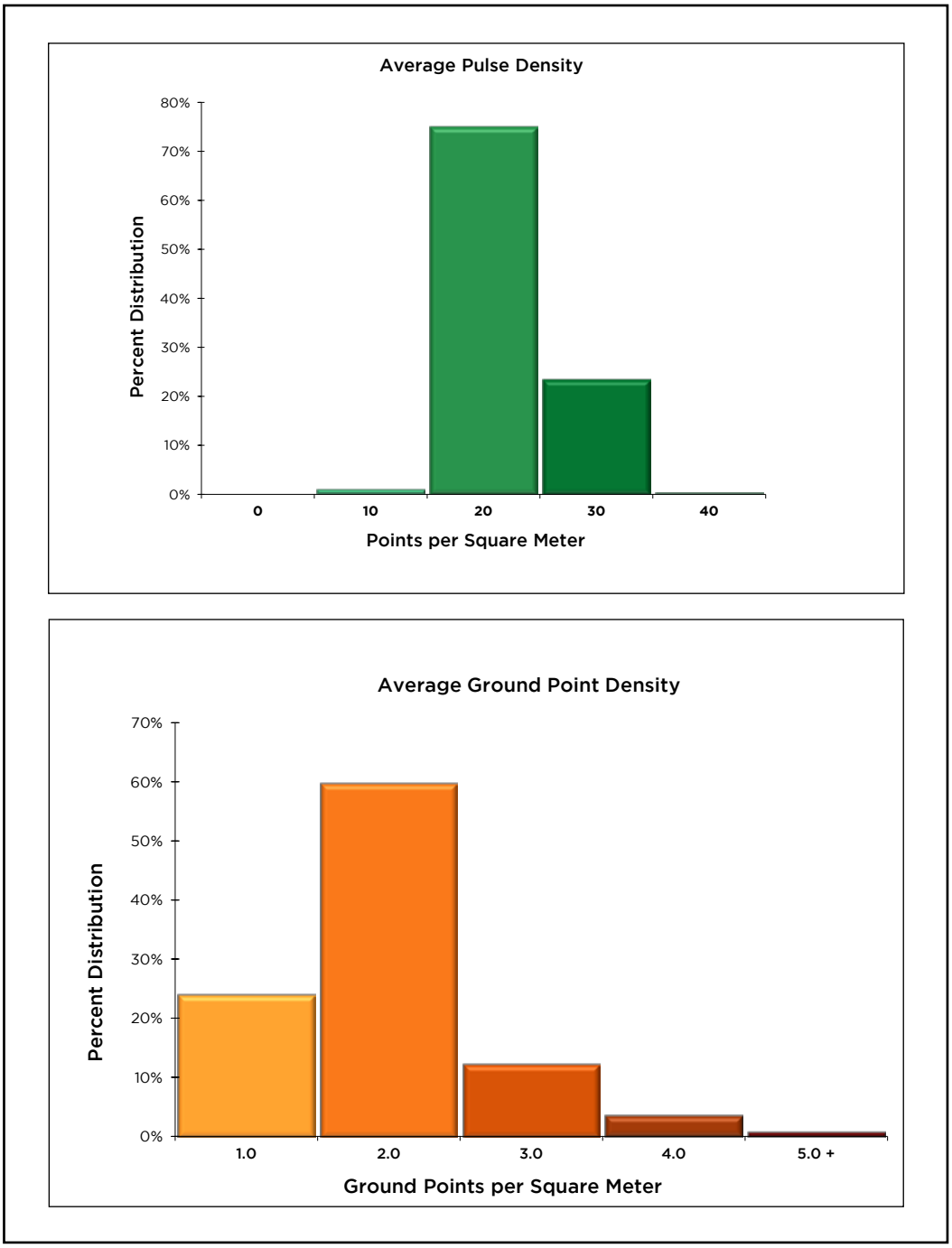

Figure 3: Frequency distribution of first return densities (above) and ground return densities (below).

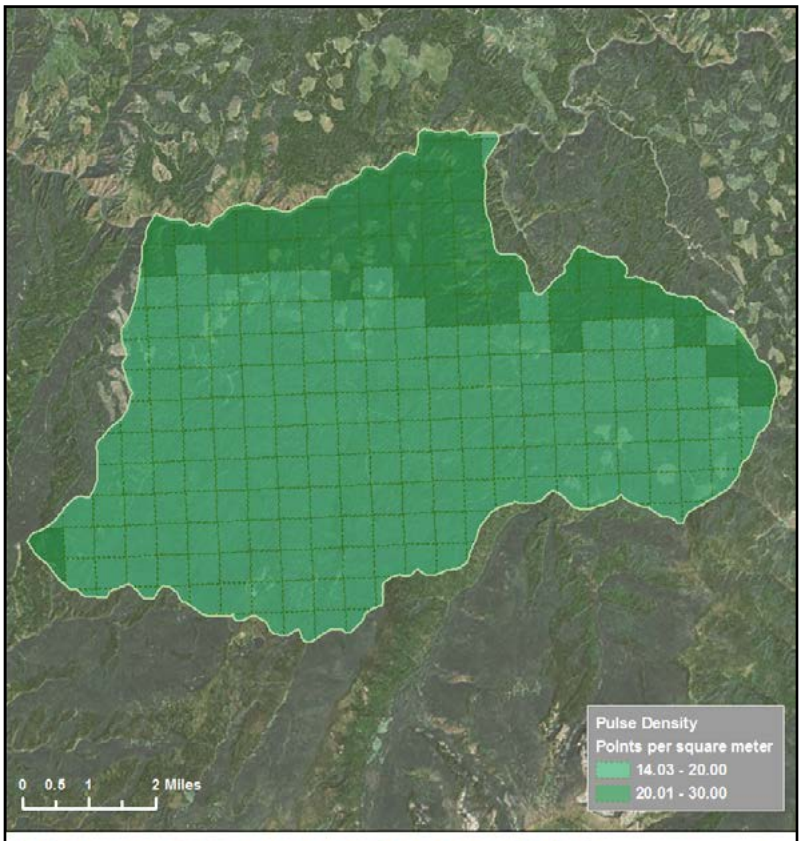

Idaho and Montana Forests 2015
Ten Twenty Mile Pulse Density

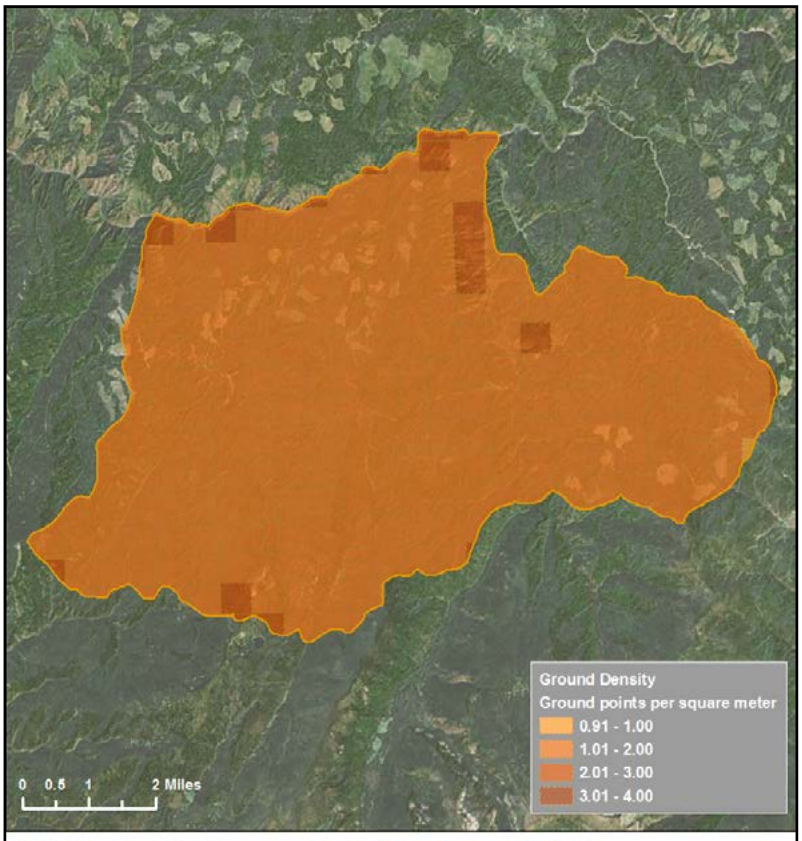

Idaho and Montana Forests 2015
Ten Twenty Mile Ground Density

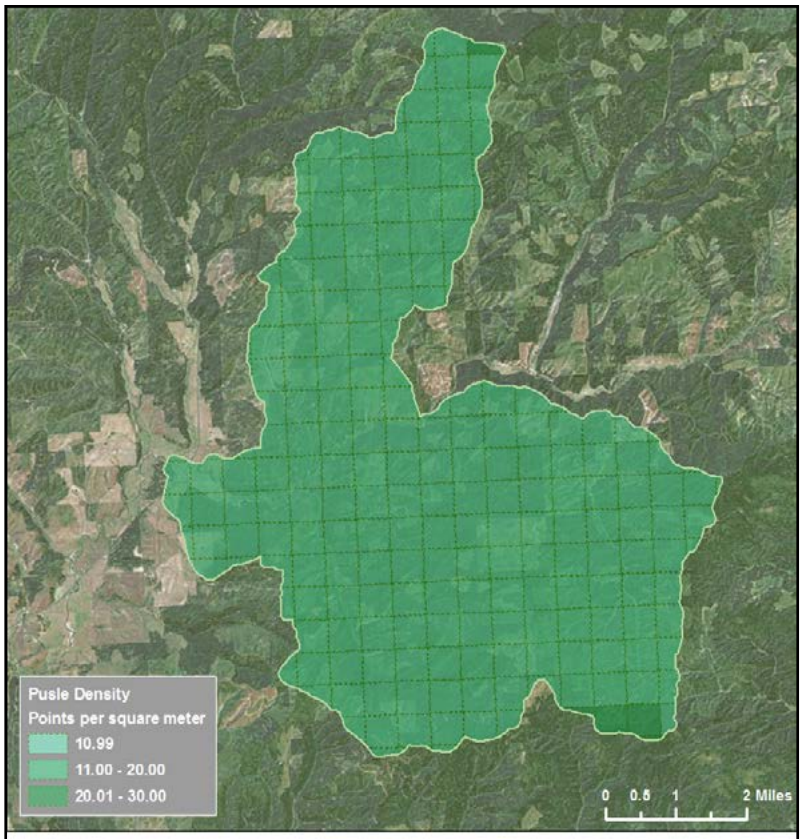

Idaho and Montana Forests 2015
Big Sand Creek Pulse Density

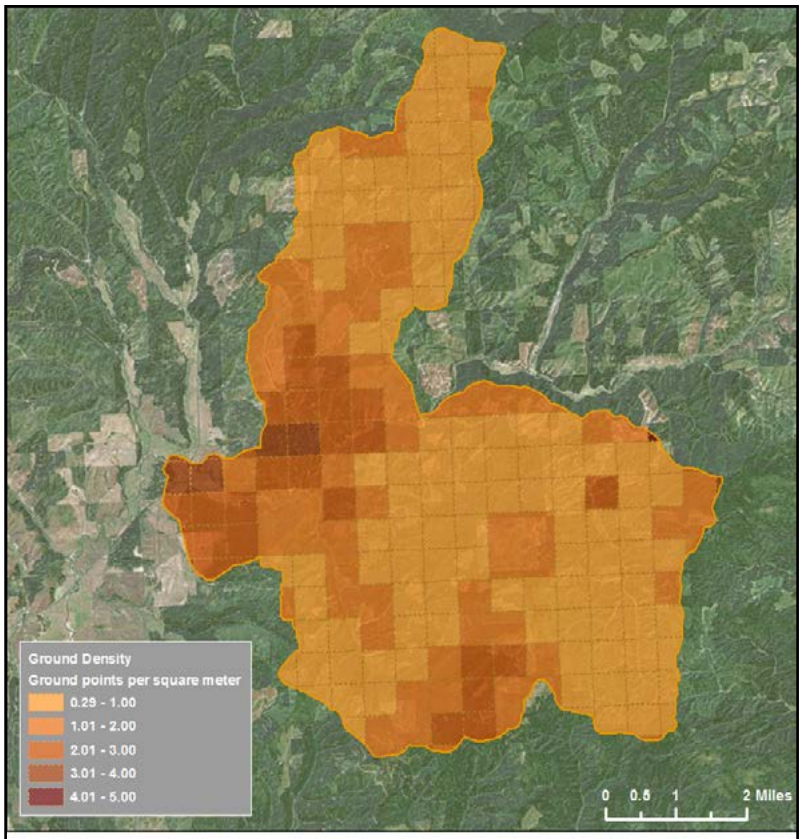

Idaho and Montana Forests 2015
Big Sand Creek Ground Density

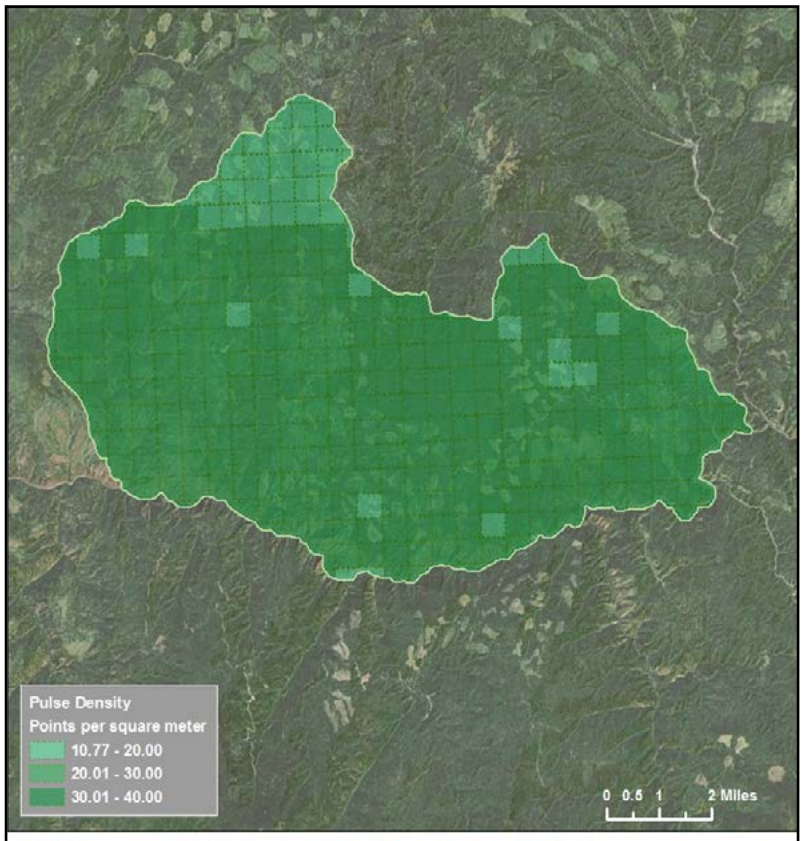

Idaho and Montana Forests 2015
Cougar Legett Pulse Density

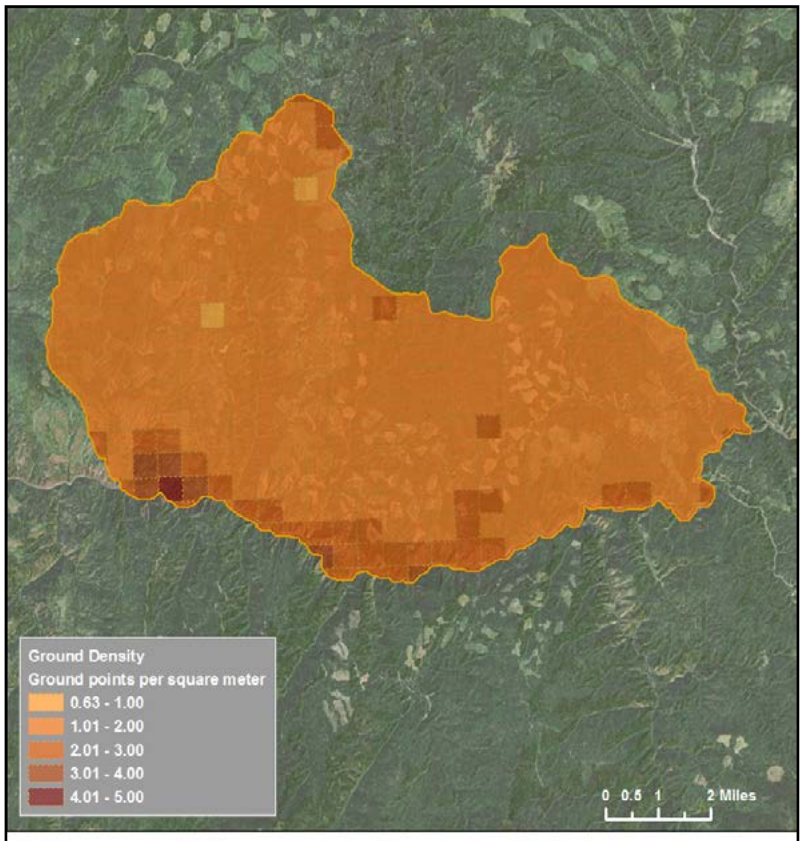

Idaho and Montana Forests 2015
Cougar Legett Ground Density

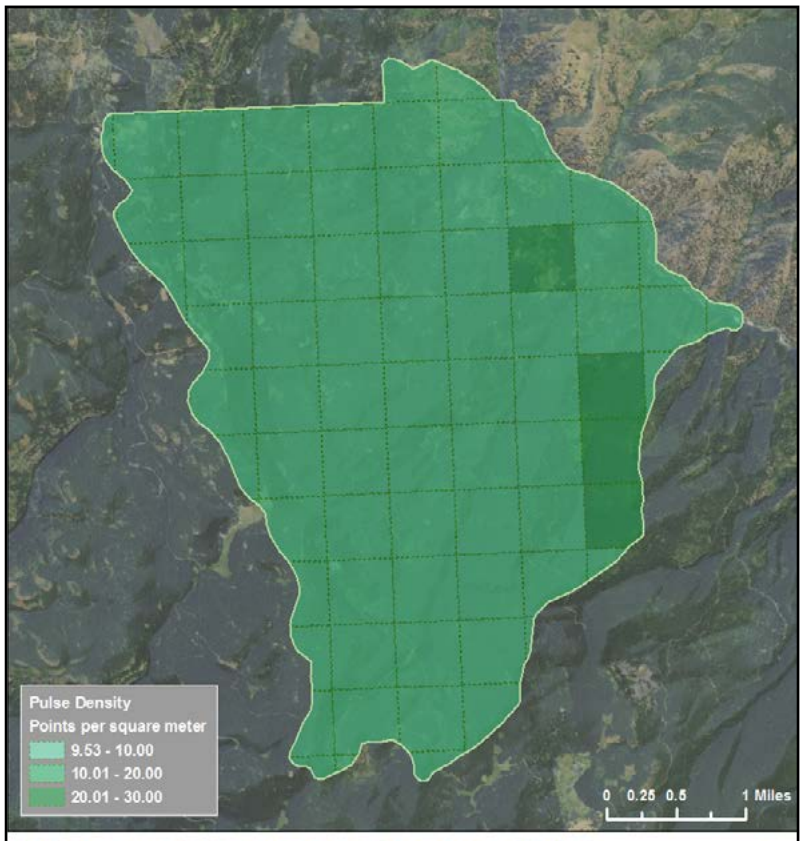

Idaho and Montana Forests 2015
Cove Restoration Pulse Density

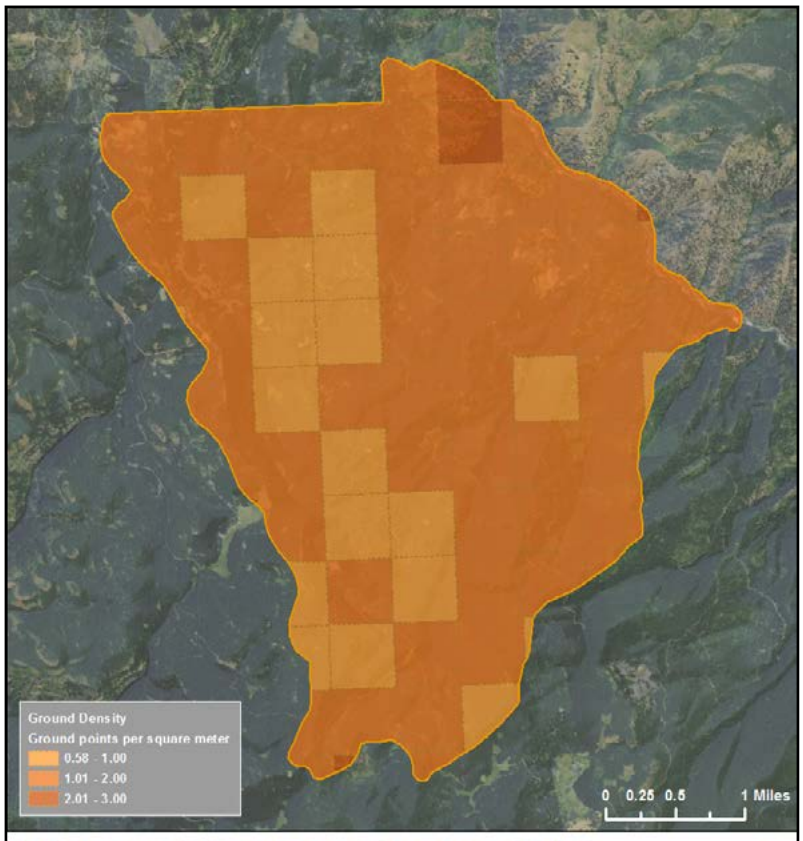

Idaho and Montana Forests 2015
Cove Restoration Ground Density

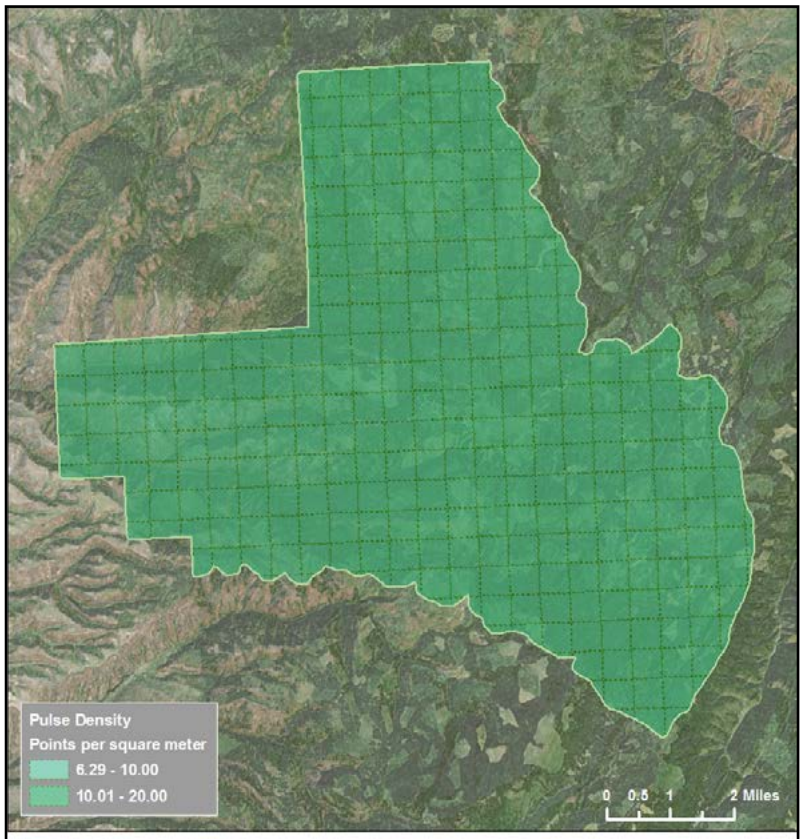

Idaho and Montana Forests 2015
Grangeville Pulse Density

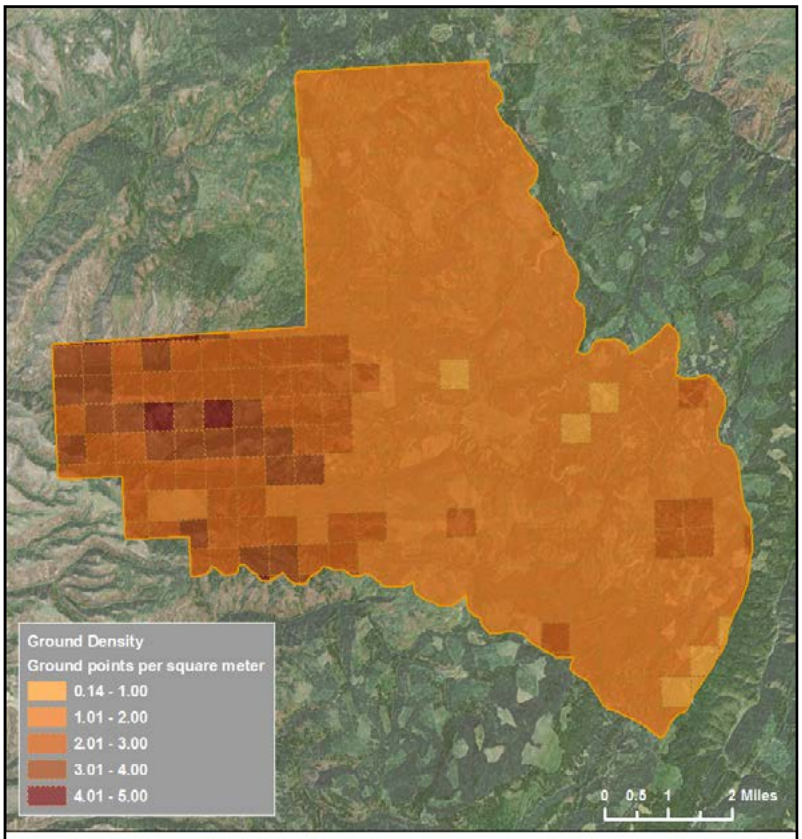

Idaho and Montana Forests 2015
Grangeville Ground Density

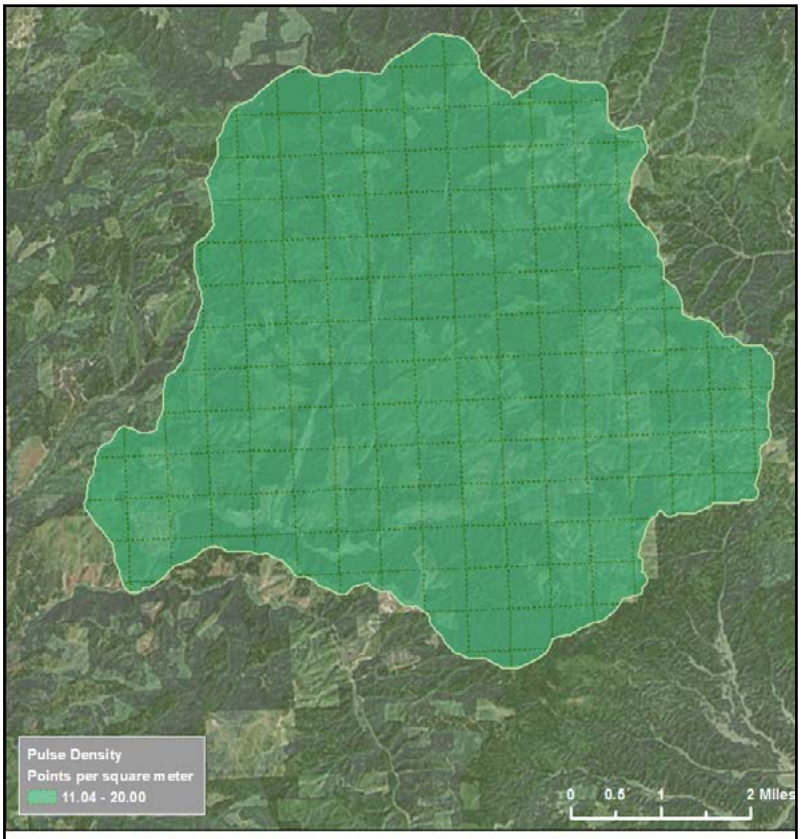

Idaho and Montana Forests 2015
Headwaters Palouse Pulse Density

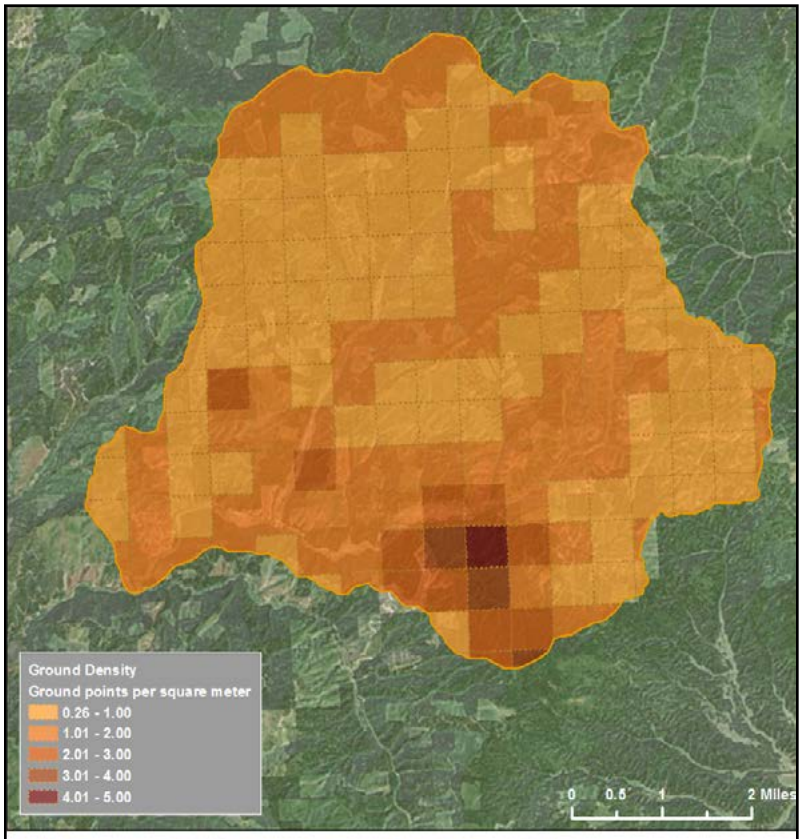

Idaho and Montana Forests 2015
Headwaters Palouse Ground Density

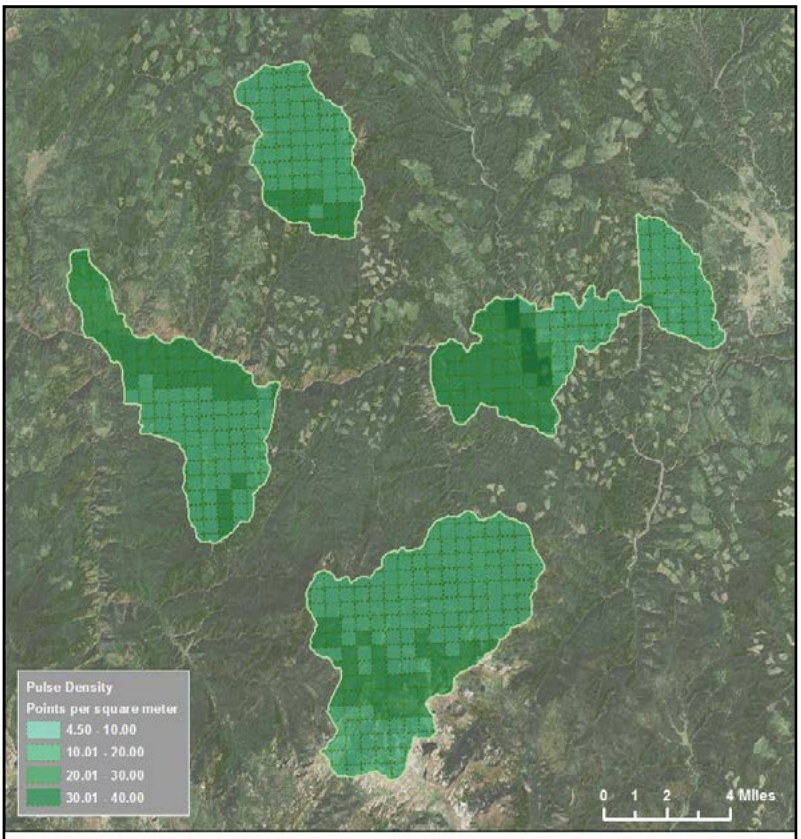

Idaho and Montana Forests 2015
HUC 10 Pulse Density

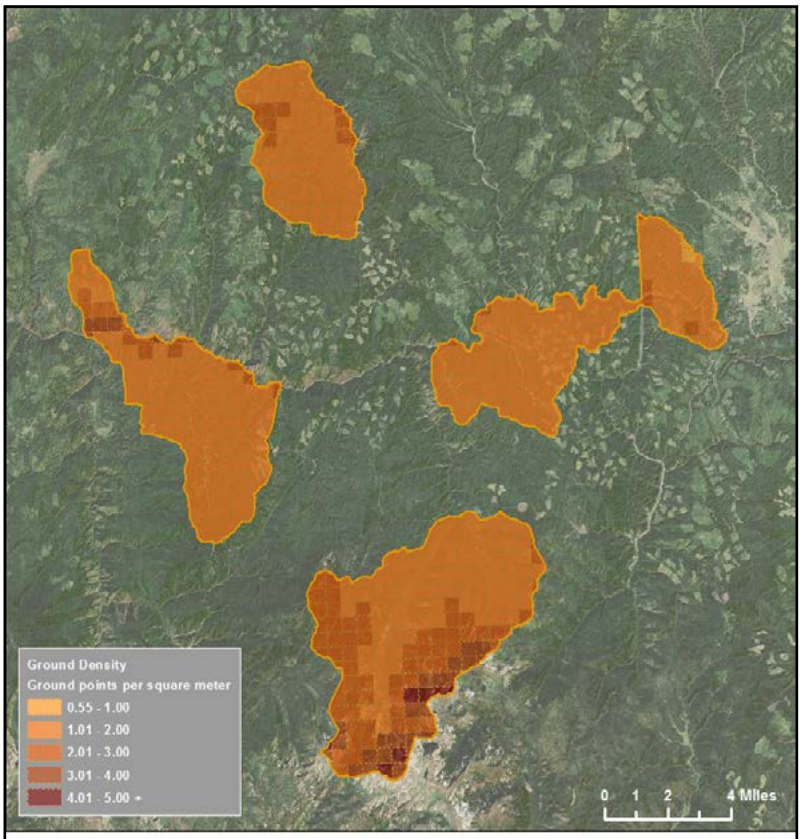

Idaho and Montana Forests 2015
HUC 10 Ground Density

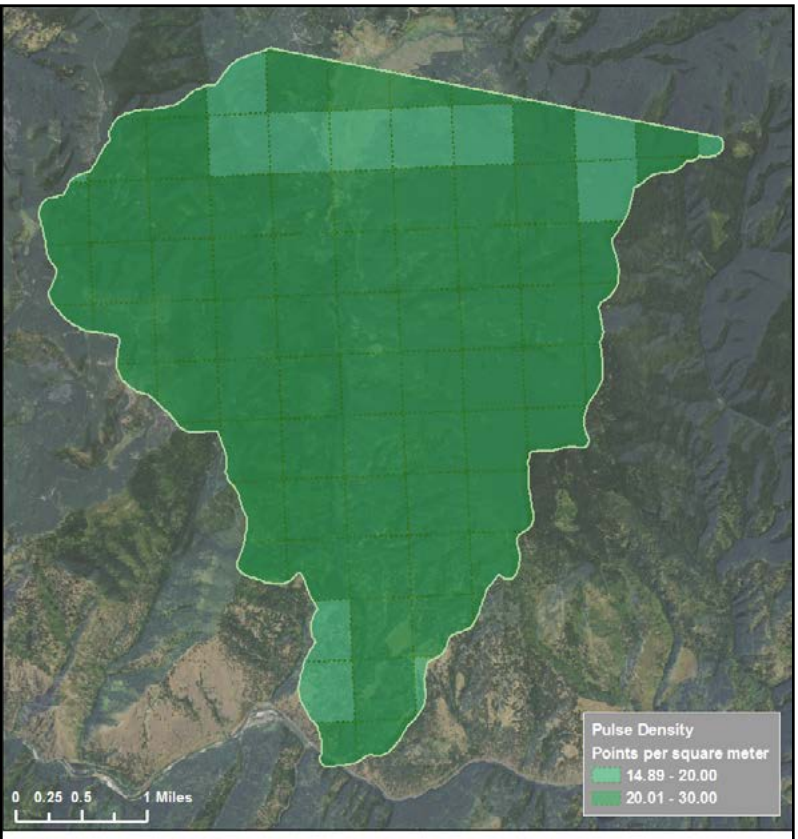

Idaho and Montana Forests 2015
Meadow Creek Addition Pulse Density

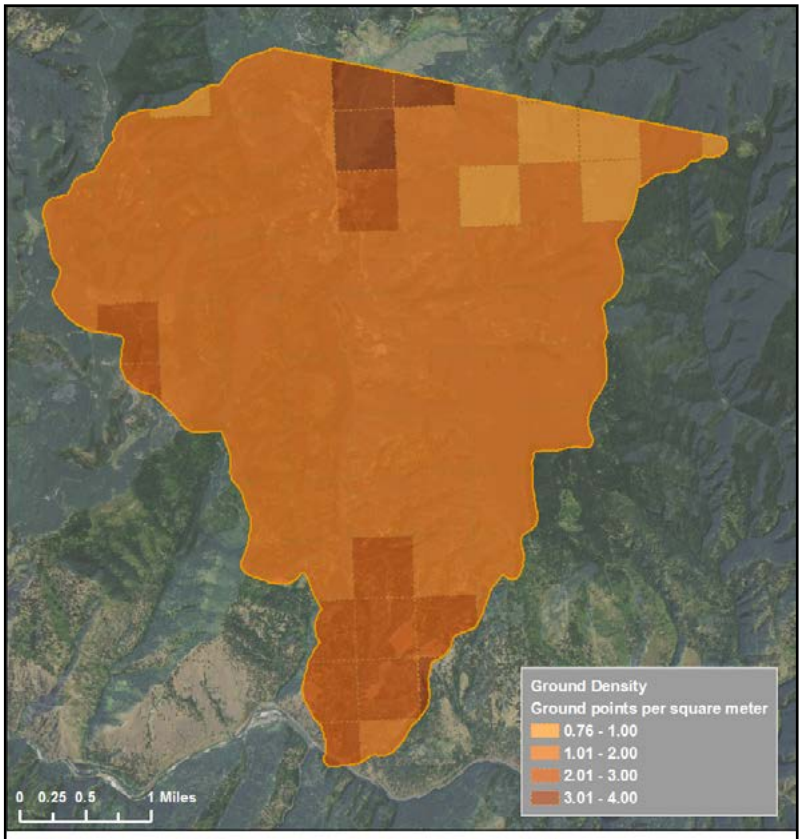

Idaho and Montana Forests 2015
Meadow Creek Addition Ground Density

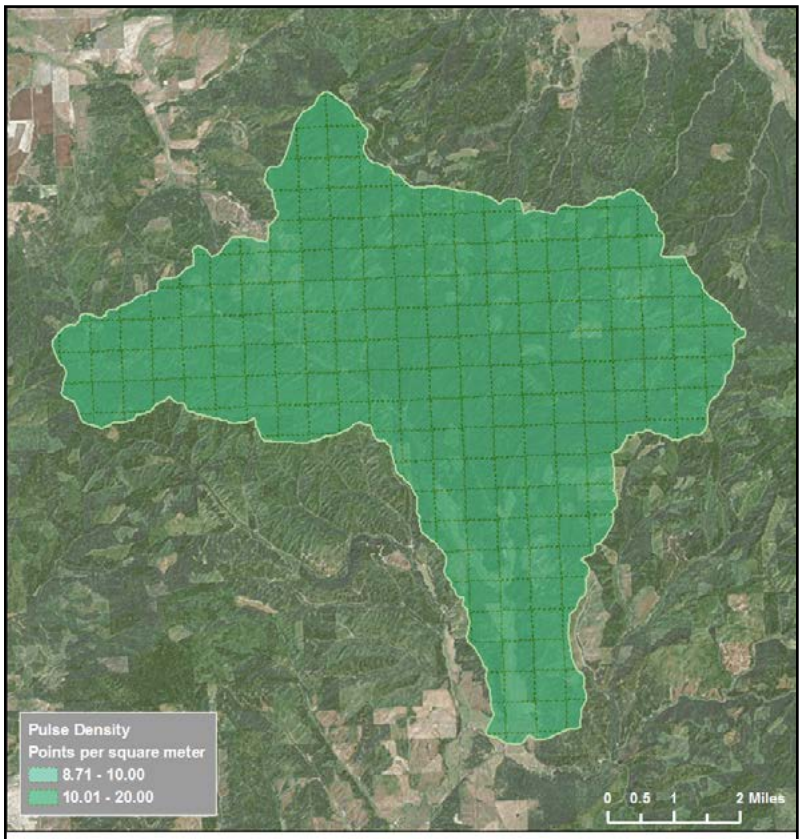

Idaho and Montana Forests 2015
Meadow Creek Pulse Density

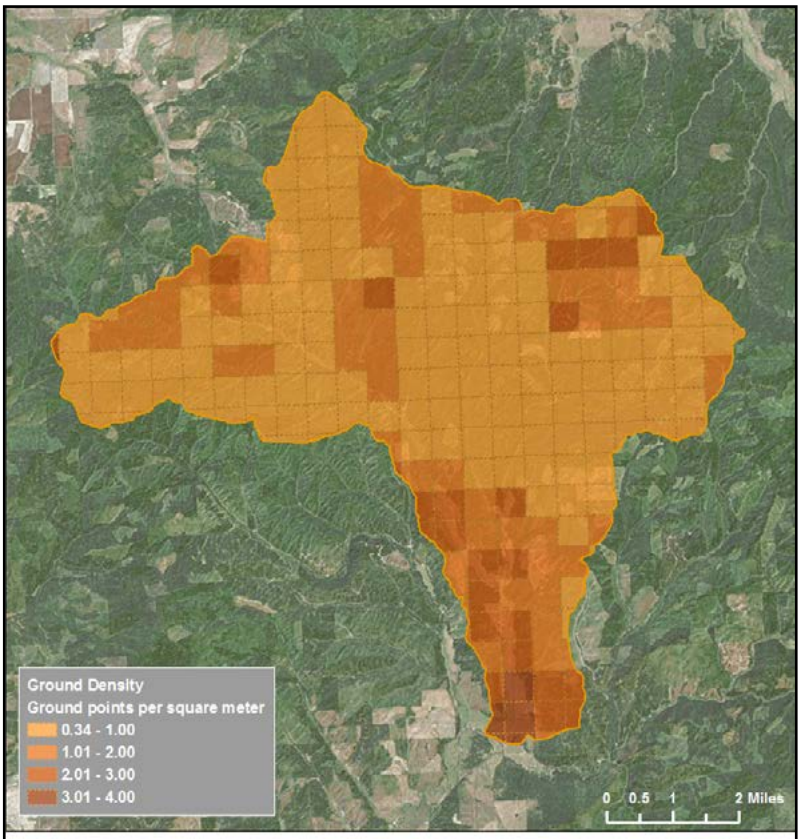

Idaho and Montana Forests 2015
Meadow Creek Ground Density

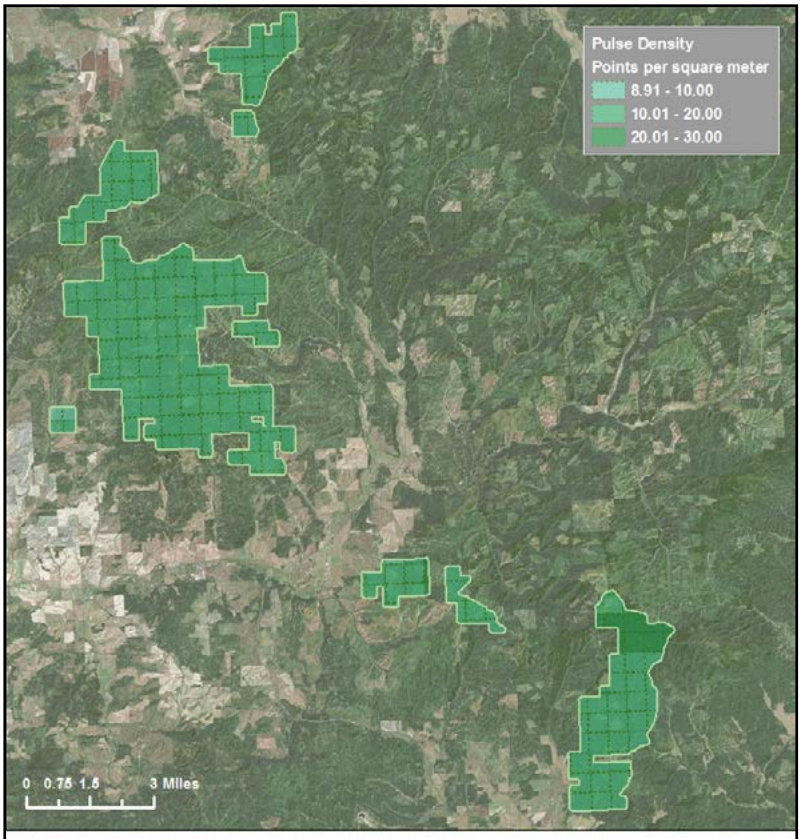

Idaho and Montana Forests 2015
Palouse Addition 1 Pulse Density

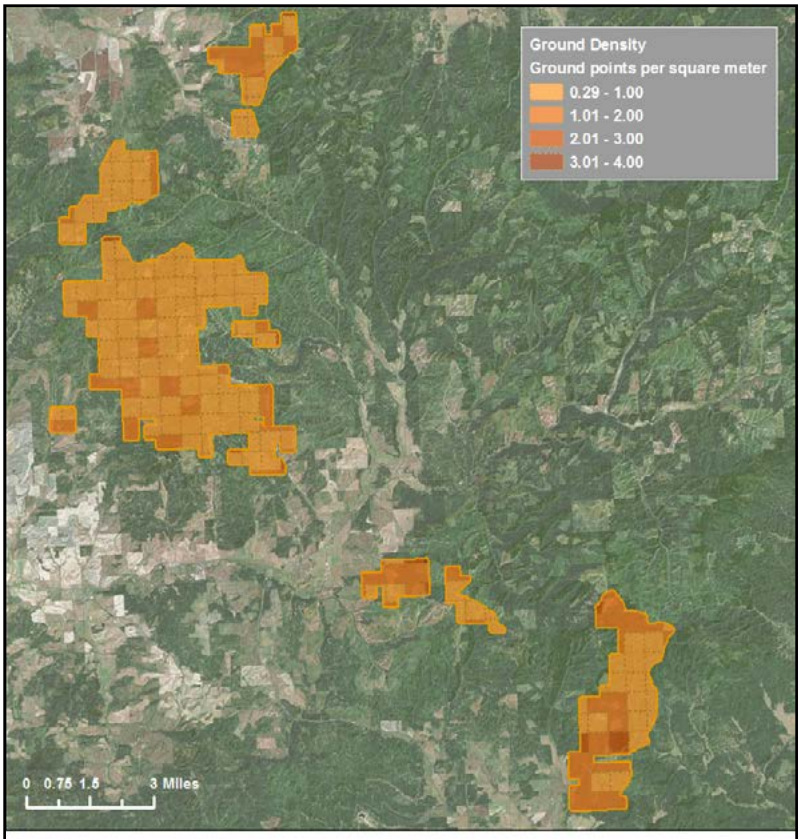

Idaho and Montana Forests 2015
Palouse Addition 1 Ground Density

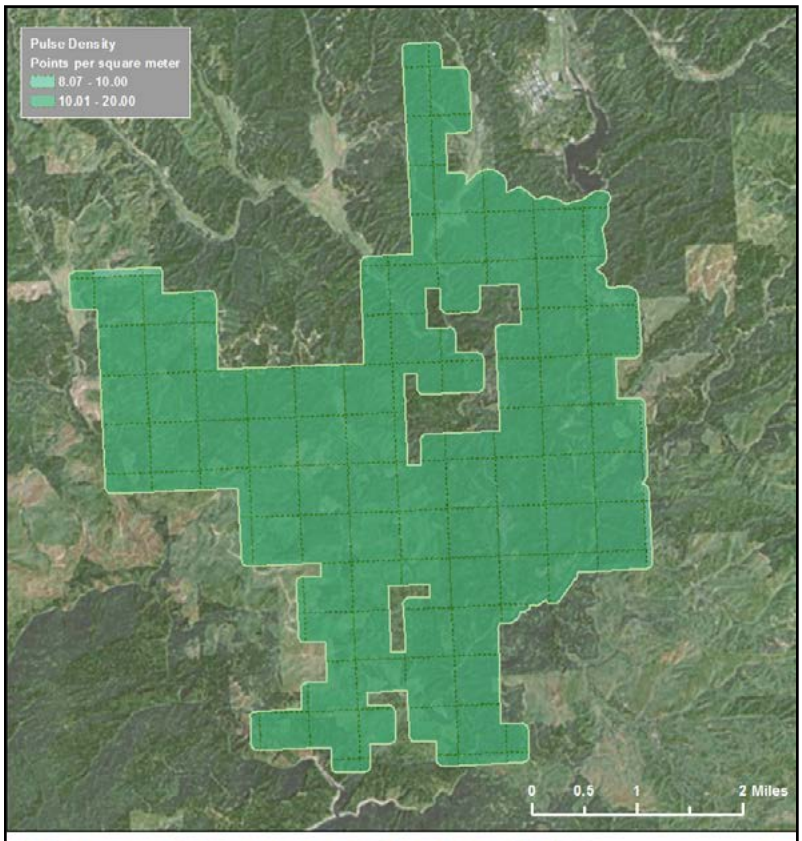

Idaho and Montana Forests 2015
Palouse Addition 2 Pulse Density

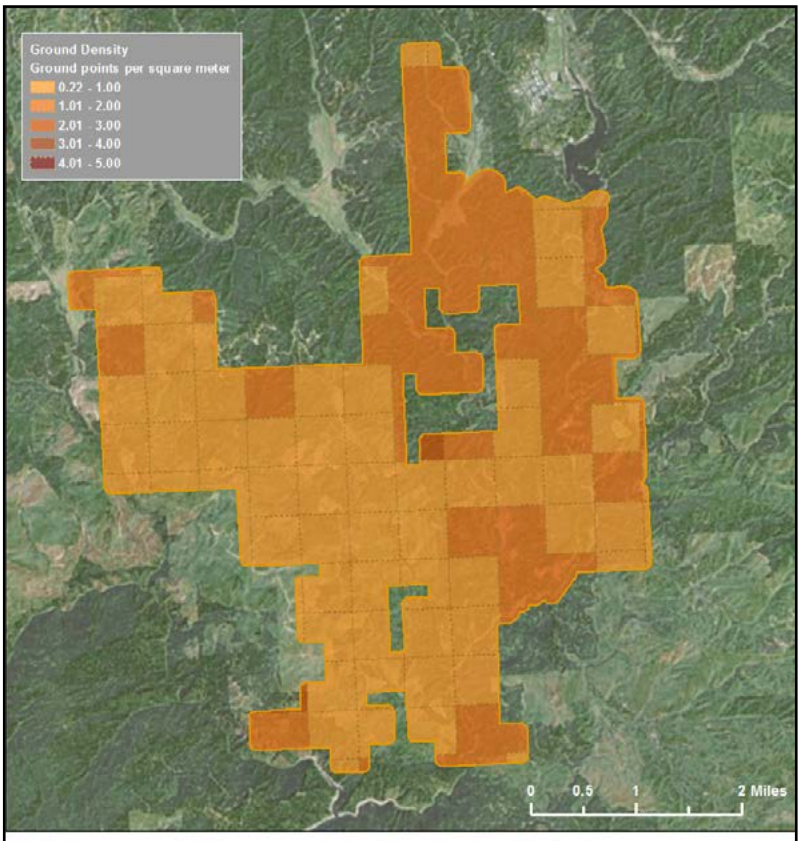

Idaho and Montana Forests 2015
Palouse Addition 2 Ground Density

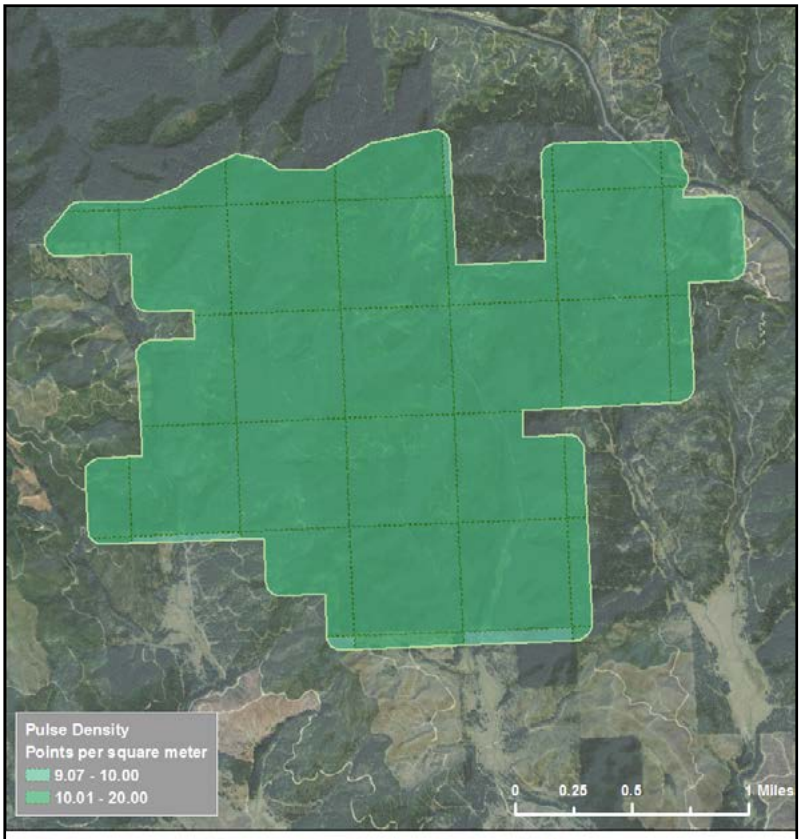

Idaho and Montana Forests 2015
Palouse Addition 3 Pulse Density

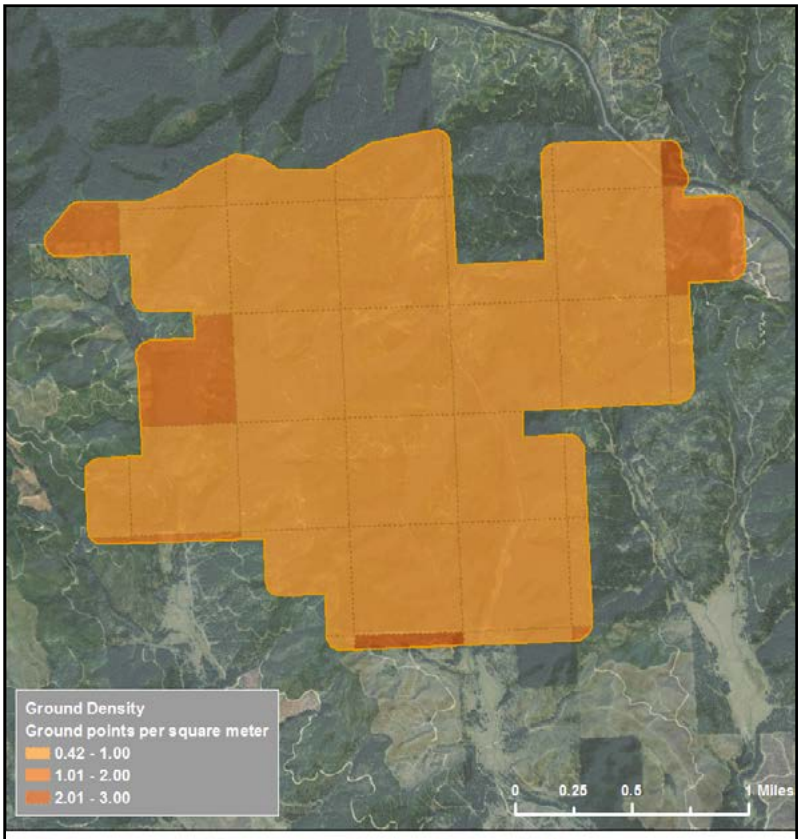

Idaho and Montana Forests 2015
Palouse Addition 3 Ground Density

LiDAR Accuracy Assessments

The accuracy of the LiDAR data collection can be described in terms of absolute accuracy (the consistency of the data with external data sources) and relative accuracy (the consistency of the dataset with itself). See Appendix A for further information on sources of error and operational measures used to improve relative accuracy.

LiDAR Absolute Accuracy

Absolute accuracy was assessed using Fundamental Vertical Accuracy (FVA) reporting designed to meet guidelines presented in the FGDC National Standard for Spatial Data Accuracy* . FVA compares known reserved RTK ground check point data collected on open, bare earth surfaces with level slope (<20°) to the triangulated surface generated by the LiDAR points. FVA is a measure of the accuracy of LiDAR point data in open areas where the LiDAR system has a high probability of measuring the ground surface and is evaluated at the 95% confidence interval (1.96 * RMSE), as shown in Table 10.

The mean and standard deviation (sigma σ) of divergence of the ground surface model from ground survey point coordinates are also considered during accuracy assessment. These statistics assume the error for x, y and z is normally distributed, and therefore the skew and kurtosis of distributions are also considered when evaluating error statistics. For the Idaho and Montana Forests survey, 2,983 ground survey points were collected in total resulting in an average accuracy of 0.026 meters (0.086 feet). An additional 158 check points were reserved for independent verification. Results for both absolute accuracy and the independent verification are located in Table 10 and Figure 4.

In addition to the hard surface land class, checkpoints were also collected across the project area for additional land cover classes (Table 11).

Table 10: Absolute Accuracy

	Absolute Accuracy	Independent Check Point Accuracy
Sample	2,983 points	158 points
FVA (1.96*RMSE)	N/A	0.061 m 0.199 ft.
Average	0.026 m 0.086 ft.	0.025 m 0.082 ft.
Median	-0.002 m -0.007 ft.	-0.010 m -0.033 ft.
RMSE	0.033 m 0.109 ft.	0.031 m 0.102 ft.
Standard Deviation (1σ)	0.031 m 0.102 ft.	0.030 m 0.098 ft.

Table 11: Land Class Accuracy

	Tall Grass	Short Grass	Shrubs	All Land Cover Classes
Sample	135 points	1,046 points	89 points	1,271 points
95th Percentile	0.098 m 0.322 ft.	0.103 m 0.338 ft.	0.185 m 0.606 ft.	0.113 m 0.371 ft.
Average	0.048 m 0.158 ft.	0.045 m 0.148 ft.	0.081 m 0.264 ft.	0.048 m 0.158 ft.
Median	0.041 m 0.135 ft.	0.036 m 0.118 ft.	0.069 m 0.226 ft.	0.039 m 0.128 ft.
RMSE	0.043 m 0.142 ft.	0.043 m 0.142 ft.	0.065 m 0.213 ft.	0.046 m 0.152 ft.
Standard Deviation (1σ)	0.056 m 0.184 ft.	0.056 m 0.184 ft.	0.099 m .0324 ft.	0.058 m 0.190 ft.

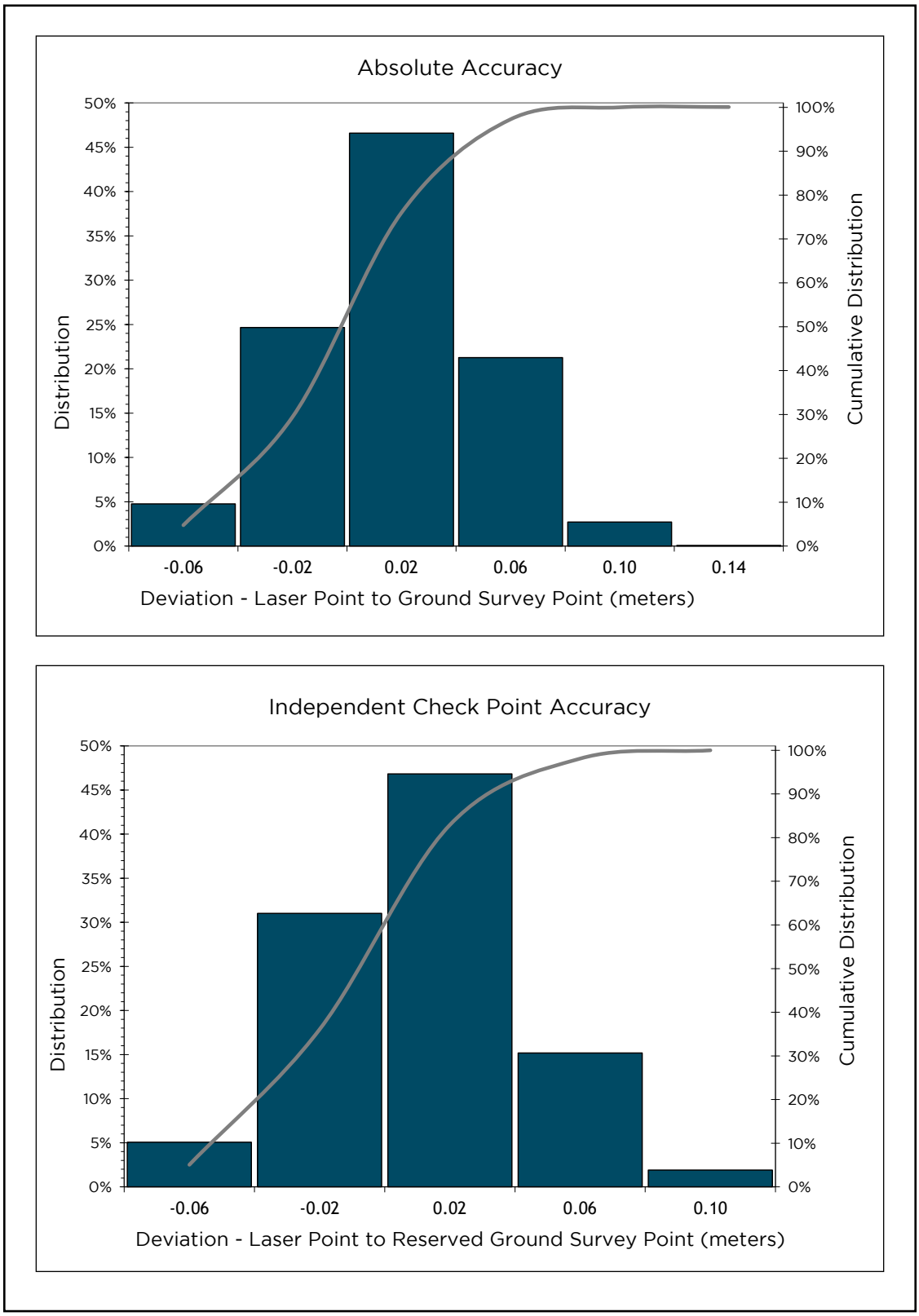

Figure 4: Frequency histograms for LiDAR surface deviation from ground survey point values (above) and for the independent check point verification (below)

LiDAR Relative Accuracy

Relative vertical accuracy refers to the internal consistency of the data set as a whole: the ability to place an object in the same location given multiple flight lines, GPS conditions, and aircraft attitudes. When the LiDAR system is well calibrated, the swath-to-swath vertical divergence is low (<0.10 meters). The relative vertical accuracy was computed by comparing the ground surface model of each individual flight line with its neighbors in overlapping regions. The average (mean) line to line relative vertical accuracy for the Idaho and Montana Forests LiDAR project was 0.061 meters (0.202 ft.) (Table 12, Figure 5).

Table 12: Relative accuracy

Relative Accuracy	
Sample	644 flightlines
Average	0.061 m
	0.202 ft.
Median	0.060 m
	0.196 ft.
Standard Deviation (1 σ)	0.063 m
	0.208 ft.

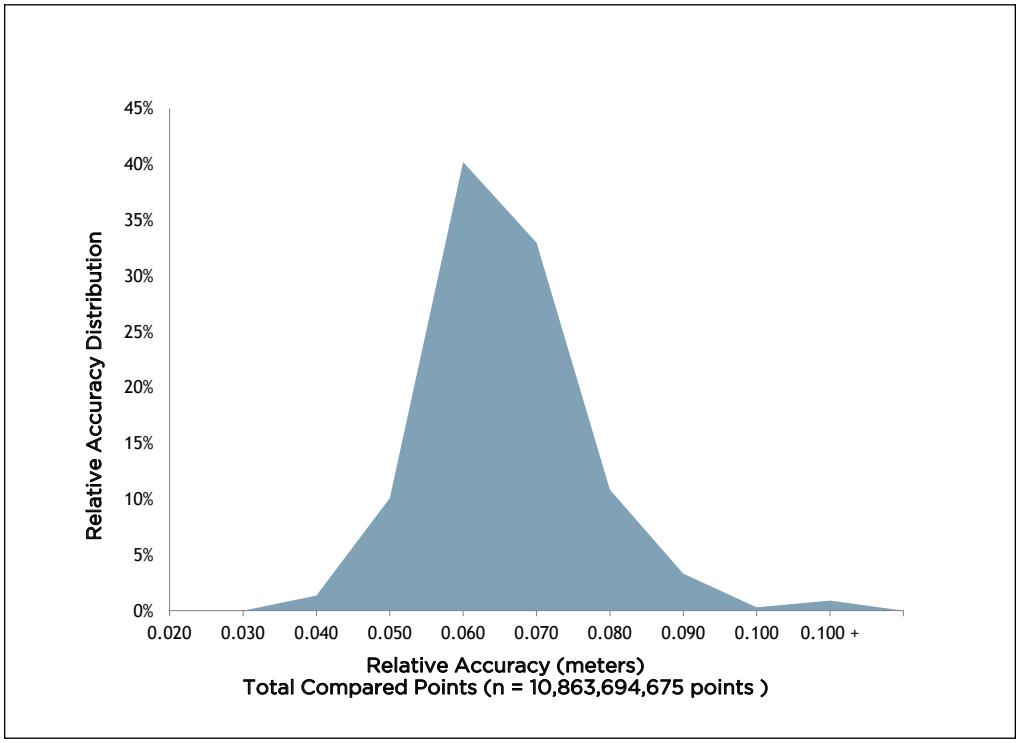

Figure 5: Frequency plot for relative vertical accuracy between flight lines.

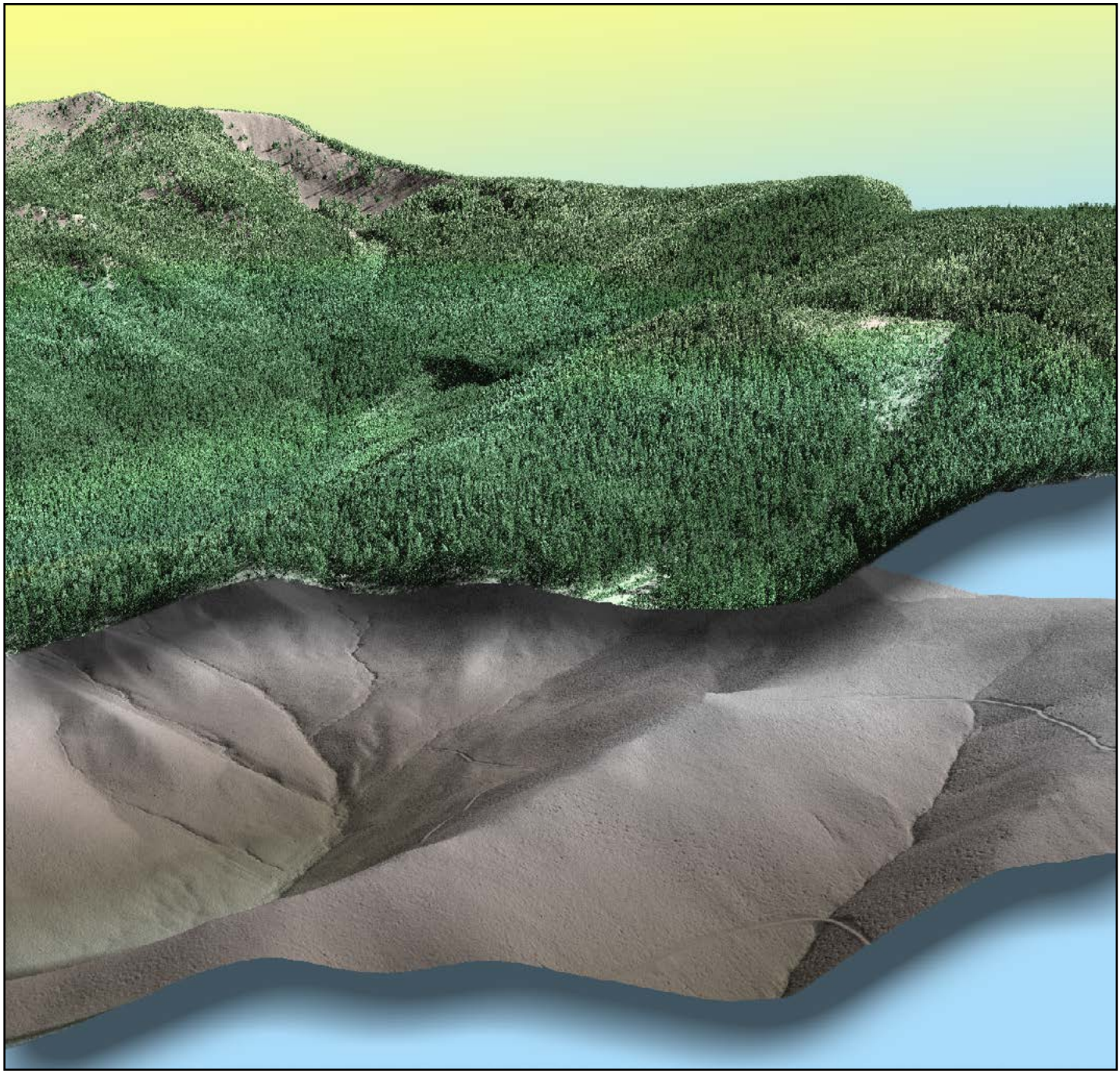

Figure 6: View looking west at Ovando Mountain in the North Lake area of interest in Montana. The images were created from the gridded LiDAR surface colored by elevation with the top image overlaid with the 3-D LiDAR point cloud.

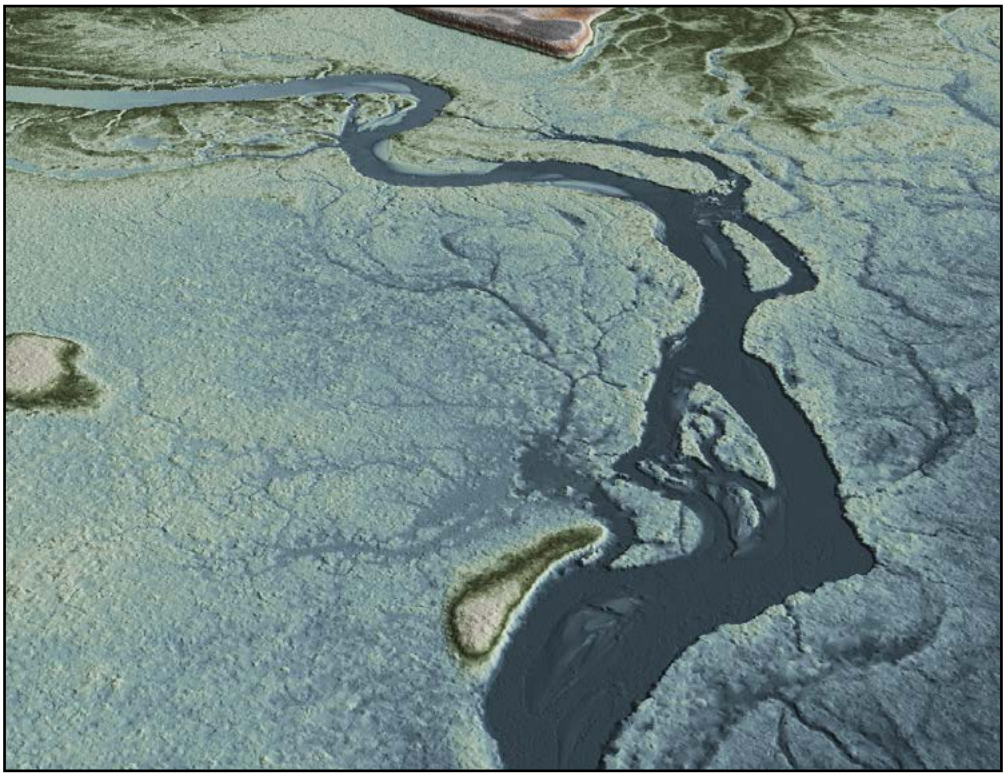

Figure 7: (Above) View looking south over the Swan River in the North Swan area of interest. The image was created from the gridded LiDAR surface colored by elevation.
(Below) View looking northeast over the Swan River in the North Swan area of interest. The image was created from the gridded LiDAR surface colored by elevation and overlaid with the 3-D LiDAR point cloud.

Glossary

1-sigma (σ) Absolute Deviation: Value for which the data are within one standard deviation (approximately 68th percentile) of a normally distributed data set.

1.96 * RMSE Absolute Deviation: Value for which the data are within two standard deviations (approximately 95th percentile) of a normally distributed data set, based on the FGDC standards for Fundamental Vertical Accuracy (FVA) reporting.

Accuracy: The statistical comparison between known (surveyed) points and laser points. Typically measured as the standard deviation (sigma σ) and root mean square error (RMSE).

Absolute Accuracy: The vertical accuracy of LiDAR data is described as the mean and standard deviation (sigma σ) of divergence of LiDAR point coordinates from ground survey point coordinates. To provide a sense of the model predictive power of the dataset, the root mean square error (RMSE) for vertical accuracy is also provided. These statistics assume the error distributions for x, y, and z are normally distributed, and thus the skew and kurtosis of distributions are also considered when evaluating error statistics.

Relative Accuracy: Relative accuracy refers to the internal consistency of the data set (i.e., the ability to place a laser point in the same location over multiple flight lines), GPS conditions, and aircraft attitudes. Affected by system attitude offsets, scale, and GPS/IMU drift, internal consistency is measured as the divergence between points from different flight lines within an overlapping area. Divergence is most apparent when flight lines are opposing. When the LiDAR system is well calibrated, the line-to-line divergence is low (<10 cm).

Root Mean Square Error (RMSE): A statistic used to approximate the difference between real-world points and the LiDAR points. It is calculated by squaring all the values, then taking the average of the squares and taking the square root of the average.

Data Density: A common measure of LiDAR resolution, measured as points per square meter.

Digital Elevation Model (DEM): File or database made from surveyed points, containing elevation points over a contiguous area. Digital terrain models (DTM) and digital surface models (DSM) are types of DEMs. DTMs consist solely of the bare earth surface (ground points), while DSMs include information about all surfaces, including vegetation and man-made structures.

Intensity Values: The peak power ratio of the laser return to the emitted laser, calculated as a function of surface reflectivity.

Nadir: A single point or locus of points on the surface of the earth directly below a sensor as it progresses along its flight line.

Overlap: The area shared between flight lines, typically measured in percent. 100% overlap is essential to ensure complete coverage and reduce laser shadows.

Pulse Rate (PR): The rate at which laser pulses are emitted from the sensor; typically measured in thousands of pulses per second (kHz).

Pulse Returns: For every laser pulse emitted, the number of wave forms (i.e., echos) reflected back to the sensor. Portions of the wave form that return first are the highest element in multi-tiered surfaces such as vegetation. Portions of the wave form that return last are the lowest element in multi-tiered surfaces.

Real-Time Kinematic (RTK) Survey: A type of surveying conducted with a GPS base station deployed over a known monument with a radio connection to a GPS rover. Both the base station and rover receive differential GPS data and the baseline correction is solved between the two. This type of ground survey is accurate to 1.5 cm or less.

Post-Processed Kinematic (PPK) Survey: GPS surveying is conducted with a GPS rover collecting concurrently with a GPS base station set up over a known monument. Differential corrections and precisions for the GNSS baselines are computed and applied after the fact during processing. This type of ground survey is accurate to 1.5 cm or less.

Scan Angle: The angle from nadir to the edge of the scan, measured in degrees. Laser point accuracy typically decreases as scan angles increase.

Native LiDAR Density: The number of pulses emitted by the LiDAR system, commonly expressed as pulses per square meter.

Appendix A - Accuracy Controls

Relative Accuracy Calibration Methodology:

Manual System Calibration: Calibration procedures for each mission require solving geometric relationships that relate measured swath-to-swath deviations to misalignments of system attitude parameters. Corrected scale, pitch, roll and heading offsets were calculated and applied to resolve misalignments. The raw divergence between lines was computed after the manual calibration was completed and reported for each survey area.

Automated Attitude Calibration: All data were tested and calibrated using TerraMatch automated sampling routines. Ground points were classified for each individual flight line and used for line-to-line testing. System misalignment offsets (pitch, roll and heading) and scale were solved for each individual mission and applied to respective mission datasets. The data from each mission were then blended when imported together to form the entire area of interest.

Automated Z Calibration: Ground points per line were used to calculate the vertical divergence between lines caused by vertical GPS drift. Automated Z calibration was the final step employed for relative accuracy calibration.

LiDAR accuracy error sources and solutions:

Type of Error	Source	Post Processing Solution
GPS (Static/Kinematic)	Long Base Lines	None
	Poor Satellite Constellation	None
	Poor Antenna Visibility	Reduce Visibility Mask
Relative Accuracy	Poor System Calibration	Recalibrate IMU and sensor offsets/settings
	Inaccurate System	None
Laser Noise	Poor Laser Timing	None
	Poor Laser Reception	None
	Poor Laser Power	None
	Irregular Laser Shape	None

Operational measures taken to improve relative accuracy:

Low Flight Altitude: Terrain following was employed to maintain a constant above ground level (AGL). Laser horizontal errors are a function of flight altitude above ground (about 1/3000th AGL flight altitude).

Focus Laser Power at narrow beam footprint: A laser return must be received by the system above a power threshold to accurately record a measurement. The strength of the laser return (i.e., intensity) is a function of laser emission power, laser footprint, flight altitude and the reflectivity of the target. While surface reflectivity cannot be controlled, laser power can be increased and low flight altitudes can be maintained.

Reduced Scan Angle: Edge-of-scan data can become inaccurate. The scan angle was reduced to a maximum of 312o from nadir, creating a narrow swath width and greatly reducing laser shadows from trees and buildings.

Quality GPS: Flights took place during optimal GPS conditions (e.g., 6 or more satellites and PDOP [Position Dilution of Precision] less than 3.0). Before each flight, the PDOP was determined for the survey day. During all flight times, a dual frequency DGPS base station recording at 1 second epochs was utilized and a maximum baseline length between the aircraft and the control points was less than 13 nm at all times.

Ground Survey: Ground survey point accuracy (<1.5 cm RMSE) occurs during optimal PDOP ranges and targets a minimal baseline distance of 4 miles between GPS rover and base. Robust statistics are, in part, a function of sample size (n) and distribution. Ground survey points are distributed to the extent possible throughout multiple flight lines and across the survey area.

50% Side-Lap (100% Overlap): Overlapping areas are optimized for relative accuracy testing. Laser shadowing is minimized to help increase target acquisition from multiple scan angles. Ideally, with a 50% side-lap, the nadir portion of one flight line coincides with the swath edge portion of overlapping flight lines. A minimum of 50% side-lap with terrain-followed acquisition prevents data gaps.

Opposing Flight Lines: All overlapping flight lines have opposing directions. Pitch, roll and heading errors are amplified by a factor of two relative to the adjacent flight line(s), making misalignments easier to detect and resolve.

September 29, 2015

USFS Idaho and Montana Forests LiDAR 2015

Block 1

Technical Data Report

Ken Marshall
USDA Forest Service
Nez Perce-Clearwater National Forests
12730 Hwy 12
Orofino, ID 83544-9333

QSI Environmental
517 SW 2nd St., Suite 400
Corvallis, OR 97333
PH: 541-752-1204

Cover Photo: A view of Little Salmon River Canyon, Idaho.

Table of Contents

Introduction 1
Planning 4
Acquisition 4
Ground Control 5
Airborne Survey 9
LiDAR 9
LiDAR Data 10
Processing 10
LiDAR Density 12
Results and Discussion 12
LiDAR Accuracy Assessments 19
LiDAR Absolute Accuracy 19
LiDAR Relative Accuracy 21
Selected Images 22
Glossary 24
Appendix A - Accuracy Controls 26
Appendix B - 2014 Data Report 28

Introduction

Little Salmon River near Riggins, Idaho.

WSI, a Quantum Spatial company (QSI), was contracted by the USDA Forest Service (USFS) to collect Light Detection and Ranging (LiDAR) data in the fall of 2014 for the Idaho and Montana Forests project. Data were collected to aid the USFS in assessing the topographic properties of the study area to support resource management.

This report accompanies the delivered LiDAR data and products for Block 1 of the 2015 USFS Idaho and Montana Forests project. Contract specifications, data acquisition procedures, processing methods, and analysis of the final dataset including LiDAR accuracy and density are included in delivery. A complete list of contracted deliverables provided to the USFS is shown in Table 1, acquisition dates and acreage are shown in Table 2 and the project extent is shown in Figure 1.

Table 1: Products delivered to the USFS Idaho and Montana Forests 2015 project area for Block 1.

Idaho and Montana Forests Products Projection: UTM Zones 11 North and 12 North Horizontal Datum: NAD83 (CORS96) Vertical Datum: NAVD88 (GEOID03) Units: Meters	
Points	LAS v 1.2 • All Returns • Ground Returns
Rasters	1.0 Meter ESRI Grids • Bare Earth DEM • Canopy Height DEM 0.5 Meter GeoTiffs • Intensity Images
Vectors	Shapefiles (*.shp) • Site Boundary • LiDAR Tile Index • DEM Tile Index • Ground Survey Shapes • Survey Monuments • Ground Check Points • Land Class Points • Quality Assurance Points

Table 2: Acquisition dates, acreage, and delivery dates for Idaho and Montana Forests project areas

Delivery Block	UTM	AOI	Contracted Acres	Buffered Acres	Acquisition Date(s)	Delivery Date
1	11	Cool Mush	33,938.3	35,386.3	6/13/2015 - 6/15/2015, 6/18/2015	9/29/15
	11	Lower Lochsa	6,637.2	7,311.3	6/21/2015	
	11	Riggins West Island	77,738.2	81,373.3	6/16/2015, 6/19/2015 - 6/21/2015	
	11	TePee Potter Creek	29,003.5	30,427.1	5/24/2015 - 5/26/2015, 5/29/2015	
	12	Stonewall	37,421.2	39,454	6/22/2015 - 6/24/2015	

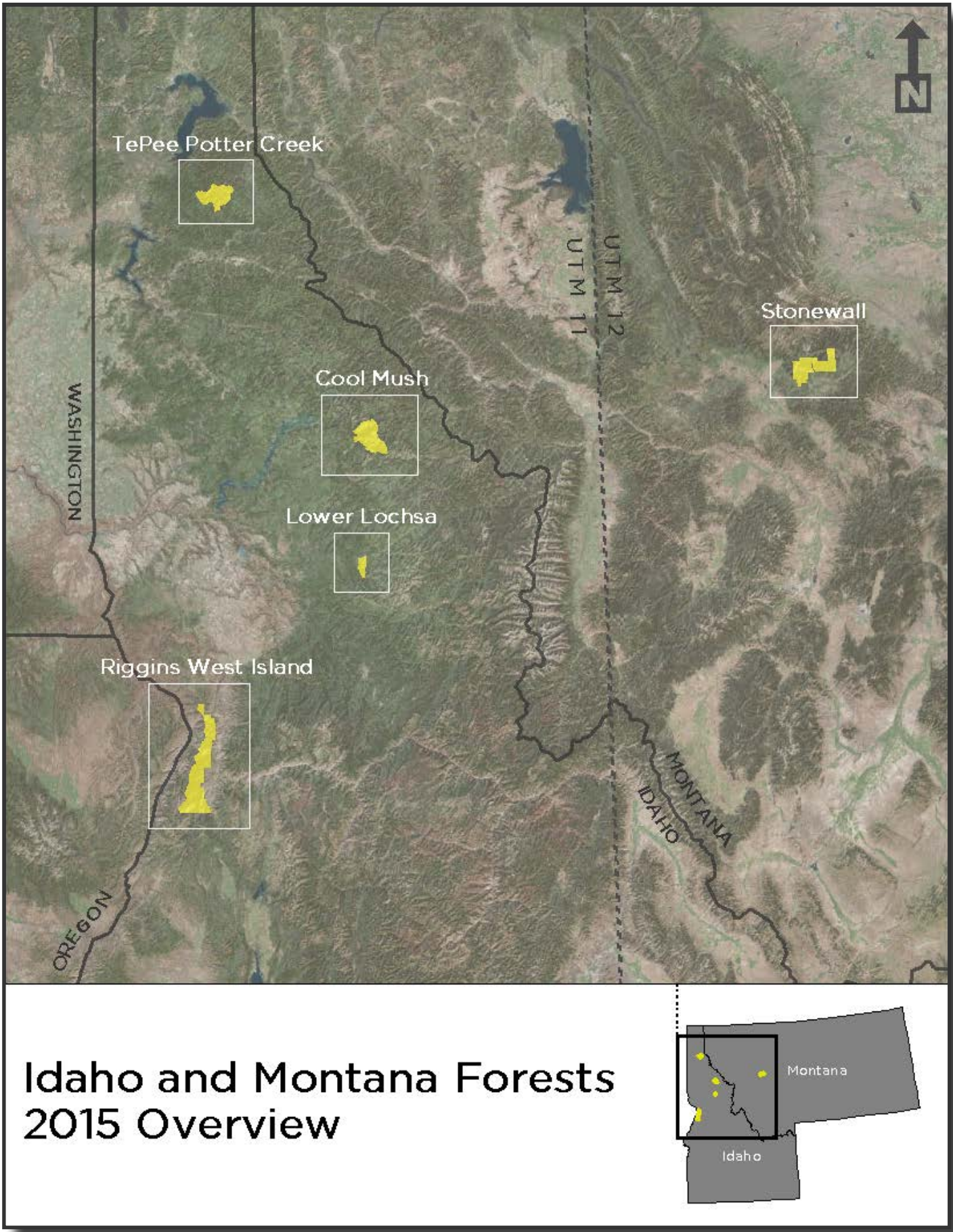

Figure 1: Location map of 2015 Idaho and Montana Forests

Acquisition

QSI Cessna 208-B Grand Caravan

Planning

In preparation for data collection, QSI reviewed the project area and developed a specialized flight plan to ensure complete coverage of the Idaho and Montana LiDAR study area at the target point density of ≥8.0 points/m^2 (0.74 points/ft^2). Acquisition parameters including orientation relative to terrain, flight altitude, pulse rate, scan angle, and ground speed were adapted to optimize flight paths and flight times while meeting all contract specifications.

Factors such as satellite constellation availability and weather windows must be considered during the planning stage. Any weather hazards or conditions affecting the flight were continuously monitored due to their potential impact on the daily success of airborne and ground operations. In addition, logistical considerations including private property access and potential air space restrictions were reviewed.

Ground Control

Ground control surveys, including monumentation, aerial targets and ground survey points (GSPs), were conducted to support the airborne acquisition. Ground control data were used to geospatially correct the aircraft positional coordinate data and to perform quality assurance checks on final LiDAR data and orthoimagery products.

QSI-Established Monument

Monumentation

The spatial configuration of ground survey monuments provided redundant control within 13 nautical miles of the mission areas for LiDAR flights. Monuments were also used for collection of ground survey points using the real time kinematic (RTK) survey technique.

Monument locations were selected with consideration for satellite visibility, field crew safety, and optimal location for GSP coverage. QSI utilized 17 existing monuments and established 43 monuments for the Idaho and Montana Forests LiDAR project (Table 3, Figure 2). New monumentation was set using 5/8" x 30" rebar topped with stamped 2" aluminum caps.

To correct the continuously recorded onboard measurements of the aircraft position, QSI concurrently conducted multiple static Global Navigation Satellite System (GNSS) ground surveys (1 Hz recording frequency) over each monument. During post-processing, the static GPS data were triangulated with nearby Continuously Operating Reference Stations (CORS) using the Online Positioning User Service (OPUS*) for precise positioning. Multiple independent sessions over the same monument were processed to confirm antenna height measurements and to refine position accuracy.

Table 3: Monuments established for the Idaho and Montana Forests acquisition. Coordinates are on the NAD83 (CORS96) datum, epoch 2002.00. Geoid03 was used to establish orthometric heights.

UTM Zone	Monument ID	Latitude	Longitude	Ellipse	NAVD88 Height (meters)
11	DUTCH_01	N45°49'45.26290"	W115°36'10.35256"	1204.157	1219.586
11	DUTCH_02	N45°49'04.40532"	W115°27'25.95805"	1184.307	1199.613
11	ELK_01A	N46°47'28.03198"	W116°10'26.76338"	844.749	861.749
11	ELK_01B	N46°47'26.96376"	W116°10'26.31241"	845.398	862.398
11	ID_MT_FOR_01	N46°17'22.58039"	W115°28'10.51282"	1593.435	1609.501
11	ID_MT_FOR_02	N46°18'52.77536"	W115°25'27.32450"	1591.161	1607.184
11	ID_MT_FOR_03	N46°50'29.54312"	W115°25'41.56738"	1422.701	1438.543
11	ID_MT_FOR_04	N46°51'25.68990"	W115°22'08.56449"	1407.036	1422.739
11	ID_MT_FOR_05	N46°44'49.01540"	W115°19'06.78184"	1391.325	1406.924
11	ID_MT_FOR_06	N46°47'19.19859"	W115°26'14.13932"	1203.404	1219.311
11	ID_MT_FOR_07	N45°50'25.67201"	W116°04'43.89199"	1510.339	1526.230
11	ID_MT_FOR_08	N45°45'54.82620"	W116°05'37.63340"	1625.654	1641.378
11	ID_MT_FOR_09	N45°22'56.30848"	W116°27'09.23563"	1920.629	1935.886
11	ID_MT_FOR_10	N45°20'49.47449"	W116°29'31.58828"	2245.68	2260.817
11	IDMT_1A	N47°50'18.42046"	W116°15'17.98418"	899.617	916.284
11	IDMT_1B (SV0057)	N47°50'18.24062"	W116°15'16.93899"	899.767	916.433

* OPUS is a free service provided by the National Geodetic Survey to process corrected monument positions. http://www.ngs.noaa.gov/OPUS.

Table 3 cont'd: Monuments established for the Idaho and Montana Forests acquisition. Coordinates are on the NAD83 (CORS96) datum, epoch 2002.00. Geoid03 was used to establish orthometric heights.

UTM Zone	Monument ID	Latitude	Longitude	Ellipse	NAVD88 Height (meters)
11	IDMT_2A	N46°57'27.12561"	W116°40'06.18645"	787.818	805.595
11	IDMT_2B	N46°57'28.08788"	W116°40'06.25244"	787.466	805.242
11	IDMT_5A	N45°32'00.80369"	W116°20'41.82002"	939.974	955.616
11	IDMT_5B	N45°32'01.16174"	W116°20'42.70169"	939.980	955.621
11	IDMT_5C	N45°32'54.30483"	W116°24'36.58737"	1582.283	1597.879
11	IDMT_7A	N45°50'21.72930"	W115°41'14.47764"	1634.779	1650.308
11	IDMT_7B	N45°49'53.60076"	W115°41'54.41542"	1687.737	1703.268
11	IDMT_9A	N45°44'57.02027"	W115°42'14.93166"	1773.361	1788.658
11	IDMT_9B	N45°44'56.75974"	W115°42'14.53746"	1773.187	1788.483
11	IDNP	N45°56'22.93594"	W116°07'16.53072"	997.096	1013.322
11	LOLO	N46°45'46.24714"	W114°05'48.67315"	1109.860	1124.614
11	LWST	N46°22'23.42428"	W117°00'08.24812"	427.607	445.852
11	P023	N44°53'54.34204"	W116°06'10.76576"	1522.130	1537.060
11	P025	N48°43'51.63137"	W116°17'14.98404"	695.902	712.342
11	P372	N45°25'41.27722"	W117°15'05.91188"	1208.817	1224.945
11	P422	N46°47'52.29765"	W116°58'46.80446"	844.199	862.601
11	RIG_01	N45°20'26.05061"	W116°23'05.08261"	1192.416	1207.805
11	RIG_02	N45°18'37.38776"	W116°22'58.98879"	1242.471	1257.785
11	RIG_03	N45°32'55.16792"	W116°24'36.66711"	1583.564	1599.162
11	SPN6	N47°31'06.10734"	W117°25'24.00164"	720.997	739.314
12	AI7923	N47°21'50.97066"	W113°35'58.61712"	1243.997	1257.895
12	AI7923-B	N47°21'51.31615"	W113°35'53.28186"	1242.297	1256.192
12	IDMT_11A	N47°52'42.03773"	W113°47'51.73762"	1000.579	1015.440
12	IDMT_11B	N47°52'45.60200"	W113°47'56.03164"	999.058	1013.924
12	IDMT_13A	N47°35'29.44346"	W113°45'20.86851"	1066.545	1081.086
12	IDMT_13B	N47°35'26.21433"	W113°45'19.28065"	1067.183	1081.722
12	IDMT_16A	N47°20'41.09926"	W113°31'20.21364"	1882.270	1895.933
12	IDMT_16B	N47°20'41.88195"	W113°31'22.51814"	1879.058	1892.724
12	IDMT_17A	N47°09'20.06465"	W113°19'00.36234"	1484.274	1497.813
12	IDMT_17B	N47°09'18.66519"	W113°19'02.82768"	1499.362	1512.904
12	IDMT_17C	N47°09'20.13816"	W113°19'00.26068"	1484.236	1497.775
12	IDMT_19A	N47°07'17.61634"	W112°59'10.39571"	1742.360	1755.295
12	IDMT_19B	N47°07'18.91084"	W112°59'10.79992"	1741.331	1754.265
12	IDMT_23A	N46°51'00.57362"	W112°43'21.63439"	1928.477	1941.441
12	IDMT_23B	N46°51'01.16231"	W112°43'21.76271"	1927.876	1940.841
12	IDMT_25A	N46°57'18.62103"	W112°30'30.38888"	1791.196	1803.960
12	IDMT_25B	N46°57'18.77823"	W112°30'28.94686"	1784.119	1796.880
12	MSOL	N46°55'45.83748"	W114°06'31.84582"	960.622	975.562
12	MTDT	N46°35'18.59106"	W111°59'36.96383"	1217.751	1230.826
12	MTFV	N48°13'38.89075"	W114°19'36.54418"	905.677	921.802
12	P046	N47°01'46.52350"	W113°19'54.18626"	1290.837	1304.661
12	PLS5	N47°39'49.55360"	W114°06'50.07818"	974.604	990.000
12	RX0477	N46°56'23.78108"	W112°40'06.70709"	1374.622	1387.584
12	RX0477B	N46°56'24.95725"	W112°40'06.69684"	1374.287	1387.249

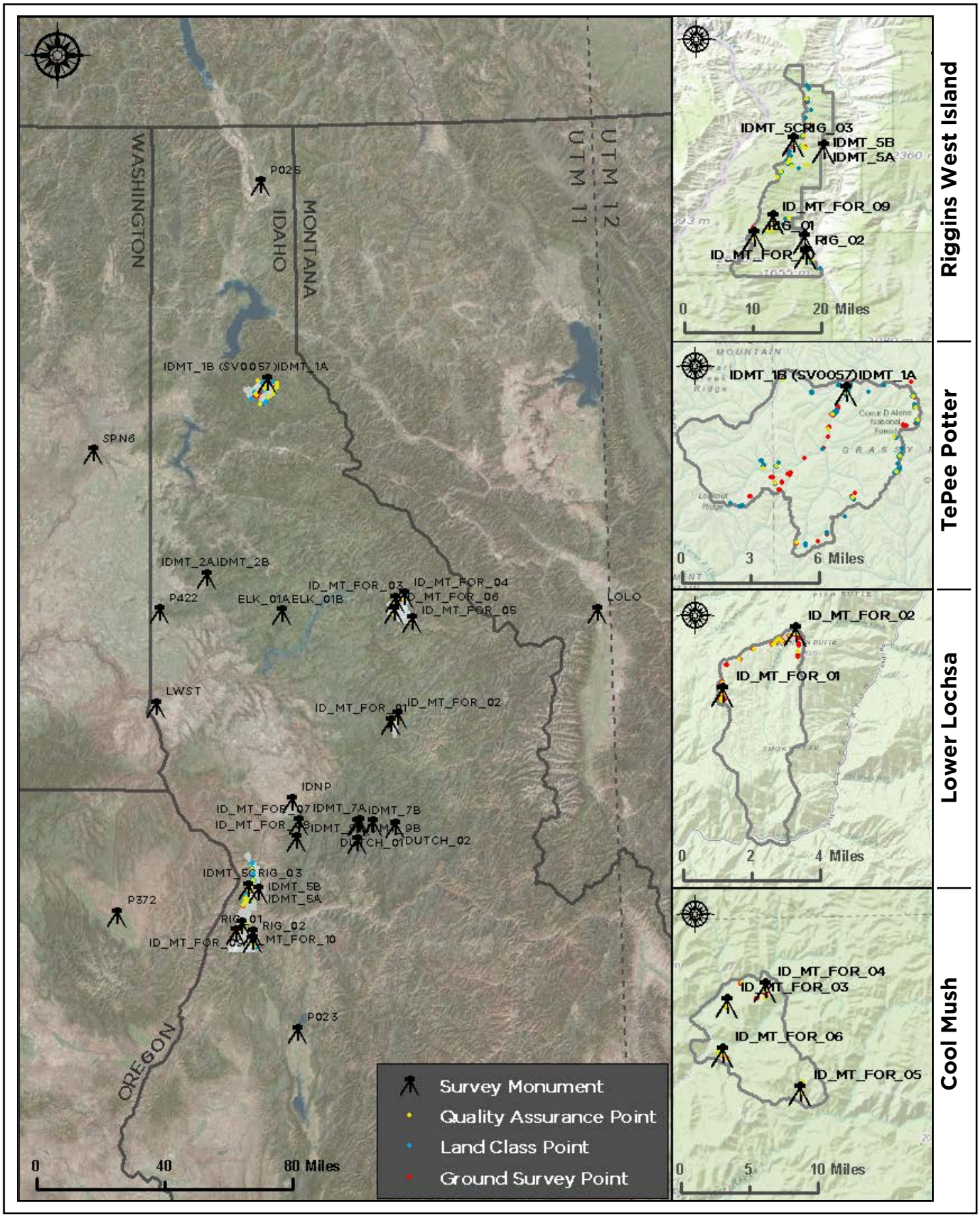

Figure 2a: Ground control location map for UTM 11

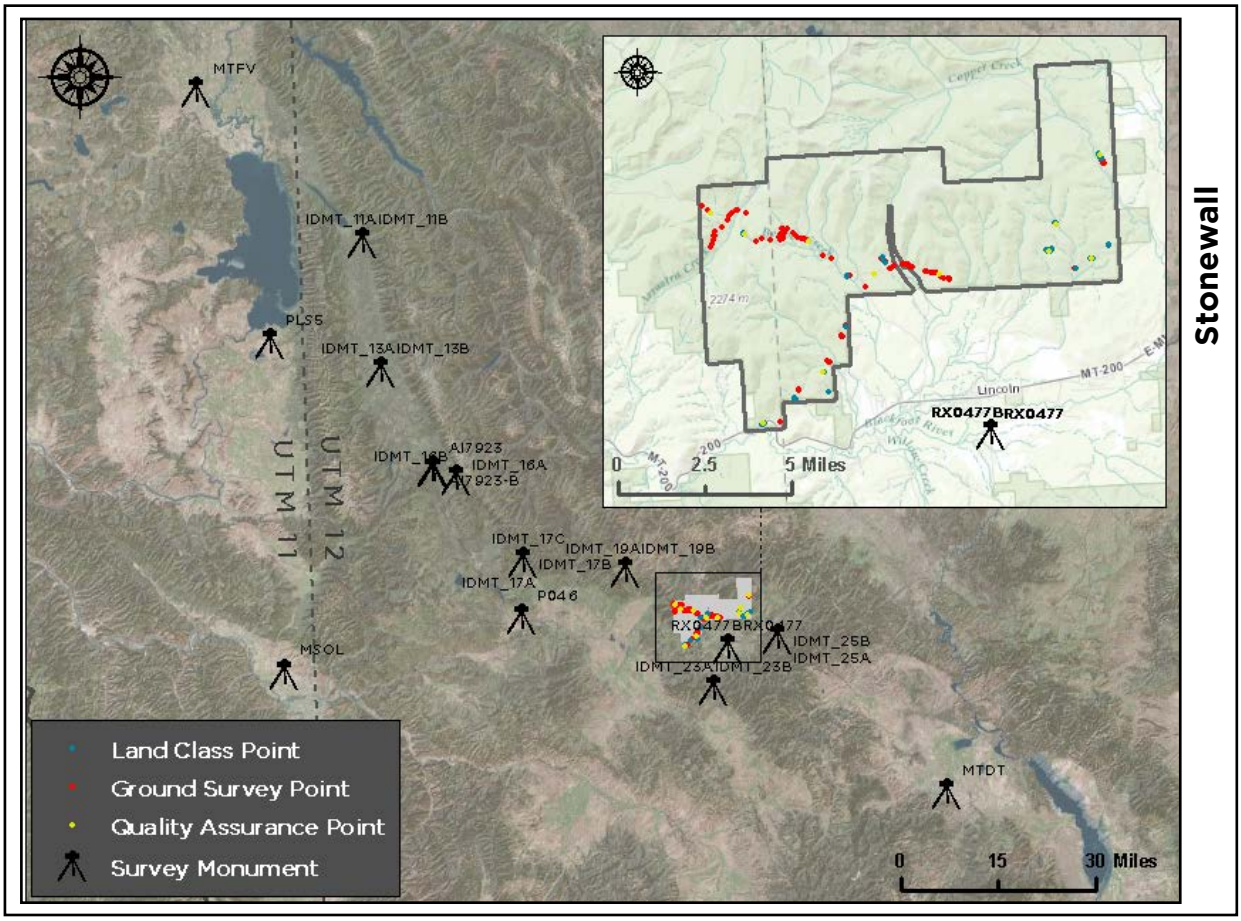

Figure 2b: Ground control location map for UTM 12

Ground Survey Points (GSPs)

Ground survey points were collected using real time kinematic, roving Trimble R6 or R8 survey techniques. A Trimble R7 base unit was positioned at a nearby monument to broadcast a kinematic correction to a roving Trimble R8 GNSS receiver. All GSP measurements were made during periods with a Position Dilution of Precision (PDOP) of ≤ 3.0 with at least six satellites in view of the stationary and roving receivers. When collecting RTK data, the rover records data while stationary for five seconds, then calculates the pseudorange position using at least three one-second epochs. Relative errors for any GSP position must be less than 1.5 cm horizontal and 2.0 cm vertical in order to be accepted. Relative errors for the position must be less than 1.5 cm horizontal and 2.0 cm vertical in order to be accepted. See Table 5 for Trimble unit specifications.

GSPs were collected in areas where good satellite visibility was achieved on paved roads and other hard surfaces such as gravel or packed dirt roads. GSP measurements were not taken on highly reflective surfaces such as center line stripes or lane markings on roads due to the increased noise seen in the laser returns over these surfaces. GSPs were collected within as many flightlines as possible, however the distribution of GSPs depended on ground access constraints and monument locations and may not be equitably distributed throughout the study area (Figures 2a and 2b).

Table 5: Trimble equipment identification

Receiver Model	Antenna	OPUS Antenna ID	Use
Trimble R6	Integrated GNSS Antenna R6	TRM_R6	Rover
Trimble R7 GNSS	Zephyr GNSS Geodetic Model 2 RoHS	TRM57971.00	Static
Trimble R8	Integrated Antenna R8 Model 2	TRM_R8_GNSS	Static, Rover

Airborne Survey

LiDAR

The LiDAR survey was accomplished using Leica ALS70 sensor systems mounted in a Cessna 208-B Grand Caravan and Partenavia P68 aircraft. Table 6 summarizes the settings used to yield an average pulse density of 8 pulses/m^2 over the Idaho and Montana Forests project area. The Leica laser system records up to four range measurements (returns) per pulse. It is not uncommon for some types of surfaces (e.g., dense vegetation or water) to return fewer pulses to the LiDAR sensor than the laser originally emitted. The discrepancy between first return and overall delivered density will vary depending on terrain, land cover, and the prevalence of water bodies. All discernible laser returns were processed for the output dataset.

Table 6: LiDAR specifications and survey set-

LiDAR Survey Settings & Specifications	
Acquisition Dates	May 24 - June 24, 2014
Aircraft Used	Cessna 208 Grand Caravan Partenavia P68
Sensor	Leica ALS70
Survey Altitude (AGL)	1,450 m
Target Pulse Rate	180-192.6 kHz
Pulse Mode	Single Pulse in Air (SPiA)
Laser Pulse Diameter	32 cm
Mirror Scan Rate	39 Hz
Field of View	30°
GPS Baselines	≤13 nm
GPS PDOP	≤3.0
GPS Satellite Constellation	≥6
Maximum Returns	Up to four per pulse
Intensity	8-bit
Resolution/Density	Average 8 pulses/m2

Leica ALS70 LiDAR sensor

All areas were surveyed with an opposing flight line side-lap of ≥56% (≥100% overlap) in order to reduce laser shadowing and increase surface laser painting. To accurately solve for laser point position (geographic coordinates x, y and z), the positional coordinates of the airborne sensor and the attitude of the aircraft were recorded continuously throughout the LiDAR data collection mission. Position of the aircraft was measured twice per second (2 Hz) by an onboard differential GPS unit, and aircraft attitude was measured 200 times per second (200 Hz) as pitch, roll and yaw (heading) from an onboard inertial measurement unit (IMU). To allow for post-processing correction and calibration, aircraft and sensor position and attitude data are indexed by GPS time.

Processing

View looking west at a regenerated clearcut on the north edge of the Woodward area of interest. The image was created from the gridded LiDAR surface colored by elevation and overlaid with the 3-D LiDAR point cloud.

LiDAR Data

Upon completion of data acquisition, QSI processing staff initiated a suite of automated and manual techniques to process the data into the requested deliverables. Processing tasks included GPS control computations, smoothed best estimate trajectory (SBET) calculations, kinematic corrections, calculation of laser point position, sensor and data calibration for optimal relative and absolute accuracy, and LiDAR point classification (Table 7). Processing methodologies were tailored for the landscape. Brief descriptions of these tasks are shown in Table 8.

Table 7: ASPRS LAS classification standards applied to the Idaho and Montana Forests dataset

Classification Number	Classification Name	Classification Description
1	Default/ Unclassified	Laser returns that are not included in the ground class, composed of vegetation and man-made structures
2	Ground	Laser returns that are determined to be ground using automated and manual cleaning algorithms
6	Buildings	Permanent structures
7	Noise	Identified by height from ground
11	Noise	Identified by intensity values of 0 or 255

Table 8: LiDAR processing workflow

Resolve kinematic corrections for aircraft position data using kinematic aircraft GPS and static ground GPS data. Develop a smoothed best estimate of trajectory (SBET) file that blends post-processed aircraft position with sensor head position and attitude recorded throughout the survey.	IPAS TC v.3.1 Waypoint Inertial Explorer v.8.5
Calculate laser point position by associating SBET position to each laser point return time, scan angle, intensity, etc. Create raw laser point cloud data for the entire survey in *.las (ASPRS v. 1.2) format. Convert data to orthometric elevations by applying a geoid correction.	ALS Post Processing Software v.2.75
Import raw laser points into manageable blocks (less than 500 MB) to perform manual relative accuracy calibration and filter erroneous points. Classify ground points for individual flight lines.	TerraScan v.15
Using ground classified points per each flight line, test the relative accuracy. Perform automated line-to-line calibrations for system attitude parameters (pitch, roll, heading), mirror flex (scale) and GPS/IMU drift. Calculate calibrations on ground classified points from paired flight lines and apply results to all points in a flight line. Use every flight line for relative accuracy calibration.	TerraMatch v.15
Classify resulting data to ground and other client designated ASPRS classifications (Table 7). Assess statistical absolute accuracy via direct comparisons of ground classified points to ground control survey data.	TerraScan v.15 TerraModeler v.15
Generate bare earth models as triangulated surfaces. Generate highest hit models as a surface expression of all classified points. Export all surface models as ESRI GRIDs in ERDAS Imagine (.img) format at a 3.0 foot 1 meter pixel resolution.	TerraScan v.15 TerraModeler v.15 ArcMap v. 10.1
Correct intensity values for variability and export intensity images as GeoTIFFs at a 1.5 foot 0.5 meter pixel resolution.	TerraScan v.15 TerraModeler v.15 ArcMap v. 10.1

Project area under snow

LiDAR Density

The acquisition parameters were designed to acquire an average first-return density of 8 points/m^2. First return density describes the density of pulses emitted from the laser that return at least one echo to the system. Multiple returns from a single pulse were not considered in first return density analysis. Some types of surfaces (e.g., breaks in terrain, water and steep slopes) may have returned fewer pulses than originally emitted by the laser. First returns typically reflect off the highest feature on the landscape within the footprint of the pulse. In forested or urban areas the highest feature could be a tree, building or power line, while in areas of unobstructed ground, the first return will be the only echo and represents the bare earth surface.

The density of ground-classified LiDAR returns was also analyzed for this project. Terrain character, land cover, and ground surface reflectivity all influenced the density of ground surface returns. In vegetated areas, fewer pulses may penetrate the canopy, resulting in lower ground density.

The average first-return density of LiDAR data for the Idaho and Montana Forests project was 19.57 points/m^2 and the average ground classified density was 1.98 points/m^2 (Table 9).

Table 9: Average LiDAR point densities

Classification	Point Density
First Return	1.92 points/ft^2
	19.57 points/m^2
Ground Classified	0.18 points/ft^2
	1.98 points/m^2

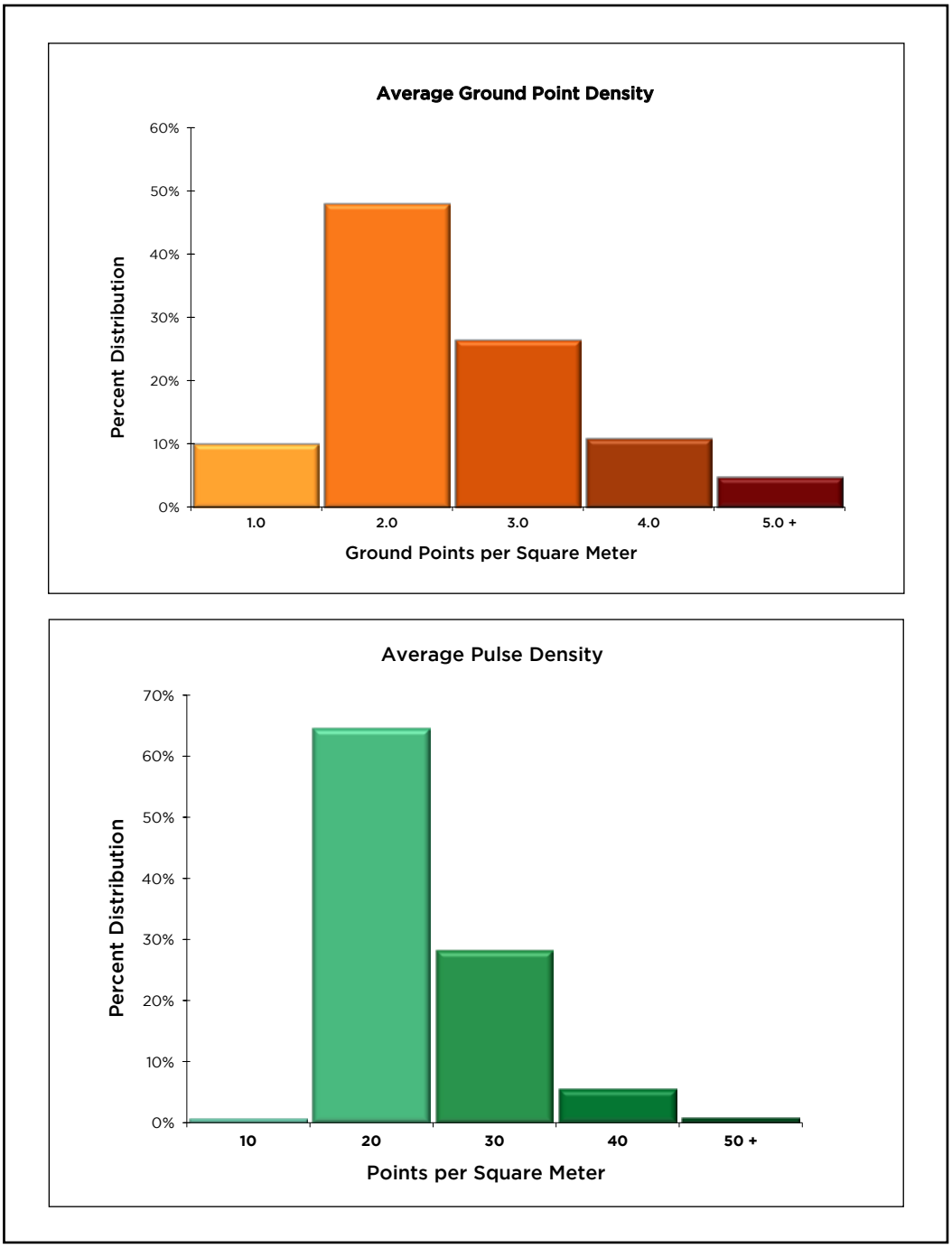

Figure 3: Frequency distribution of first return densities (above) and ground return densities (below).

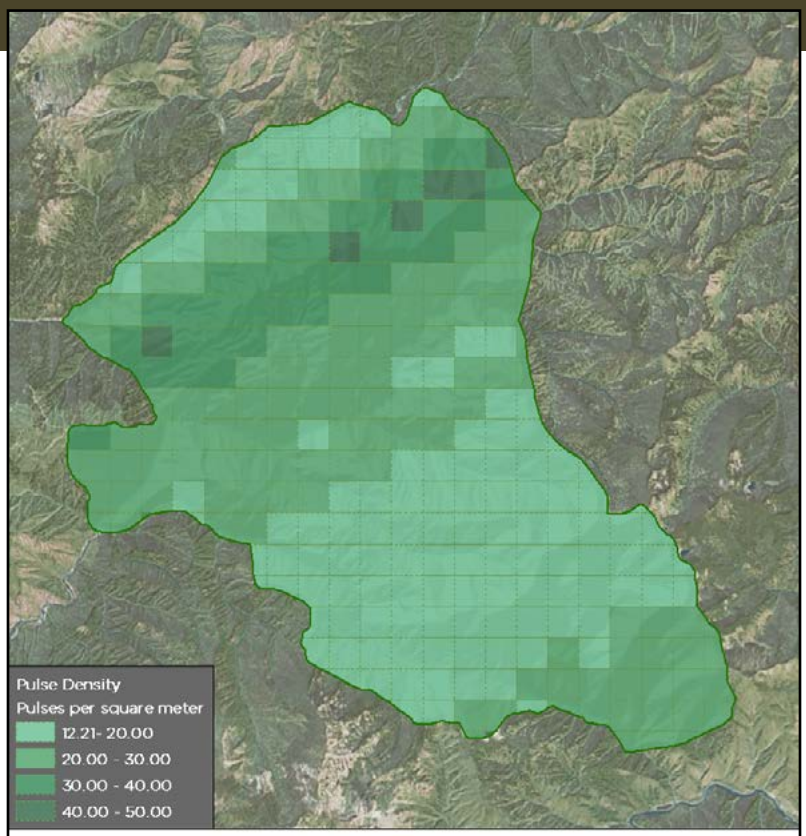

Idaho and Montana Forests 2015
Cool Mush Pulse Density

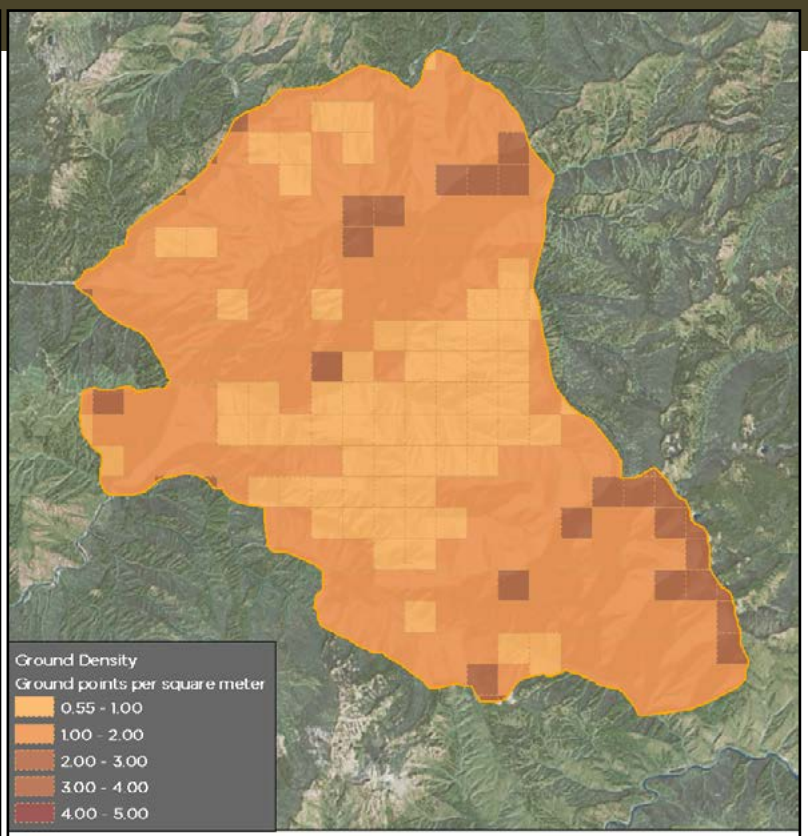

Idaho and Montana Forests 2015
Cool Mush Ground Density

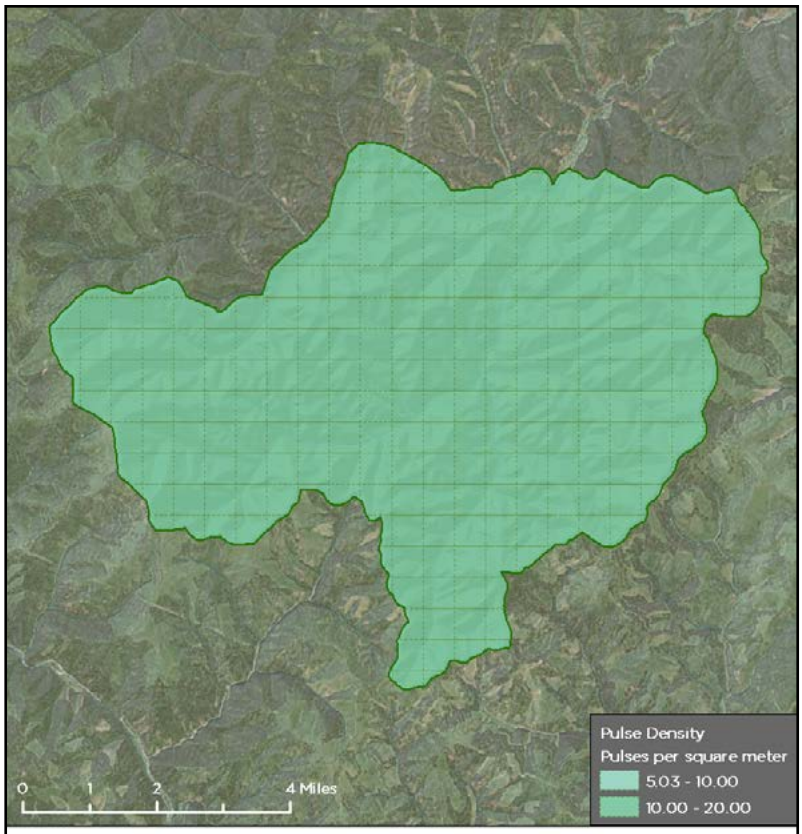

Idaho and Montana Forests 2015
TePee Potter Creek Pulse Density

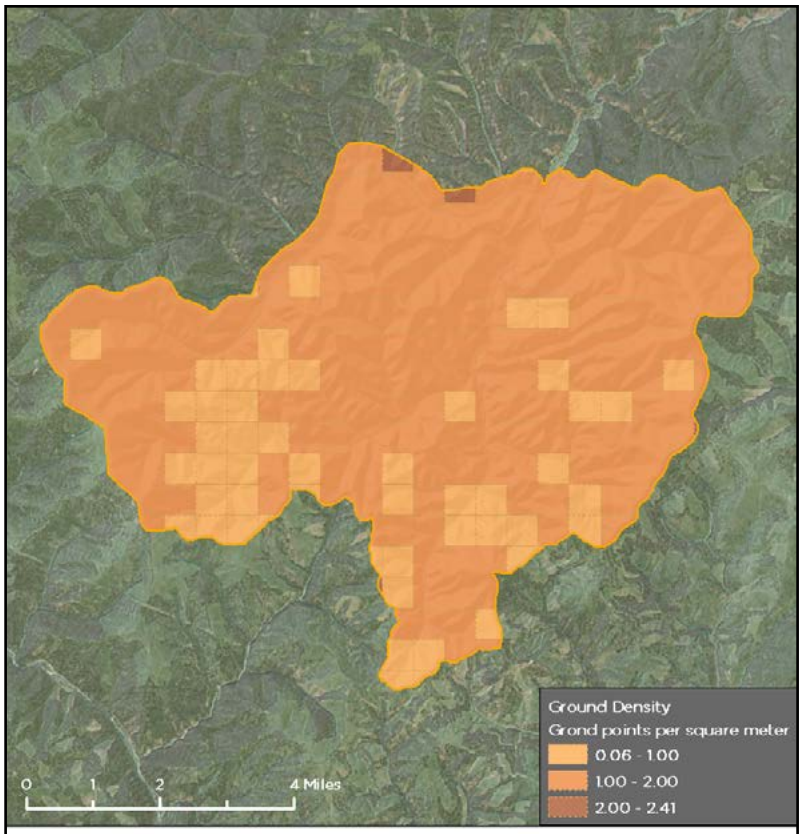

Idaho and Montana Forests 2015
TePee Potter Creek Ground Density

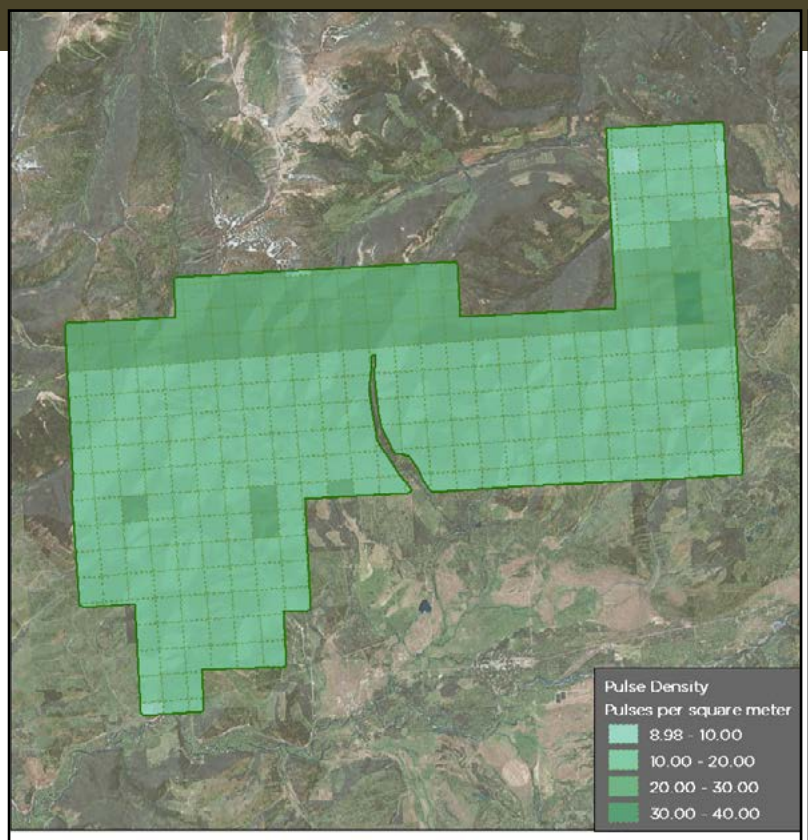

Idaho and Montana Forests 2015
Stonewall Pulse Density

0 1.5 3 Miles

N

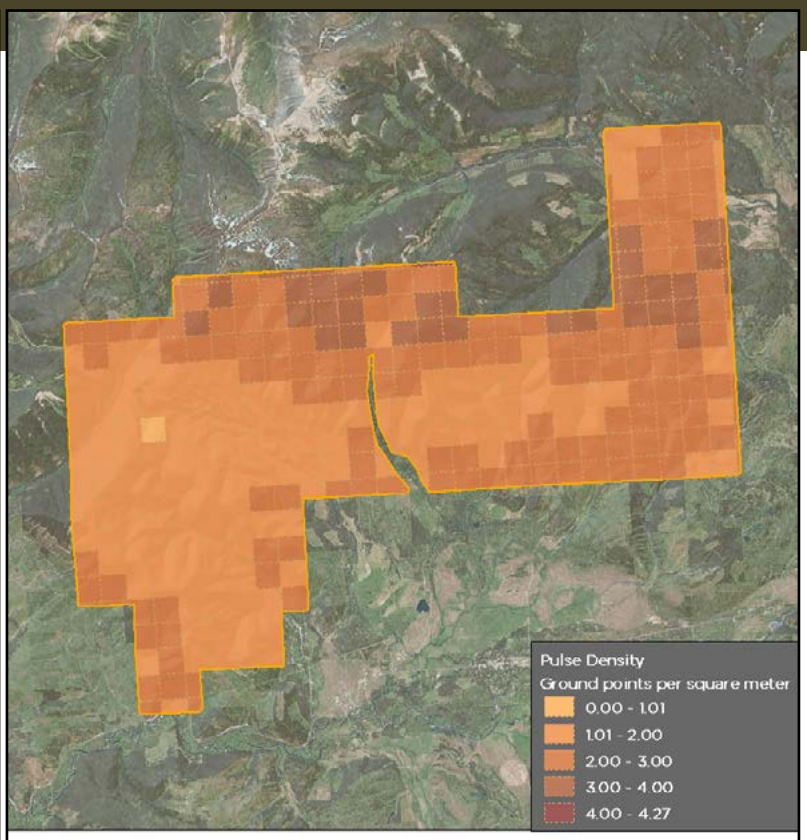

Idaho and Montana Forests 2015
Stonewall Ground Density

0 1.5 3 Miles

N

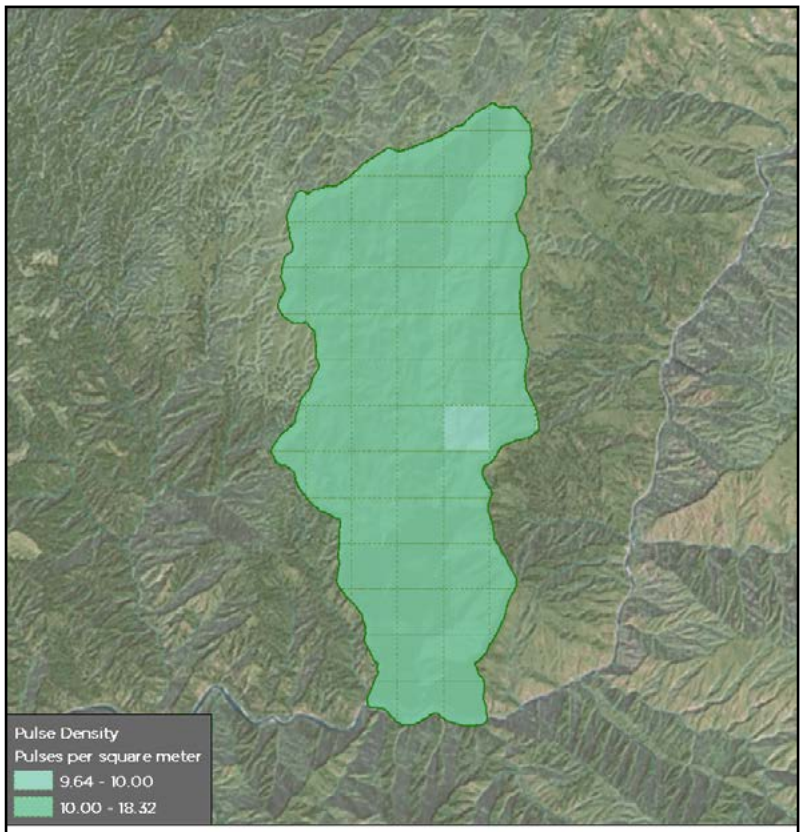

Idaho and Montana Forests 2015
Lower Lochsa Pulse Density

0 0.5 1 Miles

N

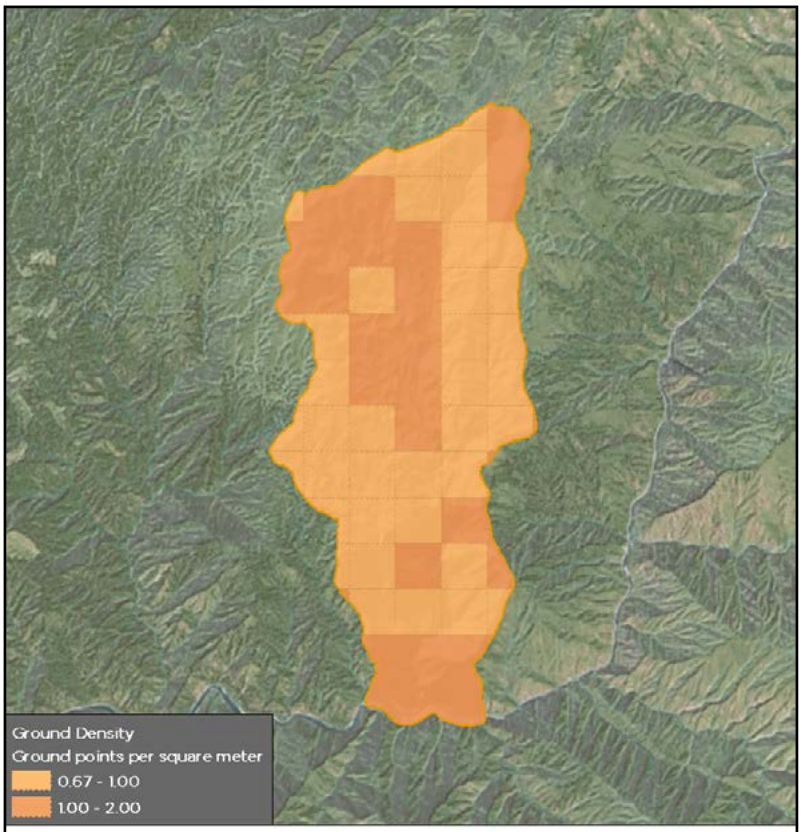

Idaho and Montana Forests 2015
Lower Lochsa Ground Density

0 0.5 1 Miles

N

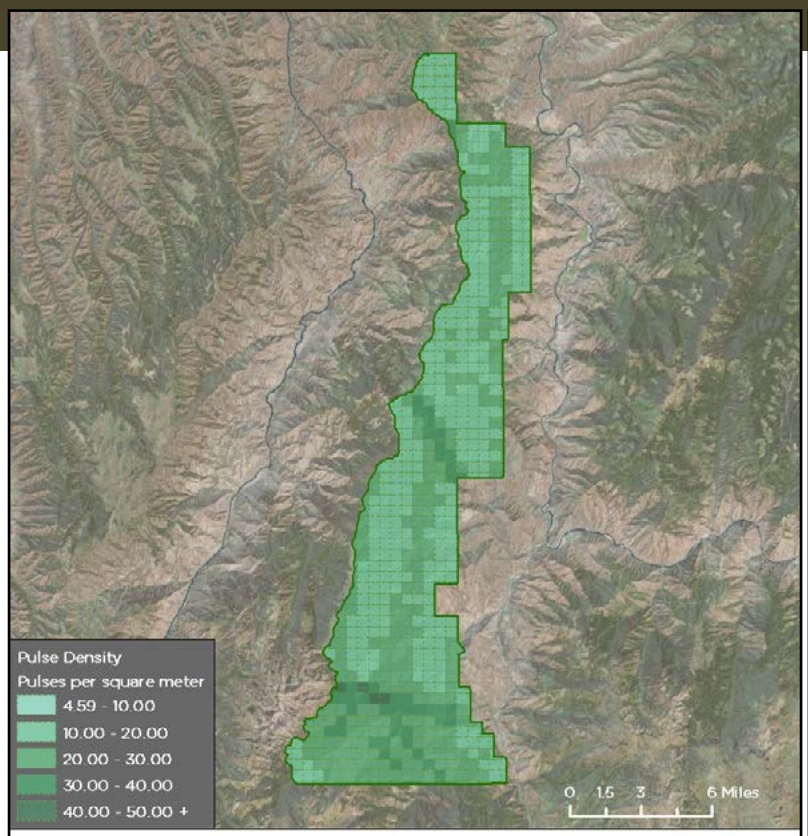

Idaho and Montana Forests 2015
Riggins West Island Pulse Density

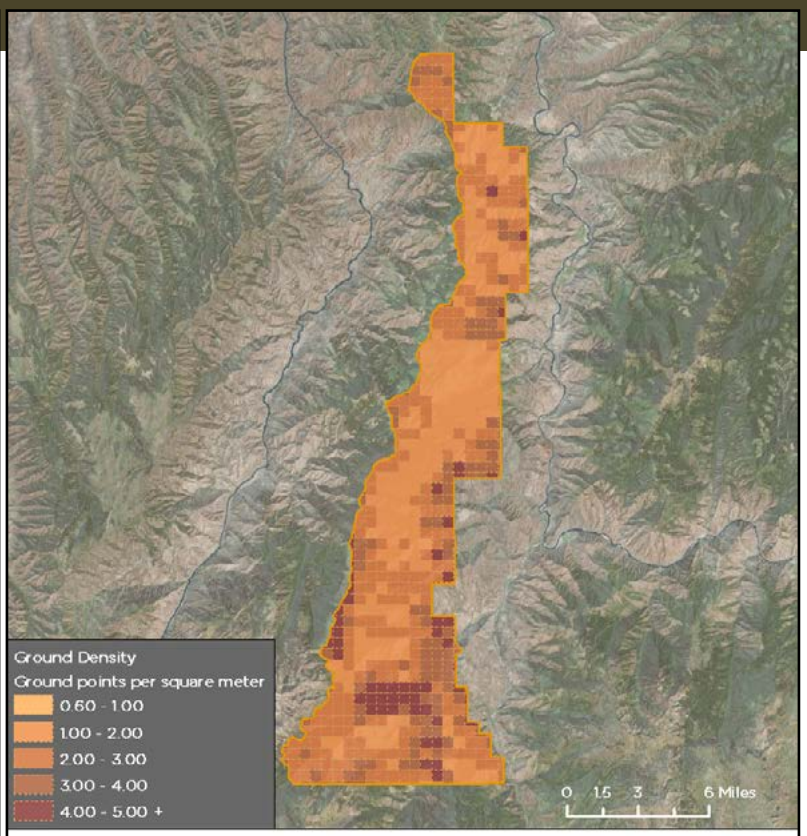

Idaho and Montana Forests 2015
Riggins West Island Ground Density

LiDAR Accuracy Assessments

The accuracy of the LiDAR data collection can be described in terms of absolute accuracy (the consistency of the data with external data sources) and relative accuracy (the consistency of the dataset with itself). See Appendix A for further information on sources of error and operational measures used to improve relative accuracy.

LiDAR Absolute Accuracy

Absolute accuracy was assessed using Fundamental Vertical Accuracy (FVA) reporting designed to meet guidelines presented in the FGDC National Standard for Spatial Data Accuracy* . FVA compares known reserved RTK ground check point data collected on open, bare earth surfaces with level slope (<20°) to the triangulated surface generated by the LiDAR points. FVA is a measure of the accuracy of LiDAR point data in open areas where the LiDAR system has a high probability of measuring the ground surface and is evaluated at the 95% confidence interval (1.96 * RMSE), as shown in Table 10.

The mean and standard deviation (sigma σ) of divergence of the ground surface model from ground survey point coordinates are also considered during accuracy assessment. These statistics assume the error for x, y and z is normally distributed, and therefore the skew and kurtosis of distributions are also considered when evaluating error statistics. For the Idaho and Montana Forests survey, 2,072 ground survey points were collected in total resulting in an average accuracy of 0.083 feet (0.025 meters). An additional 110 check points were reserved for independent verification. Results for both absolute accuracy and the independent verification are located in Table 10 and Figure 4.

In addition to the hard surface land class, checkpoints were also collected across the project area for additional land cover classes (Table 11).

Table 10: Absolute Accuracy

	Absolute Accuracy	Independent Check Point Accuracy
Sample	2,072 points	110 points
FVA (1.96*RMSE)	N/A	0.191 ft 0.058 m
Average	0.083 ft 0.025 m	0.084 ft 0.026 m
Median	-0.013 ft -0.004 m	-0.033 ft -0.010 m
RMSE	0.103 ft 0.032 m	0.097 ft 0.030 m
Standard Deviation (1σ)	0.098 ft 0.030 m	0.102 ft 0.031 m

Table 11: Land Class Accuracy

	Tall Grass	Short Grass	Moss	Shrubs	All Land Cover Classes
Sample	128 points	514 points	8 points	26 points	676 points
95th Percentile	0.299 ft 0.091 m	0.352 ft 0.107 m	0.210 ft 0.064 m	0.375 ft 0.114 m	0.375 ft 0.114 m
Average	0.139 ft 0.042 m	0.148 ft 0.045 m	0.122 ft 0.037 m	0.367 ft 0.112 m	0.154 ft 0.047 m
Median	0.107 ft 0.033 m	0.115 ft 0.035 m	0.121 ft 0.037 m	0.405 ft 0.124 m	0.118 ft 0.036 m
RMSE	0.142 ft 0.043 m	0.148 ft 0.045 m	0.072 ft 0.022 m	0.220 ft 0.067 m	0.157 ft 0.048 m
Standard Deviation (1σ)	0.181 ft 0.055 m	0.180 ft 0.055 m	0.150 ft 0.046 m	0.482 ft 0.147 m	0.184 ft 0.056 m

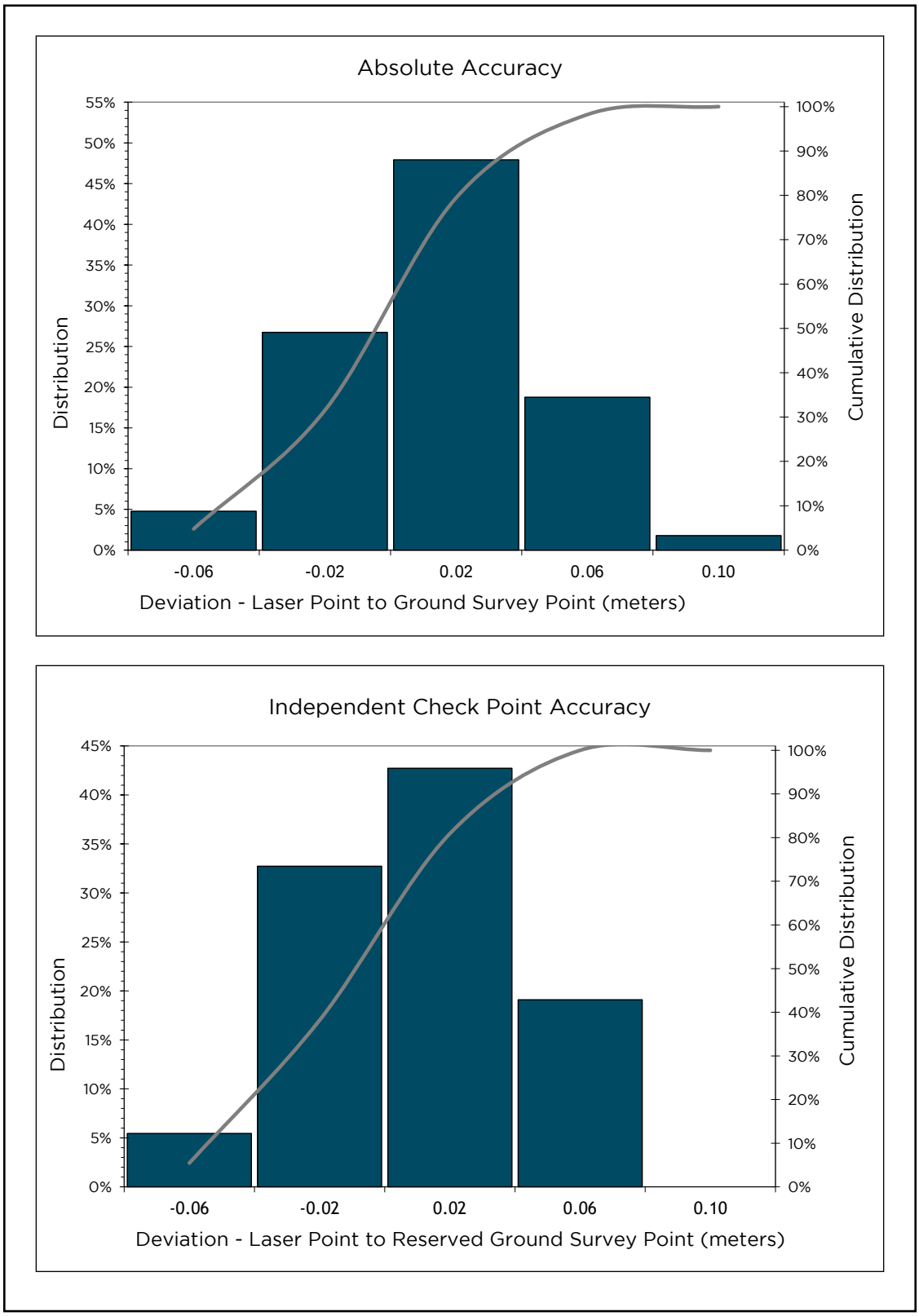

Figure 4: Frequency histograms for LiDAR surface deviation from ground survey point values (above) and for the independent check point verification (below)

LiDAR Relative Accuracy

Relative vertical accuracy refers to the internal consistency of the data set as a whole: the ability to place an object in the same location given multiple flight lines, GPS conditions, and aircraft attitudes. When the LiDAR system is well calibrated, the swath-to-swath vertical divergence is low (<0.10 meters). The relative vertical accuracy was computed by comparing the ground surface model of each individual flight line with its neighbors in overlapping regions. The average (mean) line to line relative vertical accuracy for the Idaho and Montana Forests LiDAR project was 0.102 feet (0.031 meters) (Table 12, Figure 5).

Table 12: Relative accuracy

Relative Accuracy	
Sample	533 flightlines
Average	0.102 ft
	0.031 m
Median	0.100 ft
	0.031 m
Standard Deviation (1 σ)	0.105 ft
	0.032 m

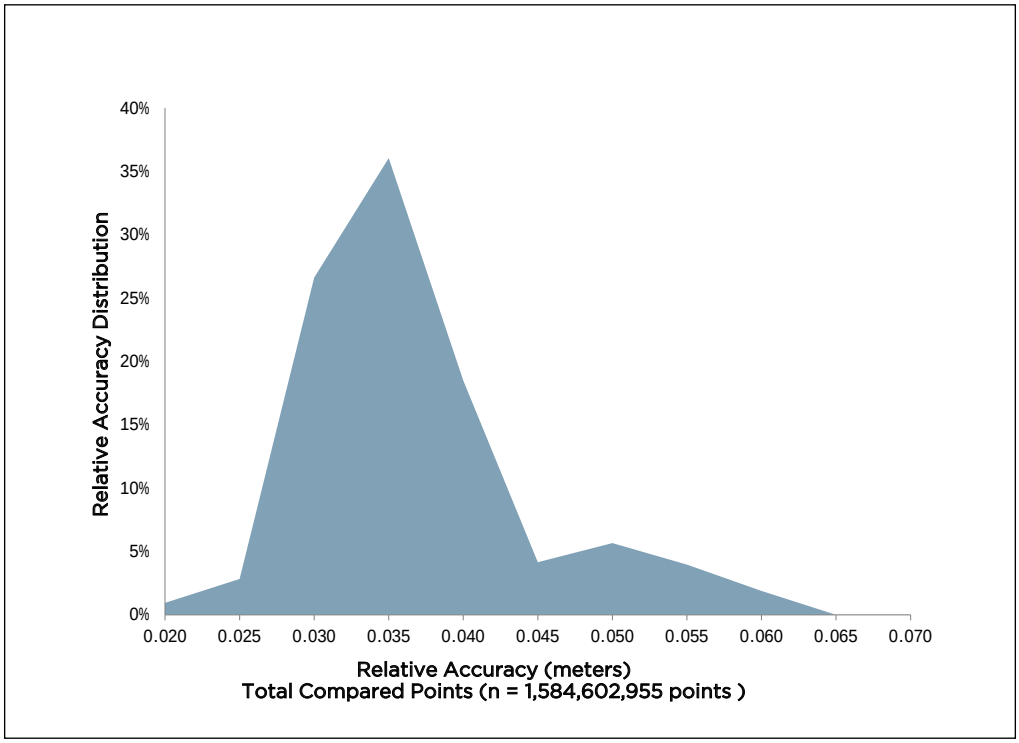

Figure 5: Frequency plot for relative vertical accuracy between flight lines.

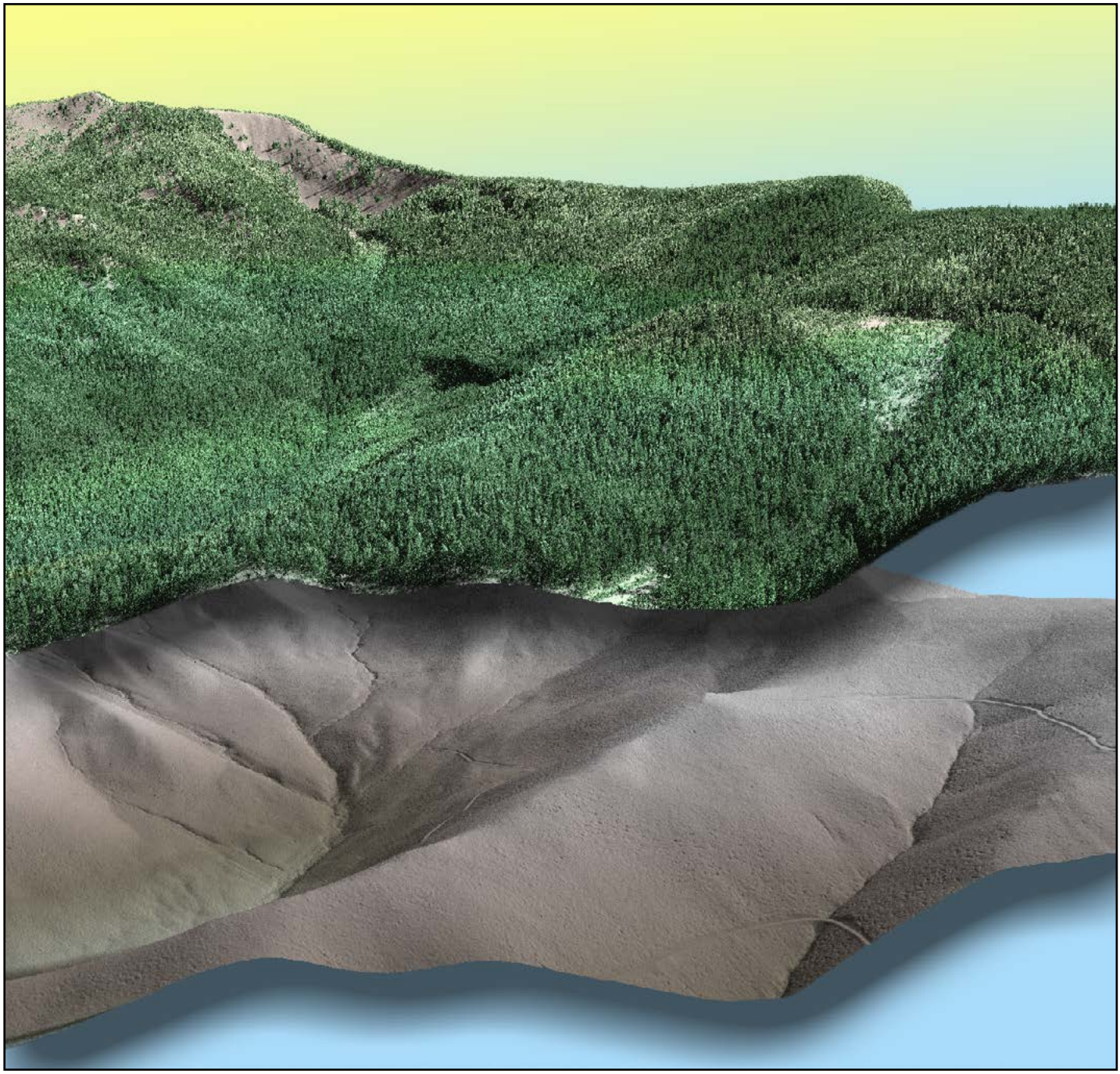

Figure 6: View looking west at Ovando Mountain in the North Lake area of interest in Montana. The images were created from the gridded LiDAR surface colored by elevation with the top image overlaid with the 3-D LiDAR point cloud.

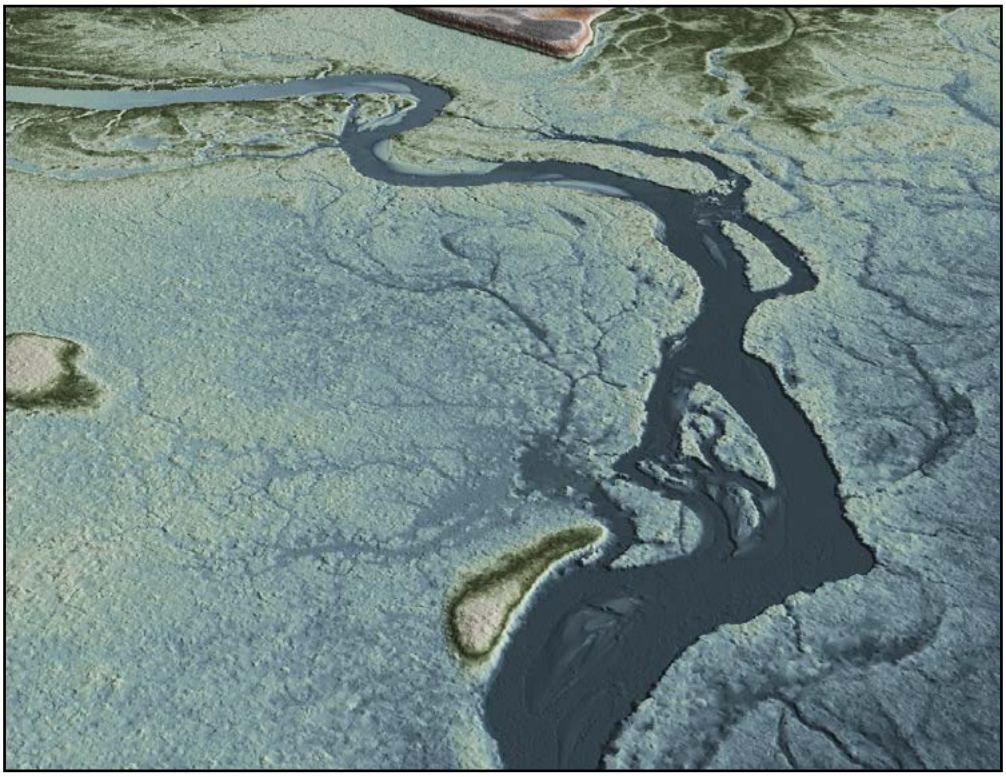

Figure 7: (Above) View looking south over the Swan River in the North Swan area of interest. The image was created from the gridded LiDAR surface colored by elevation.
(Below) View looking northeast over the Swan River in the North Swan area of interest. The image was created from the gridded LiDAR surface colored by elevation and overlaid with the 3-D LiDAR point cloud.

Glossary

1-sigma (σ) Absolute Deviation: Value for which the data are within one standard deviation (approximately 68th percentile) of a normally distributed data set.

1.96 * RMSE Absolute Deviation: Value for which the data are within two standard deviations (approximately 95th percentile) of a normally distributed data set, based on the FGDC standards for Fundamental Vertical Accuracy (FVA) reporting.

Accuracy: The statistical comparison between known (surveyed) points and laser points. Typically measured as the standard deviation (sigma σ) and root mean square error (RMSE).

Absolute Accuracy: The vertical accuracy of LiDAR data is described as the mean and standard deviation (sigma σ) of divergence of LiDAR point coordinates from ground survey point coordinates. To provide a sense of the model predictive power of the dataset, the root mean square error (RMSE) for vertical accuracy is also provided. These statistics assume the error distributions for x, y, and z are normally distributed, and thus the skew and kurtosis of distributions are also considered when evaluating error statistics.

Relative Accuracy: Relative accuracy refers to the internal consistency of the data set (i.e., the ability to place a laser point in the same location over multiple flight lines), GPS conditions, and aircraft attitudes. Affected by system attitude offsets, scale, and GPS/IMU drift, internal consistency is measured as the divergence between points from different flight lines within an overlapping area. Divergence is most apparent when flight lines are opposing. When the LiDAR system is well calibrated, the line-to-line divergence is low (<10 cm).

Root Mean Square Error (RMSE): A statistic used to approximate the difference between real-world points and the LiDAR points. It is calculated by squaring all the values, then taking the average of the squares and taking the square root of the average.

Data Density: A common measure of LiDAR resolution, measured as points per square meter.

Digital Elevation Model (DEM): File or database made from surveyed points, containing elevation points over a contiguous area. Digital terrain models (DTM) and digital surface models (DSM) are types of DEMs. DTMs consist solely of the bare earth surface (ground points), while DSMs include information about all surfaces, including vegetation and man-made structures.

Intensity Values: The peak power ratio of the laser return to the emitted laser, calculated as a function of surface reflectivity.

Nadir: A single point or locus of points on the surface of the earth directly below a sensor as it progresses along its flight line.

Overlap: The area shared between flight lines, typically measured in percent. 100% overlap is essential to ensure complete coverage and reduce laser shadows.

Pulse Rate (PR): The rate at which laser pulses are emitted from the sensor; typically measured in thousands of pulses per second (kHz).

Pulse Returns: For every laser pulse emitted, the number of wave forms (i.e., echos) reflected back to the sensor. Portions of the wave form that return first are the highest element in multi-tiered surfaces such as vegetation. Portions of the wave form that return last are the lowest element in multi-tiered surfaces.

Real-Time Kinematic (RTK) Survey: A type of surveying conducted with a GPS base station deployed over a known monument with a radio connection to a GPS rover. Both the base station and rover receive differential GPS data and the baseline correction is solved between the two. This type of ground survey is accurate to 1.5 cm or less.

Post-Processed Kinematic (PPK) Survey: GPS surveying is conducted with a GPS rover collecting concurrently with a GPS base station set up over a known monument. Differential corrections and precisions for the GNSS baselines are computed and applied after the fact during processing. This type of ground survey is accurate to 1.5 cm or less.

Scan Angle: The angle from nadir to the edge of the scan, measured in degrees. Laser point accuracy typically decreases as scan angles increase.

Native LiDAR Density: The number of pulses emitted by the LiDAR system, commonly expressed as pulses per square meter.

Appendix A - Accuracy Controls

Relative Accuracy Calibration Methodology:

Manual System Calibration: Calibration procedures for each mission require solving geometric relationships that relate measured swath-to-swath deviations to misalignments of system attitude parameters. Corrected scale, pitch, roll and heading offsets were calculated and applied to resolve misalignments. The raw divergence between lines was computed after the manual calibration was completed and reported for each survey area.

Automated Attitude Calibration: All data were tested and calibrated using TerraMatch automated sampling routines. Ground points were classified for each individual flight line and used for line-to-line testing. System misalignment offsets (pitch, roll and heading) and scale were solved for each individual mission and applied to respective mission datasets. The data from each mission were then blended when imported together to form the entire area of interest.

Automated Z Calibration: Ground points per line were used to calculate the vertical divergence between lines caused by vertical GPS drift. Automated Z calibration was the final step employed for relative accuracy calibration.

LiDAR accuracy error sources and solutions:

Type of Error	Source	Post Processing Solution
GPS (Static/Kinematic)	Long Base Lines	None
	Poor Satellite Constellation	None
	Poor Antenna Visibility	Reduce Visibility Mask
Relative Accuracy	Poor System Calibration	Recalibrate IMU and sensor offsets/settings
	Inaccurate System	None
Laser Noise	Poor Laser Timing	None
	Poor Laser Reception	None
	Poor Laser Power	None
	Irregular Laser Shape	None

Operational measures taken to improve relative accuracy:

Low Flight Altitude: Terrain following was employed to maintain a constant above ground level (AGL). Laser horizontal errors are a function of flight altitude above ground (about 1/3000th AGL flight altitude).

Focus Laser Power at narrow beam footprint: A laser return must be received by the system above a power threshold to accurately record a measurement. The strength of the laser return (i.e., intensity) is a function of laser emission power, laser footprint, flight altitude and the reflectivity of the target. While surface reflectivity cannot be controlled, laser power can be increased and low flight altitudes can be maintained.

Reduced Scan Angle: Edge-of-scan data can become inaccurate. The scan angle was reduced to a maximum of 312o from nadir, creating a narrow swath width and greatly reducing laser shadows from trees and buildings.

Quality GPS: Flights took place during optimal GPS conditions (e.g., 6 or more satellites and PDOP [Position Dilution of Precision] less than 3.0). Before each flight, the PDOP was determined for the survey day. During all flight times, a dual frequency DGPS base station recording at 1 second epochs was utilized and a maximum baseline length between the aircraft and the control points was less than 13 nm at all times.

Ground Survey: Ground survey point accuracy (<1.5 cm RMSE) occurs during optimal PDOP ranges and targets a minimal baseline distance of 4 miles between GPS rover and base. Robust statistics are, in part, a function of sample size (n) and distribution. Ground survey points are distributed to the extent possible throughout multiple flight lines and across the survey area.

50% Side-Lap (100% Overlap): Overlapping areas are optimized for relative accuracy testing. Laser shadowing is minimized to help increase target acquisition from multiple scan angles. Ideally, with a 50% side-lap, the nadir portion of one flight line coincides with the swath edge portion of overlapping flight lines. A minimum of 50% side-lap with terrain-followed acquisition prevents data gaps.

Opposing Flight Lines: All overlapping flight lines have opposing directions. Pitch, roll and heading errors are amplified by a factor of two relative to the adjacent flight line(s), making misalignments easier to detect and resolve.

February 27, 2015

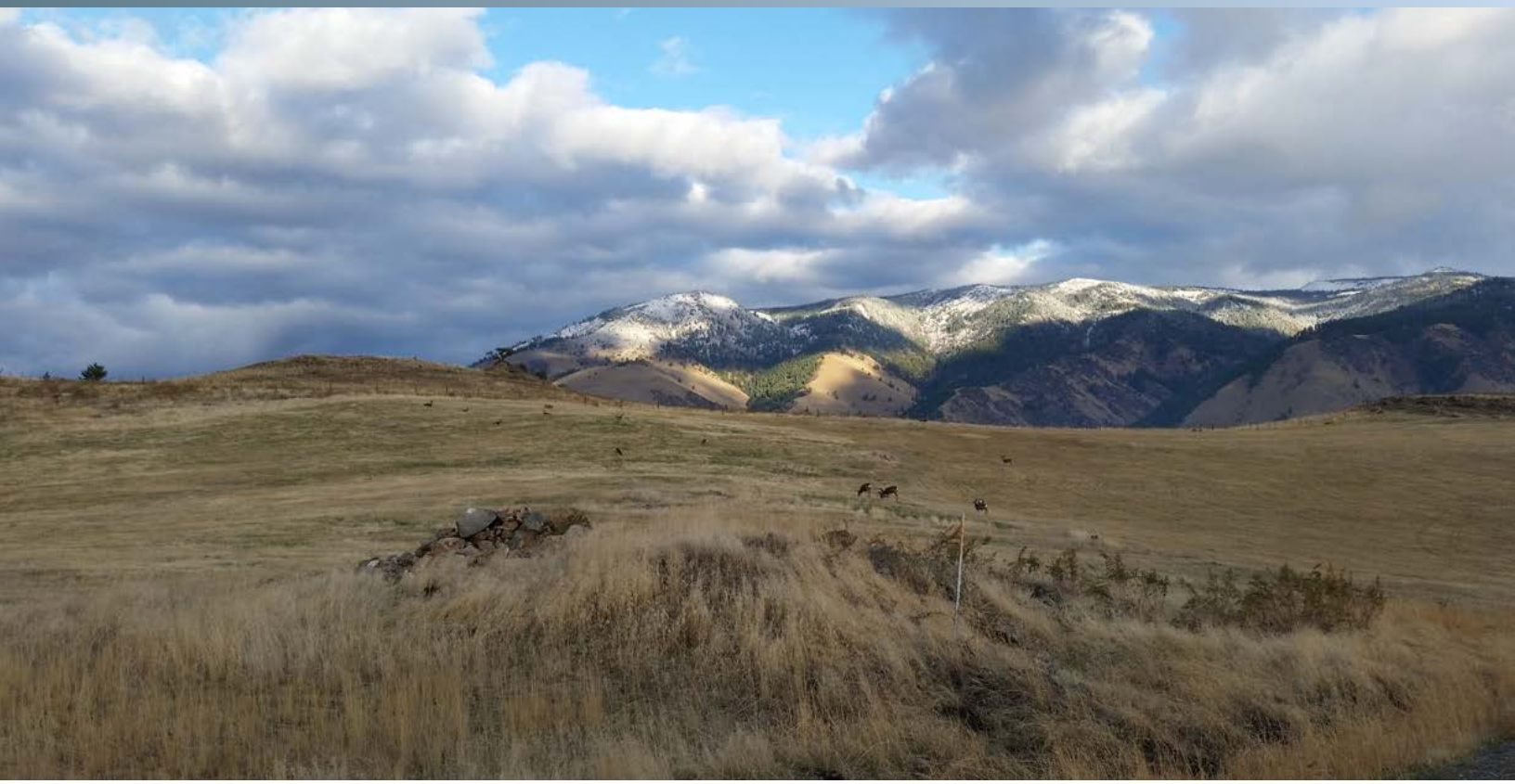

USFS Idaho and Montana Forests LiDAR 2014

Technical Data Report

Andre Snyder and Joel Harrison
USDA Forest Service
Nez Perce-Clearwater National Forests
12730 Hwy 12
Orofino, ID 83544-9333

QSI Environmental
517 SW 2nd St., Suite 400
Corvallis, OR 97333
PH: 541-752-1204

Cover Photo: A view of Little Salmon River Canyon, Idaho.

Table of Contents

Introduction 1
Planning 4

Acquisition 4
Ground Control 5
Airborne Survey 9
LiDAR 9

Processing 10
LiDAR Data 10

Results and Discussion 12
LiDAR Density 12
LiDAR Accuracy Assessments 14
LiDAR Absolute Accuracy 14
LiDAR Relative Accuracy 16

Selected Images 17

Glossary 18

Appendix A - Accuracy Controls 20

Introduction

Little Salmon River near Riggins, Idaho.

WSI, a Quantum Spatial company (QSI), was contracted by the USDA Forest Service (USFS) to collect Light Detection and Ranging (LiDAR) data in the fall of 2014 for the Idaho and Montana Forests project. Data were collected to aid the USFS in assessing the topographic properties of the study area to support resource management.

This report accompanies the delivered LiDAR data and products, and documents contract specifications, data acquisition procedures, processing methods, and analysis of the final dataset including LiDAR accuracy and density. A complete list of contracted deliverables provided to the USFS is shown in Table 1, acquisition dates and acreage are shown in Table 2 and the project extent is shown in Figure 1.

Table 1: Products delivered to the USFS

Idaho and Montana Forests Products Projection: UTM Zones 11 North and 12 North Horizontal Datum: NAD83 (CORS96) Vertical Datum: NAVD88 (GEOID03) Units: Meters	
Points	LAS v 1.2 • All Returns • Ground Returns
Rasters	1.0 Meter ESRI Grids • Bare Earth DEM • Canopy Height DEM 0.5 Meter GeoTiffs • Intensity Images
Vectors	Shapefiles (*.shp) • Site Boundary • LiDAR Tile Index • DEM Tile Index

Table 2: Acquisition dates, acreage, and delivery dates for Idaho and Montana Forests project areas

Delivery	UTM	AOI	Contracted Acres	Buffered Acres	Acquisition Date(s)	Delivery Date
1	11	Dutch Oven	6,993	7,672	10/31/14	12/31/14
2	12	North Swan	8,915	9,921	9/24, 9/25/14	1/16/15
	12	Woodward	2,180	2,556	9/24/14	
	12	North Lake	10,986	12,552	10/17/14	
3	12	Lower Cottonwood	18,319	20,004	10/9, 10/13, 10/14/14	1/23/15
	12	Lower Monture	19,148	20,271	10/9, 10/13, 10/14/14	
4	12	Buck Holland	17,587	18,567	10/5/14	2/9/15
	12	Monture Creek	1,258	1,736	10/14/14	
5	12	Meadow Smith	27,810	28,894	9/25, 9/26, 10/3/14	2/13/15
	12	Hemlock Elk	44,915	46,951	9/25, 9/26, 10/3, 10/4/14	
6	12	Blackfoot	14,351	15,610	10/18, 10/19/14	2/20/15
	12	Dalton	17,105	17,869	10/28, 10/30, 10/31, 11/1/14	
	12	Dalton B	12,265	13,024	10/30, 10/31, 11/1/14	
	12	West Flesher	24,362	25,419	10/18, 10/19/14	
	12	Stemple	28,997	30,800	10/28, 10/30, 10/31, 11/1/14	
7	12	Richmond	15,980	16,535	10/5/, 10/6, 10/9/14	2/27/15
	12	Rice	7,276	7,540	10/8, 10/9/14	
	12	Colt Bertha	6,736	7,334	10/5/14	
	12	Clearwater	10,445	10,929	10/5, 10/6/14	
	12	Lower Morell	9,936	10,513	10/6, 10/9/14	
	12	Lower Trail	11,116	11,628	10/6, 10/8, 10/9, 10/13, 10/14/14	

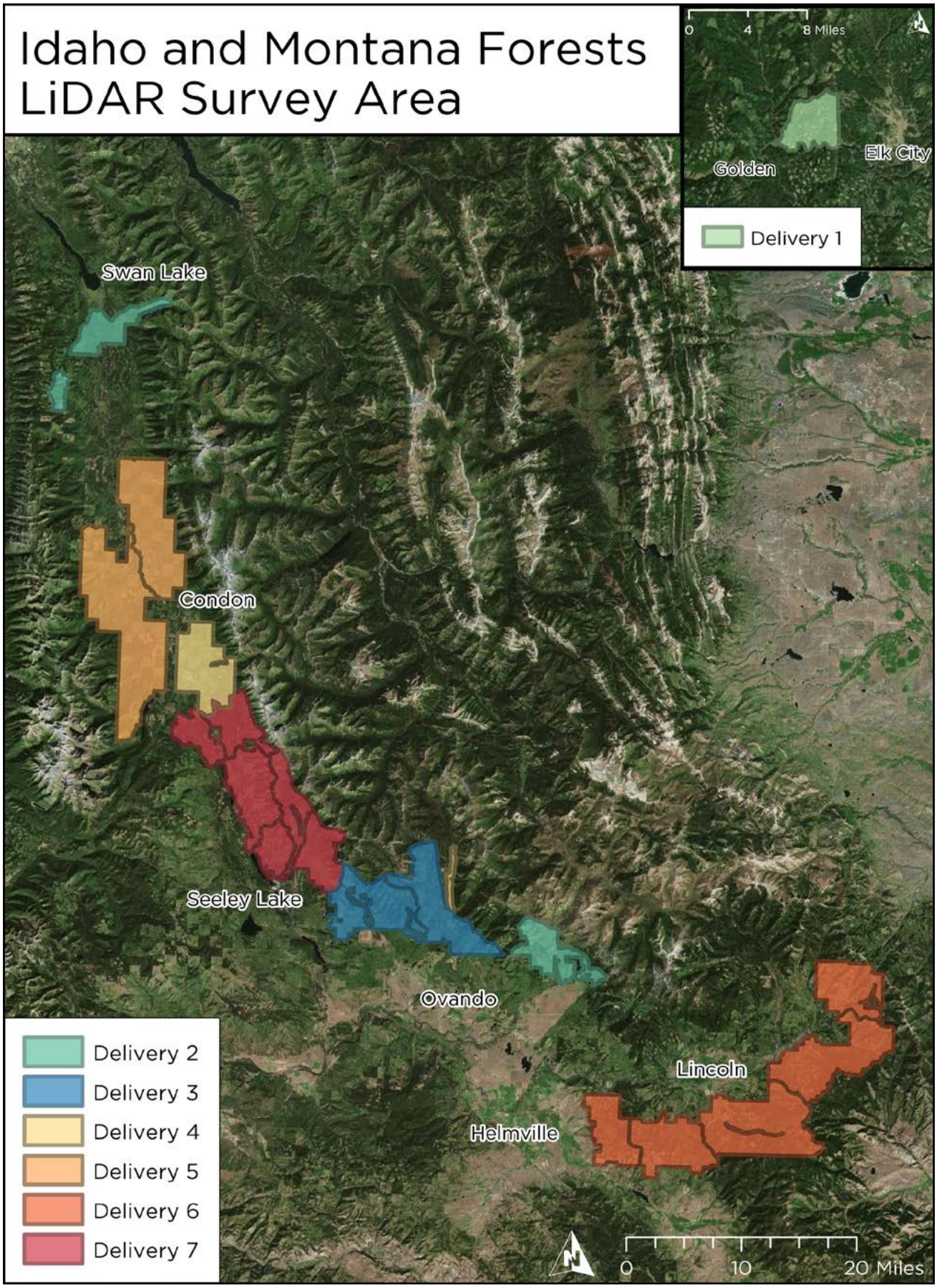

Figure 1: Location map of Idaho and Montana Forests project

Acquisition

QSI Cessna 208-B Grand Caravan

Planning

In preparation for data collection, QSI reviewed the project area and developed a specialized flight plan to ensure complete coverage of the Idaho and Montana LiDAR study area at the target point density of ≥8.0 points/m^2 (0.74 points/ft^2). Acquisition parameters including orientation relative to terrain, flight altitude, pulse rate, scan angle, and ground speed were adapted to optimize flight paths and flight times while meeting all contract specifications.

Factors such as satellite constellation availability and weather windows must be considered during the planning stage. Any weather hazards or conditions affecting the flight were continuously monitored due to their potential impact on the daily success of airborne and ground operations. In addition, logistical considerations including private property access and potential air space restrictions were reviewed.

Ground Control

Ground control surveys, including monumentation, aerial targets and ground survey points (GSPs), were conducted to support the airborne acquisition. Ground control data were used to geospatially correct the aircraft positional coordinate data and to perform quality assurance checks on final LiDAR data and orthoimagery products.

QSI-Established Monument

Monumentation

The spatial configuration of ground survey monuments provided redundant control within 13 nautical miles of the mission areas for LiDAR flights. Monuments were also used for collection of ground survey points using the real time kinematic (RTK) survey technique.

Monument locations were selected with consideration for satellite visibility, field crew safety, and optimal location for GSP coverage. QSI utilized two existing monuments and established nineteen new monuments for the Idaho and Montana Forests LiDAR project (Table 3, Figure 2). New monumentation was set using 5/8" x 30" rebar topped with stamped 2" aluminum caps.

To correct the continuously recorded onboard measurements of the aircraft position, QSI concurrently conducted multiple static Global Navigation Satellite System (GNSS) ground surveys (1 Hz recording frequency) over each monument. During post-processing, the static GPS data were triangulated with nearby Continuously Operating Reference Stations (CORS) using the Online Positioning User Service (OPUS*) for precise positioning. Multiple independent sessions over the same monument were processed to confirm antenna height measurements and to refine position accuracy.

* OPUS is a free service provided by the National Geodetic Survey to process corrected monument positions. http://www.ngs.noaa.gov/OPUS.

Table 3: Monuments established for the Idaho and Montana Forests acquisition. Coordinates are on the NAD83 (CORS96) datum, epoch 2002.00. Geoid03 was used to establish orthometric heights

Monument ID	Latitude	Longitude	Ellipsoid (meters)	NAVD88 Height (meters)
AI7923	47° 21′ 50.97066″	113° 35′ 58.61712″	1243.997	1257.895
AI7923-B	47° 21′ 51.31615″	113° 35′ 53.28186″	1242.297	1256.192
DUTCH_01	45° 49’ 45.26291”	115° 36’ 10.35228”	1204.164	1219.593
DUTCH_02	45° 49’ 04.40531”	115° 27’ 25.95767”	1184.305	1199.611
IDMT_11A	47° 52′ 42.03773″	113° 47′ 51.73762″	1000.579	1015.441
IDMT_11B	47° 52′ 45.60200″	113° 47′ 56.03164″	999.058	1013.924
IDMT_13A	47° 35′ 29.44346″	113° 45′ 20.86851″	1066.545	1081.086
IDMT_13B	47° 35′ 26.21433″	113° 45′ 19.28065″	1067.183	1081.722
IDMT_16A	47° 20′ 41.09926″	113° 31’ 20.21364″	1882.270	1895.933
IDMT_16B	47° 20′ 41.88195″	113° 31′ 22.51814″	1879.058	1892.724
IDMT_17A	47° 09′ 20.06465″	113° 19′ 00.36234″	1484.274	1497.813
IDMT_17B	47° 09′ 18.66519″	113° 19′ 02.82768″	1499.362	1512.904
IDMT_17C	47° 09′ 20.13816″	113° 19′ 00.26068″	1484.236	1497.775
IDMT_19A	47° 07′ 17.61634″	112° 59′ 10.39571″	1742.360	1755.295
IDMT_19B	47° 07′ 18.91084″	112° 59′ 10.79992″	1741.331	1754.265
IDMT_23A	46° 51′ 00.57362″	112° 43′ 21.63439″	1928.477	1941.441
IDMT_23B	46° 51′ 01.16231″	112° 43′ 21.76271″	1927.876	1940.841
IDMT_25A	46° 57′ 18.62103″	112° 30′ 30.38888″	1791.196	1803.955
IDMT_25B	46° 57′ 18.77823″	112° 30′ 28.94686″	1784.119	1796.893
RX0477	46° 56′ 23.78108″	112° 40′ 06.70709″	1374.622	1387.584
RX0477B	46°56′24.95725″	112°40′06.69684″	1374.287	1387.249

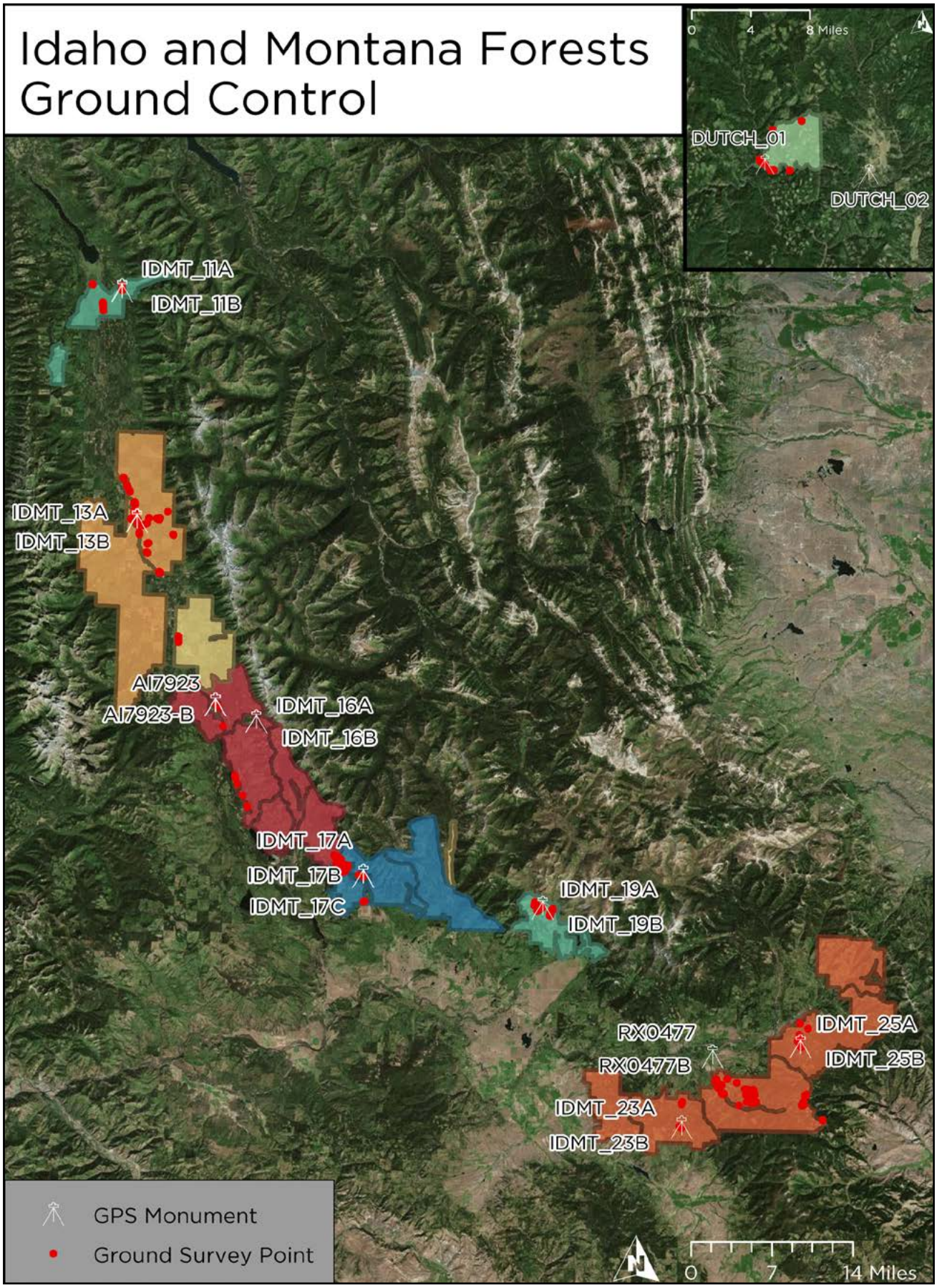

Figure 2: Ground control location map

Ground Survey Points (GSPs)

Ground survey points were collected using real time kinematic, roving Trimble R6 or R8 survey techniques. A Trimble R7 base unit was positioned at a nearby monument to broadcast a kinematic correction to a roving Trimble R8 GNSS receiver. All GSP measurements were made during periods with a Position Dilution of Precision (PDOP) of ≤ 3.0 with at least six satellites in view of the stationary and roving receivers. When collecting RTK data, the rover records data while stationary for five seconds, then calculates the pseudorange position using at least three one-second epochs..Relative errors for any GSP position must be less than 1.5 cm horizontal and 2.0 cm vertical in order to be accepted. Relative errors for the position must be less than 1.5 cm horizontal and 2.0 cm vertical in order to be accepted. See Table 5 for Trimble unit specifications.

GSPs were collected in areas where good satellite visibility was achieved on paved roads and other hard surfaces such as gravel or packed dirt roads. GSP measurements were not taken on highly reflective surfaces such as center line stripes or lane markings on roads due to the increased noise seen in the laser returns over these surfaces. GSPs were collected within as many flightlines as possible, however the distribution of GSPs depended on ground access constraints and monument locations and may not be equitably distributed throughout the study area (Figure 2).

Table 5: Trimble equipment identification

Receiver Model	Antenna	OPUS Antenna ID	Use
Trimble R6	Integrated GNSS Antenna R6	TRM_R6	Rover
Trimble R7 GNSS	Zephyr GNSS Geodetic Model 2 RoHS	TRM57971.00	Static
Trimble R8	Integrated Antenna R8 Model 2	TRM_R8_GNSS	Static, Rover

Airborne Survey

LiDAR

The LiDAR survey was accomplished using a Leica ALS70 sensor system mounted in a Cessna 208-B Grand Caravan aircraft. Table 6 summarizes the settings used to yield an average pulse density of 8 pulses/m^2 over the Idaho and Montana Forests project area. The Leica laser system records up to four range measurements (returns) per pulse. It is not uncommon for some types of surfaces (e.g., dense vegetation or water) to return fewer pulses to the LiDAR sensor than the laser originally emitted. The discrepancy between first return and overall delivered density will vary depending on terrain, land cover, and the prevalence of water bodies. All discernible laser returns were processed for the output dataset.

Table 6: LiDAR specifications and survey set-

LiDAR Survey Settings & Specifications	
Acquisition Dates	September 24 - November 1, 2014
Aircraft Used	Cessna 208
Sensor	Leica ALS70
Survey Altitude (AGL)	1,450 m
Target Pulse Rate	180-192.6 kHz
Pulse Mode	Single Pulse in Air (SPiA)
Laser Pulse Diameter	32 cm
Mirror Scan Rate	39 Hz
Field of View	30°
GPS Baselines	≤13 nm
GPS PDOP	≤3.0
GPS Satellite Constellation	≥6
Maximum Returns	Up to four per pulse
Intensity	8-bit
Resolution/Density	Average 8 pulses/m2
Accuracy	RMSEZ ≤ 15 cm

Leica ALS70 LiDAR sensor

All areas were surveyed with an opposing flight line side-lap of ≥56% (≥100% overlap) in order to reduce laser shadowing and increase surface laser painting. To accurately solve for laser point position (geographic coordinates x, y and z), the positional coordinates of the airborne sensor and the attitude of the aircraft were recorded continuously throughout the LiDAR data collection mission. Position of the aircraft was measured twice per second (2 Hz) by an onboard differential GPS unit, and aircraft attitude was measured 200 times per second (200 Hz) as pitch, roll and yaw (heading) from an onboard inertial measurement unit (IMU). To allow for post-processing correction and calibration, aircraft and sensor position and attitude data are indexed by GPS time.

Processing

View looking west at a regenerated clearcut on the north edge of the Woodward area of interest. The image was created from the gridded LiDAR surface colored by elevation and overlaid with the 3-D LiDAR point cloud.

LiDAR Data

Upon completion of data acquisition, QSI processing staff initiated a suite of automated and manual techniques to process the data into the requested deliverables. Processing tasks included GPS control computations, smoothed best estimate trajectory (SBET) calculations, kinematic corrections, calculation of laser point position, sensor and data calibration for optimal relative and absolute accuracy, and LiDAR point classification (Table 7). Processing methodologies were tailored for the landscape. Brief descriptions of these tasks are shown in Table 8.

Table 7: ASPRS LAS classification standards applied to the Idaho and Montana Forests dataset

Classification Number	Classification Name	Classification Description
1	Default/ Unclassified	Laser returns that are not included in the ground class, composed of vegetation and man-made structures
2	Ground	Laser returns that are determined to be ground using automated and manual cleaning algorithms
6	Buildings	Permanent structures
7	Noise	Identified by height from ground
11	Noise	Identified by intensity values of 0 or 255

Table 8: LiDAR processing workflow

Resolve kinematic corrections for aircraft position data using kinematic aircraft GPS and static ground GPS data. Develop a smoothed best estimate of trajectory (SBET) file that blends post-processed aircraft position with sensor head position and attitude recorded throughout the survey.	IPAS TC v.3.1 Waypoint Inertial Explorer v.8.5
Calculate laser point position by associating SBET position to each laser point return time, scan angle, intensity, etc. Create raw laser point cloud data for the entire survey in *.las (ASPRS v. 1.2) format. Convert data to orthometric elevations by applying a geoid correction.	ALS Post Processing Software v.2.75
Import raw laser points into manageable blocks (less than 500 MB) to perform manual relative accuracy calibration and filter erroneous points. Classify ground points for individual flight lines.	TerraScan v.14
Using ground classified points per each flight line, test the relative accuracy. Perform automated line-to-line calibrations for system attitude parameters (pitch, roll, heading), mirror flex (scale) and GPS/IMU drift. Calculate calibrations on ground classified points from paired flight lines and apply results to all points in a flight line. Use every flight line for relative accuracy calibration.	TerraMatch v.14
Classify resulting data to ground and other client designated ASPRS classifications (Table 7). Assess statistical absolute accuracy via direct comparisons of ground classified points to ground control survey data.	TerraScan v.14 TerraModeler v.14
Generate bare earth models as triangulated surfaces. Generate highest hit models as a surface expression of all classified points. Export all surface models as ESRI GRIDs in EDRAS Imagine (.img) format at a 3.0 foot 1 meter pixel resolution.	TerraScan v.14 TerraModeler v.14 ArcMap v. 10.1
Correct intensity values for variability and export intensity images as GeoTIFFs at a 1.5 foot 0.5 meter pixel resolution.	TerraScan v.14 TerraModeler v.14 ArcMap v. 10.1

Project area under snow

LiDAR Density

The acquisition parameters were designed to acquire an average first-return density of 8 points/m^2. First return density describes the density of pulses emitted from the laser that return at least one echo to the system. Multiple returns from a single pulse were not considered in first return density analysis. Some types of surfaces (e.g., breaks in terrain, water and steep slopes) may have returned fewer pulses than originally emitted by the laser. First returns typically reflect off the highest feature on the landscape within the footprint of the pulse. In forested or urban areas the highest feature could be a tree, building or power line, while in areas of unobstructed ground, the first return will be the only echo and represents the bare earth surface.

The density of ground-classified LiDAR returns was also analyzed for this project. Terrain character, land cover, and ground surface reflectivity all influenced the density of ground surface returns. In vegetated areas, fewer pulses may penetrate the canopy, resulting in lower ground density.

The average first-return density of LiDAR data for the Idaho and Montana Forests project was 17.72 points/m^2 and the average ground classified density was 4.35 points/m^2 (Table 9).

Table 9: Average LiDAR point densities

Classification	Point Density
First Return	1.65 points/ft^2
	17.72 points/m^2
Ground Classified	0.40 points/ft^2
	4.35 points/m^2

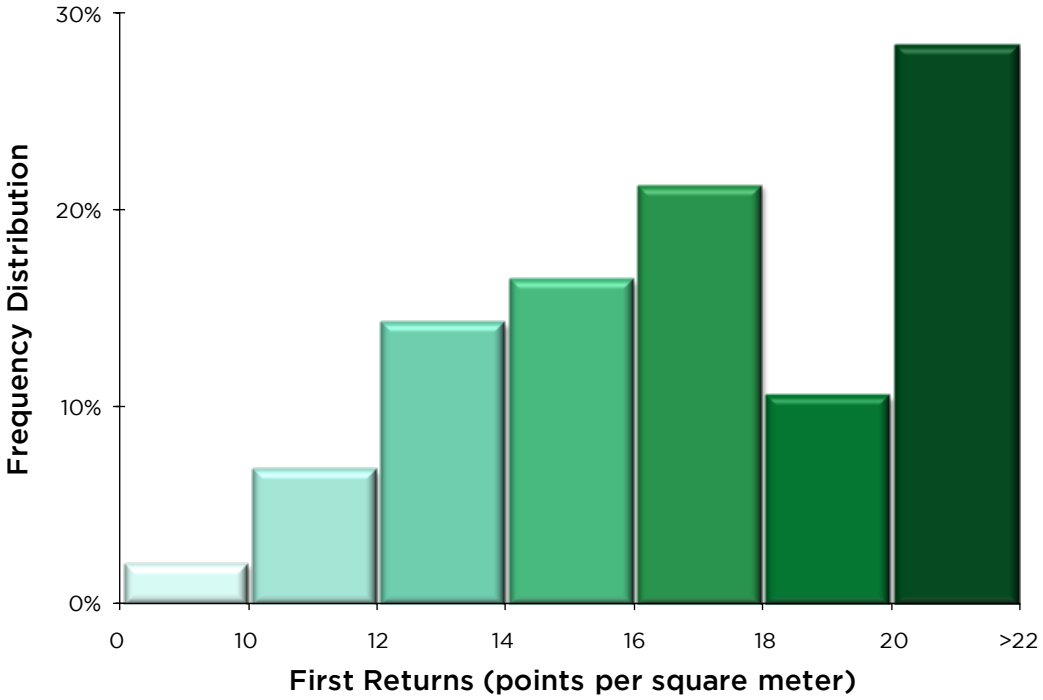

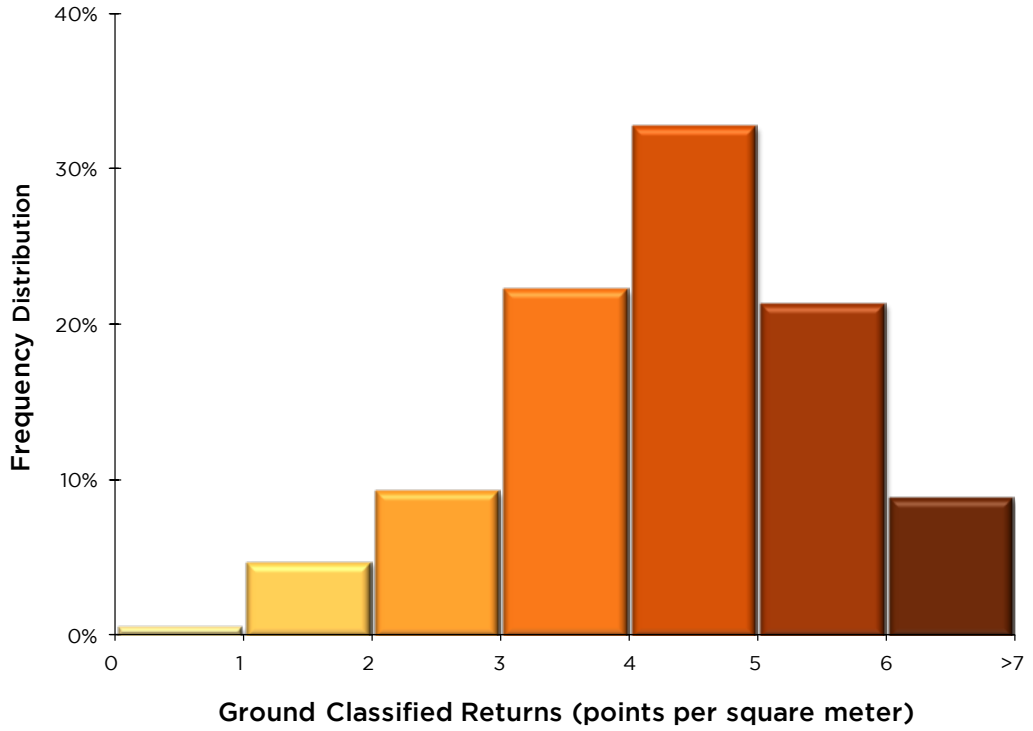

Figure 3: Frequency distribution of first return densities (above) and ground return densities (below).

LiDAR Accuracy Assessments

The accuracy of the LiDAR data collection can be described in terms of absolute accuracy (the consistency of the data with external data sources) and relative accuracy (the consistency of the dataset with itself). See Appendix A for further information on sources of error and operational measures used to improve relative accuracy.

LiDAR Absolute Accuracy

Absolute accuracy was assessed using Fundamental Vertical Accuracy (FVA) reporting designed to meet guidelines presented in the FGDC National Standard for Spatial Data Accuracy* . FVA compares known RTK ground check point data collected on open, bare earth surfaces with level slope (<20°) to the triangulated surface generated by the LiDAR points. FVA is a measure of the accuracy of LiDAR point data in open areas where the LiDAR system has a high probability of measuring the ground surface and is evaluated at the 95% confidence interval (1.96 * RMSE), as shown in Table 10.

The mean and standard deviation (sigma σ) of divergence of the ground surface model from ground survey point coordinates are also considered during accuracy assessment. These statistics assume the error for x, y and z is normally distributed, and therefore the skew and kurtosis of distributions are also considered when evaluating error statistics. For the Idaho and Montana Forests survey, 1,346 ground survey points were collected in total resulting in an average accuracy of 0.06 feet (0.02 meters). An additional 824 check points were reserved for independent verification. Results for both absolute accuracy and the independent verification are located in Table 10 and Figure 4.

In addition to the hard surface land class, checkpoints were also collected across the project area for additional land cover classes (Table 11).

Table 10: Absolute Accuracy

	Absolute Accuracy	Independent Check Point Accuracy
Sample	1,346 points	824 points
FVA (1.96*RMSE)	0.15 ft 0.04 m	0.21 ft 0.06 m
Average	0.06 ft 0.02 m	0.08 ft 0.03 m
Median	0.05 ft 0.01 m	0.07 ft 0.02 m
RMSE	0.07 ft 0.02 m	0.11 ft 0.03 m
Standard Deviation (1σ)	0.07 ft 0.02 m	0.10 ft 0.03 m

Table 11: Land Class Accuracy*

	Bare Earth	Short Grass	Tall Grass	Short Grass w/ Trees	All Land Cover Classes
Sample	595 points	1,655 points	560 points	26 points	2,836 points
95th Percentile	0.313 ft 0.095 m	0.431 ft 0.131 m	0.886 ft 0.270 m	0.334 ft 0.102 m	0.502 ft 0.153 m
Average	0.064 ft 0.020 m	0.117 ft 0.036 m	0.294 ft 0.090 m	0.136 ft 0.041 m	0.141 ft 0.043 m
Median	0.082 ft 0.025 m	0.108 ft 0.033 m	0.223 ft 0.068 m	0.136 ft 0.042 m	0.121 ft 0.037 m
RMSE	0.170 ft 0.052 m	0.216 ft 0.066 m	0.426 ft 0.130 m	0.178 ft 0.054 m	0.263 ft 0.080 m
Standard Deviation (1σ)	0.158 ft 0.048 m	0.181 ft 0.055 m	0.309 ft 0.094 m	0.118 ft 0.036 m	0.223 ft 0.068 m

* A total of 117 client collected landclass points were not used in the analysis. 115 client collected data points were outside the extent of the data. Four data points were not labeled with a landclass. Two of the four data points that were not labeled with a landclass were also outside the extent of the data.

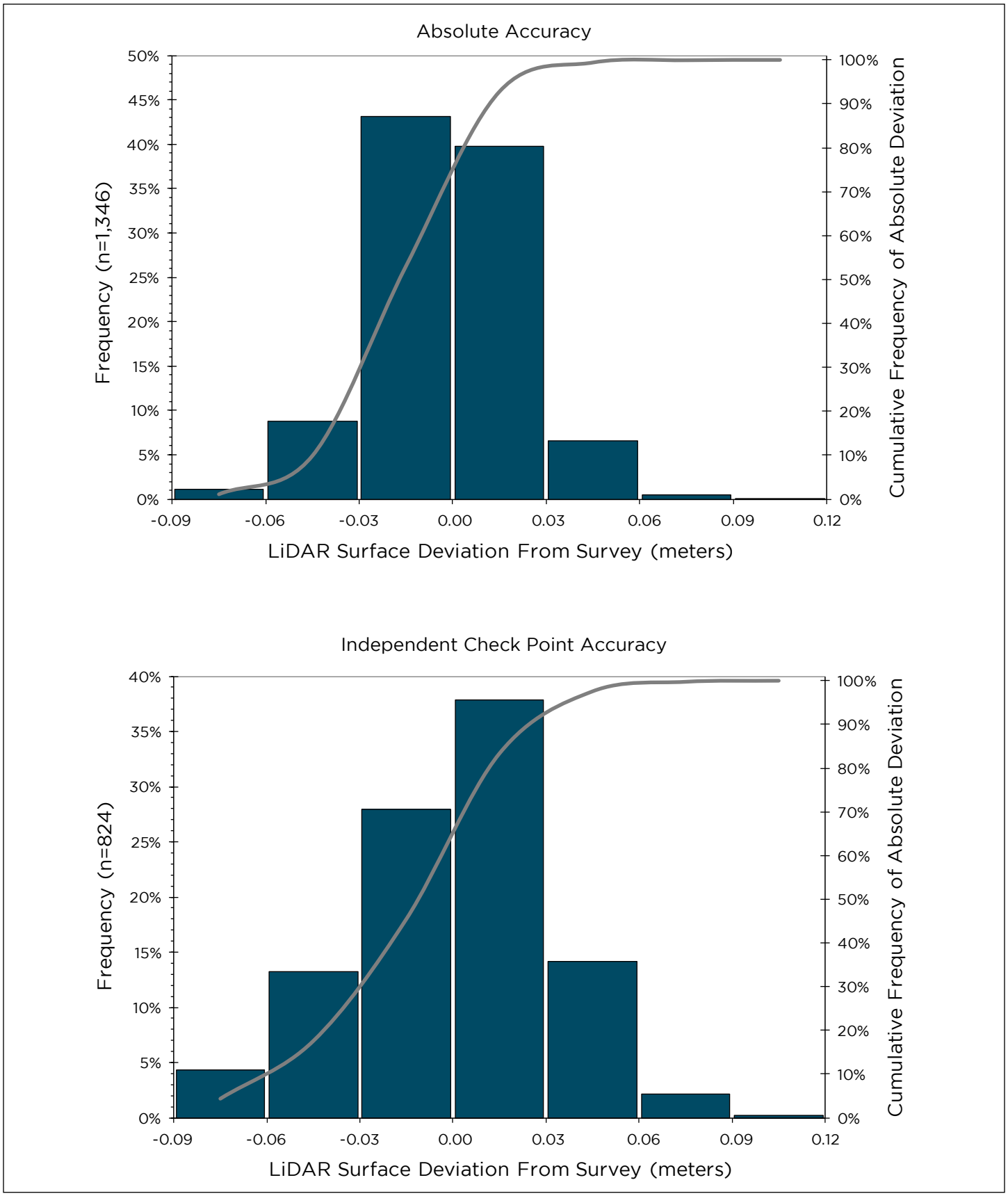

Figure 4: Frequency histograms for LiDAR surface deviation from ground survey point values (above) and for the independent check point verification (below)

LiDAR Relative Accuracy

Relative vertical accuracy refers to the internal consistency of the data set as a whole: the ability to place an object in the same location given multiple flight lines, GPS conditions, and aircraft attitudes. When the LiDAR system is well calibrated, the swath-to-swath vertical divergence is low (<0.10 meters). The relative vertical accuracy was computed by comparing the ground surface model of each individual flight line with its neighbors in overlapping regions. The average (mean) line to line relative vertical accuracy for the Idaho and Montana Forests LiDAR project was 0.17 feet (0.05 meters) (Table 12, Figure 5).

Table 12: Relative accuracy

Relative Accuracy	
Sample	690 flightlines
Average	0.17 ft
	0.05 m
Median	0.15 ft
	0.05 m
RMSE	0.05 ft
	0.02 m
Standard Deviation (1 σ)	0.17 ft
	0.05 m
1.96 σ	0.10 ft
	0.03 m

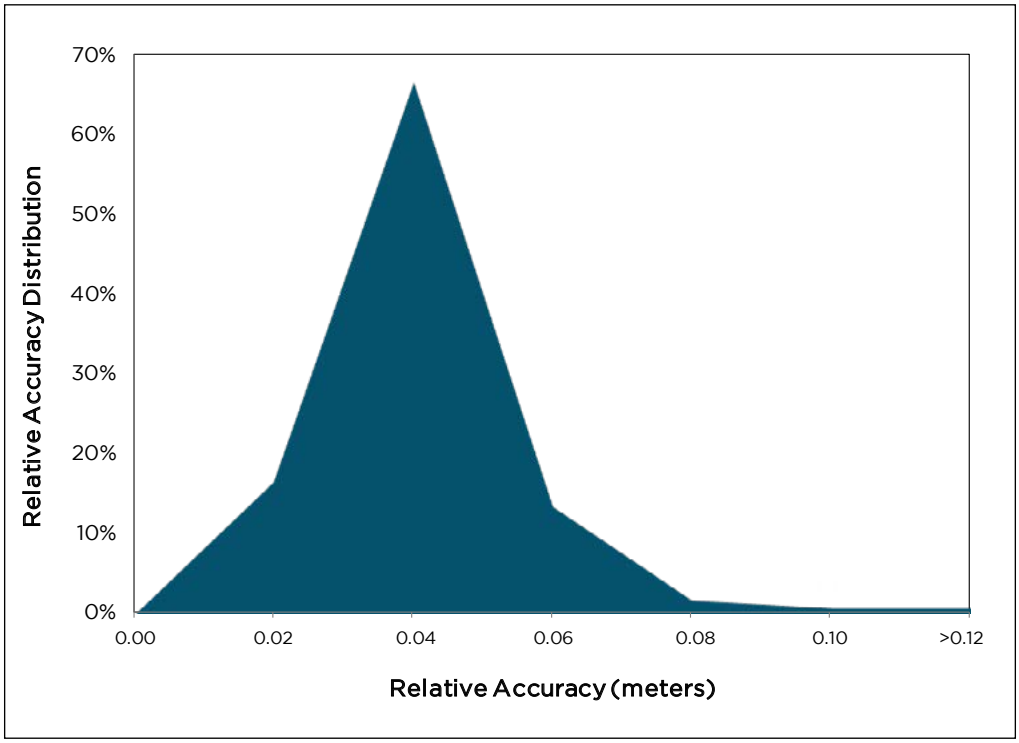

Figure 5: Frequency plot for relative vertical accuracy between flight lines.

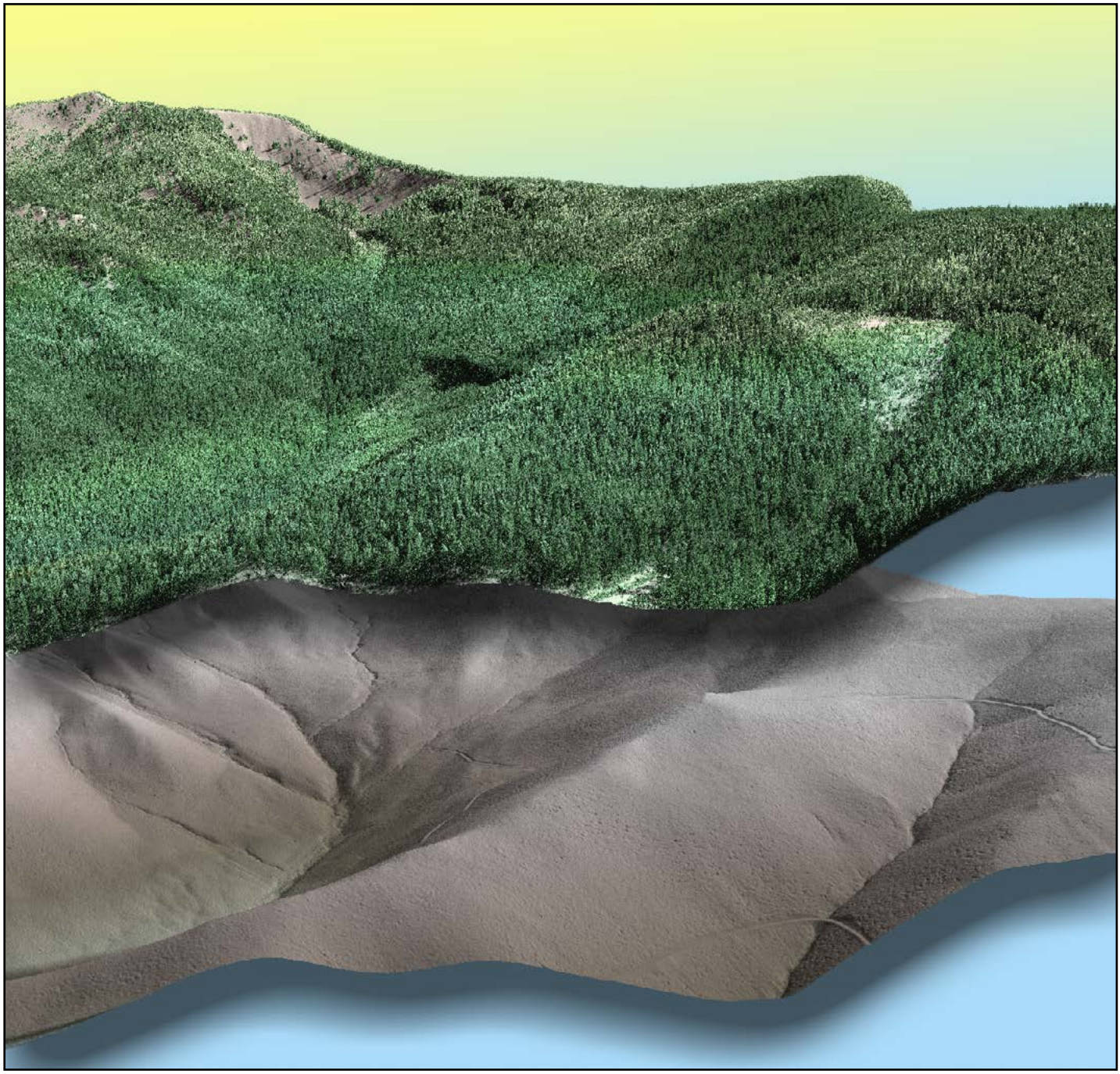

Figure 6: View looking west at Ovando Mountain in the North Lake area of interest in Montana. The images were created from the gridded LiDAR surface colored by elevation with the top image overlaid with the 3-D LiDAR point cloud.

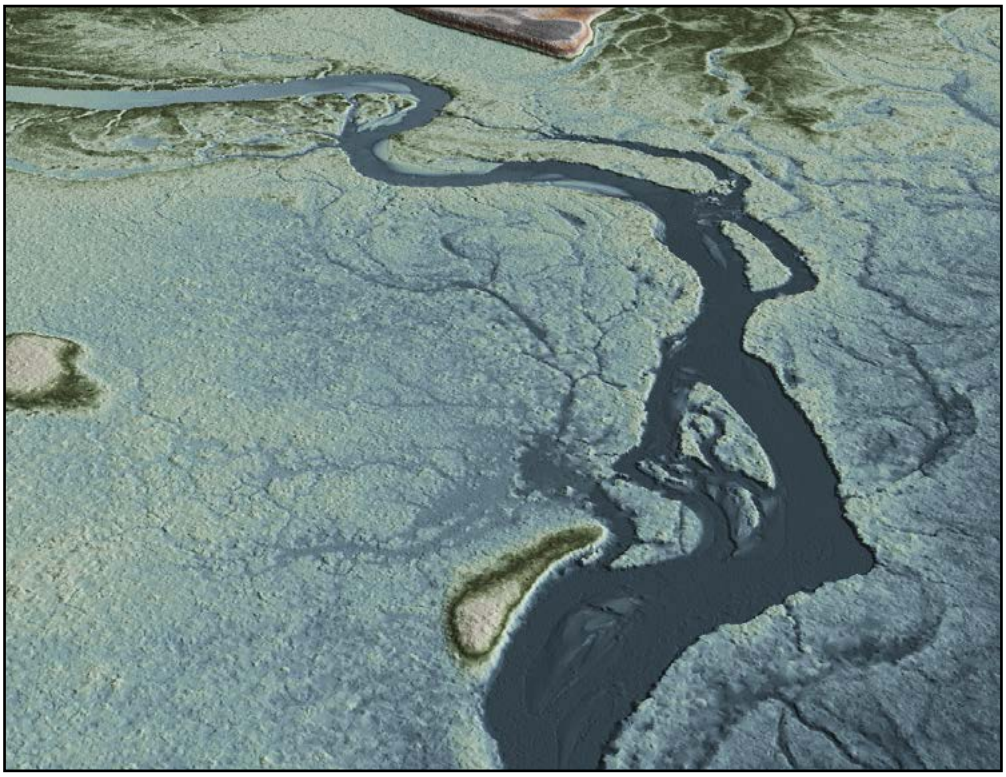

Figure 7: (Above) View looking south over the Swan River in the North Swan area of interest. The image was created from the gridded LiDAR surface colored by elevation.
(Below) View looking northeast over the Swan River in the North Swan area of interest. The image was created from the gridded LiDAR surface colored by elevation and overlaid with the 3-D LiDAR point cloud.

Glossary

1-sigma (σ) Absolute Deviation: Value for which the data are within one standard deviation (approximately 68th percentile) of a normally distributed data set.

1.96 * RMSE Absolute Deviation: Value for which the data are within two standard deviations (approximately 95th percentile) of a normally distributed data set, based on the FGDC standards for Fundamental Vertical Accuracy (FVA) reporting.

Accuracy: The statistical comparison between known (surveyed) points and laser points. Typically measured as the standard deviation (sigma σ) and root mean square error (RMSE).

Absolute Accuracy: The vertical accuracy of LiDAR data is described as the mean and standard deviation (sigma σ) of divergence of LiDAR point coordinates from ground survey point coordinates. To provide a sense of the model predictive power of the dataset, the root mean square error (RMSE) for vertical accuracy is also provided. These statistics assume the error distributions for x, y, and z are normally distributed, and thus the skew and kurtosis of distributions are also considered when evaluating error statistics.

Relative Accuracy: Relative accuracy refers to the internal consistency of the data set (i.e., the ability to place a laser point in the same location over multiple flight lines), GPS conditions, and aircraft attitudes. Affected by system attitude offsets, scale, and GPS/IMU drift, internal consistency is measured as the divergence between points from different flight lines within an overlapping area. Divergence is most apparent when flight lines are opposing. When the LiDAR system is well calibrated, the line-to-line divergence is low (<10 cm).

Root Mean Square Error (RMSE): A statistic used to approximate the difference between real-world points and the LiDAR points. It is calculated by squaring all the values, then taking the average of the squares and taking the square root of the average.

Data Density: A common measure of LiDAR resolution, measured as points per square meter.

Digital Elevation Model (DEM): File or database made from surveyed points, containing elevation points over a contiguous area. Digital terrain models (DTM) and digital surface models (DSM) are types of DEMs. DTMs consist solely of the bare earth surface (ground points), while DSMs include information about all surfaces, including vegetation and man-made structures.

Intensity Values: The peak power ratio of the laser return to the emitted laser, calculated as a function of surface reflectivity.

Nadir: A single point or locus of points on the surface of the earth directly below a sensor as it progresses along its flight line.

Overlap: The area shared between flight lines, typically measured in percent. 100% overlap is essential to ensure complete coverage and reduce laser shadows.

Pulse Rate (PR): The rate at which laser pulses are emitted from the sensor; typically measured in thousands of pulses per second (kHz).

Pulse Returns: For every laser pulse emitted, the number of wave forms (i.e., echos) reflected back to the sensor. Portions of the wave form that return first are the highest element in multi-tiered surfaces such as vegetation. Portions of the wave form that return last are the lowest element in multi-tiered surfaces.

Real-Time Kinematic (RTK) Survey: A type of surveying conducted with a GPS base station deployed over a known monument with a radio connection to a GPS rover. Both the base station and rover receive differential GPS data and the baseline correction is solved between the two. This type of ground survey is accurate to 1.5 cm or less.

Post-Processed Kinematic (PPK) Survey: GPS surveying is conducted with a GPS rover collecting concurrently with a GPS base station set up over a known monument. Differential corrections and precisions for the GNSS baselines are computed and applied after the fact during processing. This type of ground survey is accurate to 1.5 cm or less.

Scan Angle: The angle from nadir to the edge of the scan, measured in degrees. Laser point accuracy typically decreases as scan angles increase.

Native LiDAR Density: The number of pulses emitted by the LiDAR system, commonly expressed as pulses per square meter.

Appendix A - Accuracy Controls

Relative Accuracy Calibration Methodology:

Manual System Calibration: Calibration procedures for each mission require solving geometric relationships that relate measured swath-to-swath deviations to misalignments of system attitude parameters. Corrected scale, pitch, roll and heading offsets were calculated and applied to resolve misalignments. The raw divergence between lines was computed after the manual calibration was completed and reported for each survey area.

Automated Attitude Calibration: All data were tested and calibrated using TerraMatch automated sampling routines. Ground points were classified for each individual flight line and used for line-to-line testing. System misalignment offsets (pitch, roll and heading) and scale were solved for each individual mission and applied to respective mission datasets. The data from each mission were then blended when imported together to form the entire area of interest.

Automated Z Calibration: Ground points per line were used to calculate the vertical divergence between lines caused by vertical GPS drift. Automated Z calibration was the final step employed for relative accuracy calibration.

LiDAR accuracy error sources and solutions:

Type of Error	Source	Post Processing Solution
GPS (Static/Kinematic)	Long Base Lines	None
	Poor Satellite Constellation	None
	Poor Antenna Visibility	Reduce Visibility Mask
Relative Accuracy	Poor System Calibration	Recalibrate IMU and sensor offsets/settings
	Inaccurate System	None
Laser Noise	Poor Laser Timing	None
	Poor Laser Reception	None
	Poor Laser Power	None
	Irregular Laser Shape	None

Operational measures taken to improve relative accuracy:

Low Flight Altitude: Terrain following was employed to maintain a constant above ground level (AGL). Laser horizontal errors are a function of flight altitude above ground (about 1/3000th AGL flight altitude).

Focus Laser Power at narrow beam footprint: A laser return must be received by the system above a power threshold to accurately record a measurement. The strength of the laser return (i.e., intensity) is a function of laser emission power, laser footprint, flight altitude and the reflectivity of the target. While surface reflectivity cannot be controlled, laser power can be increased and low flight altitudes can be maintained.

Reduced Scan Angle: Edge-of-scan data can become inaccurate. The scan angle was reduced to a maximum of 312o from nadir, creating a narrow swath width and greatly reducing laser shadows from trees and buildings.

Quality GPS: Flights took place during optimal GPS conditions (e.g., 6 or more satellites and PDOP [Position Dilution of Precision] less than 3.0). Before each flight, the PDOP was determined for the survey day. During all flight times, a dual frequency DGPS base station recording at 1 second epochs was utilized and a maximum baseline length between the aircraft and the control points was less than 13 nm at all times.

Ground Survey: Ground survey point accuracy (<1.5 cm RMSE) occurs during optimal PDOP ranges and targets a minimal baseline distance of 4 miles between GPS rover and base. Robust statistics are, in part, a function of sample size (n) and distribution. Ground survey points are distributed to the extent possible throughout multiple flight lines and across the survey area.

50% Side-Lap (100% Overlap): Overlapping areas are optimized for relative accuracy testing. Laser shadowing is minimized to help increase target acquisition from multiple scan angles. Ideally, with a 50% side-lap, the nadir portion of one flight line coincides with the swath edge portion of overlapping flight lines. A minimum of 50% side-lap with terrain-followed acquisition prevents data gaps.

Opposing Flight Lines: All overlapping flight lines have opposing directions. Pitch, roll and heading errors are amplified by a factor of two relative to the adjacent flight line(s), making misalignments easier to detect and resolve.